

TEXTE

94/2023

Final report

Satellite-based Emission Verification

Pilot study

by:

Enrico Dammers, Janot Tokaya, Renske Timmermans, Martijn Schaap, Peter Coenen
TNO, Utrecht (The Netherlands)

publisher:

German Environment Agency

TEXTE 94/2023

Ressortforschungsplan of the Federal Ministry for the
Environment, Nature Conservation, Nuclear Safety and
Consumer Protection

Project No. FKZ 3720 51 501 0

Report No. (UBA-FB) FB001010/ENG

Final report

Satellite-based Emission Verification

Pilot study

by


Enrico Dammers, Janot Tokaya, Renske Timmermans,
Martijn Schaap, Peter Coenen
TNO, Utrecht (The Netherlands)


On behalf of the German Environment Agency

Imprint

Publisher

Umweltbundesamt
Wörlitzer Platz 1
06844 Dessau-Roßlau
Tel: +49 340-2103-0
Fax: +49 340-2103-2285
buergerservice@uba.de
Internet: www.umweltbundesamt.de

 [umweltbundesamt.de](https://www.facebook.com/umweltbundesamt.de)

 [umweltbundesamt](https://twitter.com/umweltbundesamt)

Report performed by:

TNO
Princetonlaan 6
3584 CB Utrecht
The Netherlands

Report completed in:

November 2022

Edited by:

Section V 1.6 Emissionssituation
Christian Mielke and Kevin Hausmann

Publication as pdf:

<http://www.umweltbundesamt.de/publikationen>

ISSN 1862-4804

Dessau-Roßlau, June 2023

The responsibility for the content of this publication lies with the author(s).

Abstract:

Satellites that measure the chemical composition of the atmosphere are becoming more accurate and numerous, providing a unique opportunity to independently monitor emissions for large geographical regions in a consistent way. This report elaborates the development of a software tool which is able to process satellite observation data and estimate NO_x emissions from it for a pre-defined area. The tool is fully operational for processing satellite observations from the TROPospheric Monitoring Instrument (TROPOMI) and the Ozone Monitoring Instrument (OMI). The tool is modular in design with the capability in mind to digest satellite data from various satellites and for pollutants. It is furthermore designed to be relatively simple and operates without a dependence on complicated and computationally demanding atmospheric models. The methods for satellite based emission estimation can complement data from emission inventories by incorporating independent measurement techniques into the reporting scheme. This would help to identify room for improvement in the compilation of inventories as well as boost the transparency and confidence in the reported data.

The developed capabilities of the tool are applied to derive German national emissions for the year 2019 as well as the trend in NO_x emissions between 2005 and 2019. Three methods to derive NO_x emissions estimates from satellite observations are developed and applied to TROPOMI data for the year 2019. Derivation of emissions through direct integration of atmospheric concentrations over the vertical columns within a region (called the Naïve method) results in an estimate of German NO_x emission of 1097.1 kton. A Gaussian plume-based fitting routine (Fioletov et al., 2017) led to an estimated 1241.0 kton and a computation based on the divergence of the pollutant flux field (Beirle et al., 2019) resulted in an estimate of 1260.7 kton. All three estimates are within 15% of the reported total emissions for 2019 (1108.82, NFR, [Submission 2022 \(europa.eu\)](#)).

To derive the trend in NO_x emissions within the past 15 years, the Fioletov method was applied to OMI observations between 2005 and 2019, showing an average decrease of around 25% between the 2005-2007 and 2017-2019 period, which is in agreement with the reduction reported in emission inventories (20% reduction between 2005-2007 and 2014-2016 period and 23% between 2005-2007 and 2017-2019 period found in the 2022 NFR reported totals based on fuel sold [Submission 2022]). TROPOMI was launched in October 2017 hence its data cannot be used to monitor long term trends.

While all three methods show comparable results for 2019 at country level, differences were observed at smaller administrative scales, notably the Naïve method not being able to reproduce local emission gradients to the same level as the other methods. At the highest administrative level (Districts) the Gaussian plume method starts to outperform the divergence method. Both methods can be further improved to reach higher levels of accuracy. The majority of the uncertainties relate to the estimated NO_x lifetime in the calculations and inaccuracies in the TROPOMI-NO₂ product.

An important issue when comparing emission estimates from satellite observations with the official inventory data is the fact that the inventories (by convention) do not include all emission sources which contribute to the observed concentrations. Adding estimates for natural emissions and emissions from the so called “Memo” items¹ from the IIR to the national total as reported in the IIR bring the inventory data and the satellite observation closer together.

¹ : Emissions to be reported in the IIR, but these will not be included in the national total emissions.

Kurzbeschreibung:

Satelliten, die die chemische Zusammensetzung der Atmosphäre messen, werden immer zahlreicher und genauer. Sie bieten die Option, Emissionen über große geografische Regionen hinweg und auf einheitliche Weise unabhängig zu überwachen. Dieser Bericht erläutert die Entwicklung eines Softwaretools, welches in der Lage ist, Satellitenbeobachtungsdaten zu verarbeiten und daraus NO_x-Emissionen für ein vordefiniertes Gebiet abzuschätzen. Das Werkzeug ist auf die Verarbeitung von Satellitenbeobachtungen des TROPospheric Monitoring Instrument (TROPOMI) und des Ozone Monitoring Instrument (OMI) optimiert, bietet aber einen modularen Aufbau, um Satellitendaten von verschiedenen Satelliten und zu unterschiedlichen Schadstoffen zu verarbeiten. Es ist darüber hinaus so konzipiert, dass es relativ einfach funktionsfähig ist, ohne von komplizierten und rechenintensiven atmosphärischen Modellen abhängig zu sein. Die Methoden zur satellitengestützten Emissionsschätzung können Daten aus Emissionsinventaren ergänzen, indem sie unabhängige Datenreihen in das Berichtssystem einbeziehen. Dies trägt bei, Verbesserungspotenziale bei der Erstellung von Inventaren zu identifizieren und die Transparenz und das Vertrauen in die gemeldeten Daten zu stärken.

Die entwickelten Features der Software werden angewendet, um die deutschen nationalen Emissionen für das Jahr 2019 sowie den Trend der NO_x-Emissionen zwischen 2005 und 2019 nachzuvollziehen. Zu diesem Zweck werden insgesamt drei Methoden zur Ableitung der NO_x-Emissionen aus Satellitenbeobachtungen entwickelt und auf TROPOMI-Daten für das Jahr 2019 angewendet um eine Schätzung der nationalen deutschen NO_x-Emissionen zu erhalten. Die einfache Ableitung einer Emissionsschätzung durch Integration der atmosphärischen Konzentrationen über die vertikalen Säulen innerhalb einer Region (als „naive Methode“ bezeichnet) führt zu einer Schätzung der deutschen NO_x-Emissionen von 1097,1 kt in 2019. Eine zweite Methode auf Basis von Abgasfahnen (Fioletov et al., 2017) führte zu einer Schätzung von 1241,0 kt und der dritte Ansatz auf der Grundlage der Divergenz des Schadstoffflussfeldes (Beirle et al., 2019) ergab eine Schätzung von 1260,7 kt. Alle drei Berechnungen liegen innerhalb von 15% der von Deutschland berichteten Gesamtemissionen für 2019 (1108,82 kt, NFR-Submission 2022).

Um den Trend der NO_x-Emissionen über die letzten 15 Jahre abzuleiten, wurde die Fioletov-Methode auf OMI-Beobachtungen aus der Zeit zwischen 2005 und 2019 angewendet, die einen Rückgang der Emissionen um etwa 25% zwischen 2005 und 2019 zeigt, in guter Übereinstimmung mit den Emissionsinventaren (20% bis 25% Abnahme, je nach Grundlage). Das TROPOMI-Instrument wurde erst im Oktober 2017 in Betrieb genommen und seine Daten können daher noch nicht zur Überwachung langfristiger Trends verwendet werden.

Während alle drei Methoden für 2019 auf Bundesebene vergleichbare Ergebnisse zeigen, wurden Unterschiede auf kleineren Verwaltungsskalen offenbar, wobei insbesondere die „naive“ Methode lokale Emissionsgradienten nicht reproduzieren kann. Auf der höchsten Verwaltungsebene der Gemeinden beginnt die Gaußsche Fahnenmethode die Divergenz Methode zu übertreffen. Alle Methoden können weiter verbessert werden, um eine höhere Genauigkeit zu erreichen. Der größte Teil der Unsicherheiten bei den Berechnungen ergibt sich aus der geschätzten NO_x-Lebensdauer in der Luft und den Ungenauigkeiten im TROPOMI-NO₂-Produkt.

Eine grundlegende Schwierigkeit beim Vergleich von Emissionsschätzungen aus Satellitenbeobachtungen mit den amtlichen Inventardaten ist die Tatsache, dass die Inventare per Definition nicht alle Emissionsquellen enthalten, die zu den beobachteten Konzentrationen beitragen. Das Hinzurechnen von Schätzungen für natürliche Emissionsquellen (etwa Gewitter

und Vegetation) sowie Emissionen aus den sogenannten „Memo-Items“, deren Emissionen zwar berichtet aber nicht zu den nationalen Gesamtmengen gerechnet werden, bringt die Inventardaten und die Satellitenbeobachtung näher zusammen.

Table of content

List of Figures.....	11
List of Tables.....	13
List of Abbreviations.....	14
Summary	16
Zusammenfassung.....	19
1 Background.....	22
1.1 Introduction	22
1.2 Aim of the project	22
2 Approach	24
2.1 Introduction	24
2.2 Methodological structure	24
2.2.1 Literature research	24
2.2.2 Data sources and Compatibility issues	25
2.2.3 Satellite data processing and method development.....	26
2.2.4 Development of a Verification Tool and its implementation	28
2.2.5 Conclusion.....	28
3 Results	29
3.1 Literature research.....	29
3.1.1 Satellite observations of atmospheric composition	29
3.1.2 NO ₂ satellite products.....	30
3.1.3 NH ₃ satellite products.....	30
3.1.4 Methods for satellite-based emission estimates.....	31
3.1.4.1 Mass balance	33
3.1.4.2 Gaussian plume models.....	36
3.1.4.3 (Ensemble / Adjustment) Kalman Filter-based studies	37
3.1.4.4 Adjoint based methods.....	39
3.1.4.5 Trend estimates	41
3.1.4.6 Overview of relevant research projects	44
3.1.5 Use of satellite data in official national emission reporting	47
3.1.6 Summary of methods and characteristics	47
3.1.7 Overview and recommendation of most appropriate methods	50
3.2 Data sources and Compatibility issues.....	51
3.2.1 Introduction	51

3.2.2	Recommendations for satellite data used to estimate NO ₂ emission	52
3.2.3	NO ₂ Satellite products.....	53
3.2.4	NH ₃ Satellite products	54
3.2.5	Data providers.....	56
3.2.5.1	NO _x data	56
3.2.5.2	NH ₃ data	57
3.2.5.3	Combinations of data sources	59
3.2.6	Limitations and compatibility issues.....	59
3.2.6.1	Spatial resolution	60
3.2.6.2	Instrument sensitivity	60
3.2.6.3	Product uncertainty	60
3.2.6.4	Product biases.....	60
3.2.6.5	Temporal resolution of satellite product and temporal variability in emissions.....	61
3.2.6.6	Unavailability of data	61
3.2.6.7	Gaps in a-priori emission data	61
3.2.7	Outlook on future satellite instruments	61
3.3	Satellite data processing and method development.....	62
3.3.1	Tool description	62
3.3.1.1	Workflow – an example for NO _x emission estimates based on the Gaussian plume method.....	63
3.3.1.2	Data selection	65
3.3.2	Mitigation of compatibility issues.....	66
3.3.2.1	Mass-balance methods.....	67
3.3.2.2	Gaussian plume-based method	68
3.3.2.3	(Ensemble / Adjustment) Kalman Filter-based studies	70
3.3.2.4	Adjoint based methods.....	71
3.3.3	Other openly available software.....	72
3.3.4	Potential role of a CTM	73
3.4	Development of the tool.....	73
3.4.1	General Description	73
3.4.2	Open Source version.....	74
3.5	Tool results.....	76
3.5.1	The German 2019 National Emission data	76
3.5.2	Trends in German National Emissions based on OMI data	83

3.5.3	Discussion on comparison of NFR national and satellite derived emission estimates.....	86
	International aviation cruise (civil) (139.5 kt):	86
	Domestic aviation cruise (civil) (8.4 kton);	87
	International maritime navigation (59.4 kt).....	87
	Multilateral operations (not estimated in Germany).....	87
	Other not included in national total of the entire territory (not occurring in Germany)	88
	Volcanoes (not occurring in Germany).....	88
	Forest fires (0.34 kt)	88
	Other natural emissions: (Not occurring in Germany)	88
3.6	Dissemination.....	92
4	Conclusions and recommendations	93
4.1	Conclusions	93
4.2	Outlook.....	93
A	Appendices	96
A.1	Detailed description of satellite products - NO ₂	96
A.2	Detailed description of satellite products - NH ₃	100
5	Bibliography.....	101

List of Figures

Figure 1:	Example of improved resolution of TROPOMI versus OMI tropospheric NO ₂ data product over India.....	30
Figure 2:	Comparison of emission total, as well as the modelled OMI-NO ₂ column in 2005 and 2020 for the Czech Republic (CZE) (left) and Denmark (DNK) (right). Both the emissions (left two) and modelled (right two) columns are separated into the major sectors.	33
Figure 3:	Monthly time series for northern Spain for OMI-NO ₂ and LOTOS-EUROS NO ₂ columns for the period 2005–2010. Histograms provide the number of data points included in the average.	43
Figure 4:	Comparison of reported emission trend per year and the derived trends from OMI and AIRBASE in-situ data for European countries. The total national NO _x emissions reported in July 2012 for 2005–2010 were used and the changes relative to 2005 were computed (Curier <i>et al.</i> , 2014).....	45
Figure 5:	Comparison of trend for Germany derived with approach 3 (blue), with emissions from official reports (red) and satellite-derived emissions with approach 4 (green) and the trend in those (dashed green).....	46
Figure 6:	Overview of past, current and future approved tropospheric NO ₂ missions over Europe. The currently operational systems are in dark green. UVAS is in orange because this mission was unable to provide any retrievals due to a launch failure.	54
Figure 7:	Overview of past, current and future approved tropospheric NH ₃ missions over Europe. The currently operational systems are in dark green. Specific satellites are operational beyond their expected mission duration which is denoted by arrows for the extended periods.	56
Figure 8:	General framework for the developed tool. The tool should eventually work for a multitude of pollutants, for which available satellite products will be selected based on the query of a user.	63
Figure 9:	Graphical representation of the workflow(s) that has been developed in this project. The main workflow is displayed in black. (As an example, the Gaussian plume method is chosen, but the divergence method is likewise developed. Emissions derived from satellite data are compared to inventory data...)	65
Figure 10:	An overview of the tool components in the GitHub repository.	75

Figure 11:	Maps of Germany with yearly total NO _x emissions in kg/m ² . A) Emissions according to the gridded NFR (GNFR) inventory (CLRTAP) for 2019 B) Estimate using the divergence method for 2019 (Beirle et al., 2019) C) Estimate using the Gaussian plume-based fitting routine for 2019 (Fioletov et al., 2017) D) Estimate using the Naïve method(direct VCD summation) for 2019.....78
Figure 12:	Scatter plot of the inventory vs estimated emissions for the various methods applied at various scales.....81
Figure 13:	Line plots to compare the inventory with estimated emissions for the various methods applied at the ADM 3 level (admin code 3, i.e. district level).....83
Figure 14:	Trend line in national German NO _x emissions (in kt NO _x). The blue line in the top figure shows the emissions per year derived from OMI observations with the Gaussian plume fitting routine and the orange line shows the inventory. Colored dots show the TROPOMI-based estimates for 2019. The bottom graph shows the relative decrease with respect to the average annual emission estimate for the 2005-2007 period85
Figure 15:	Trend in reported German national NO _x emissions. Source: 2021 NFR submission. The contributions of the various sectors to the total emissions are distinguished. It is clear that the total reduction is mainly realized through a reduction in traffic emissions (F_RoadTransport).....85
Figure 16:	Soil NO _x emissions split between fertilizer induced and other emissions as in the CAMS-GLOB-SOIL inventory (2018 emissions, 0.5°x0.5° resolution). Combined emissions (Total) are shown on the right). Note that the colormap upper range is 10x smaller than those used in Figure 11.....90
Figure 17:	Screenshot of the WebApp Showing the NO _x emission estimate for Germany (in 2021) based on TROPOMI satellite data92

List of Tables

Table 1:	Methods to derive emission estimates from satellite data.	49
Table 2:	Overview satellite instruments capable of NO ₂ observations..	53
Table 3:	Overview satellite instruments capable of observing NH ₃ . D stands for diameter in case of round pixels.	55
Table 4:	The annual emission totals of German federal states (in kt/yr and excluding city states) according to the GNFR inventory, the divergence method, the Gaussian plume fitting method and the naive summation method.	79
Table 5:	Statistics of the scatter plots in Figure 12 that quantify the performance of the various methods.....	83
Table 6:	NO _x Level 2 products. Operational* means the product is still being provided, but a couple of days lag between the retrieval and the release of the processed data might be present.	96
Table 7:	Level 3 products:	98
Table 8:	Summary of the openly available ammonia satellite products (L2/L3), with a summary of the period of observations, provider, summary of quality, and download location. Operational* means the product is still being provided, but a couple of days lag between the retrieval and the release of the processed data might occur.	100

List of Abbreviations

Acronym	Explanation
ADM	ADMINistrative division of a country
AOD	Aerosol Optical Depth
CAMS	Copernicus Atmosphere Monitoring Service
CDS	Climate Data Store
CLRTAP	Convention on Long-range Transboundary Air Pollution
CO ₂	Carbon dioxide
CrIS	Cross-track Infrared Sounder
CTM	Chemical Transport Model
DECISO	Daily Emission estimates Constrained by Satellite Observation
EDGAR	Emission Database for Global Atmospheric Research
EIONet	The European Environment Information and Observation Network
EMG	Exponentially-Modified Gaussian
EnKF	Ensemble Kalman Filter
EUMETSAT	European Organisation for the Exploitation of Meteorological Satellites
ESA	European Space Agency
FTIP	Federal Transport Infrastructure Plan
GEMS	Global Environmental Monitoring Satellite
GHG	GreenHouse Gas
GOME	Global Ozone Monitoring Experiment
GOSAT	Greenhouse gases Observing SATellite
HPC	High Performance Computing cluster (supercomputing)
IASI	Infrared Atmospheric Sounding Interferometer
IIR	Informative Inventory Report
IMAGES	Intermediate Model of Global Evolution of Species
JAXA	Japan Aerospace Exploration Agency
LEO	Lower-Earth Orbital
MOPITT	Measurements of Pollution in the Troposphere
N ₂ O	Nitrous oxide (laughing gas)
NO	Nitric Oxide
NO ₂	Nitrogen dioxide
NO _x	The nitrogen oxides, the combination of nitric oxide and nitrogen dioxide.
NUTS	Nomenclature des Unités Territoriales Statistiques
OMI	Ozone Monitoring Instrument
PM	Particulate Matter
SCIAMACHY	SCanning Imaging Absorption SpectroMeter for Atmospheric CHartographY
SNAP	Selected Nomenclature for sources of Air Pollution

SNR	Signal to Noise Ratio
SO₂	Sulphur dioxide
TEMPO	Tropospheric Emissions: Monitoring of Pollution
TES	Tropospheric Emission Spectrometer
TFEIP	Task Force on Emission Inventories and Projections
TNO	Dutch organisation for Toegepast-Natuurwetenschappelijk Onderzoek (Applied Scientific Research)
TROPOMI	TROPOspheric Monitoring Instrument
UBA	UmweltBundesAmt (German Environment Agency)
UNFCCC	United Nations Framework Convention on Climate Change
UV	Ultraviolet
VCD	Vertical Column Density

Summary

Within the past decade satellite-based air pollutant measurements have increased tremendously in quality, coverage and frequency. Considering the number of planned missions with a focus on air quality monitoring, this growth is expected to continue in the forthcoming years. With an increase in instrument sensitivity, spatial and temporal resolution, and more products focusing on the lower layers of the atmosphere, these satellite-based measurements are becoming more and more attractive for air quality monitoring and emission studies.

Out of the currently available satellite products, tropospheric NO₂ data has found most applications in air quality modelling and monitoring, because of its superior quality compared to products of other measured pollutants. The current standard practices with NO₂ can function as examples for species that only the latest generation instruments were able to observe at high spatial scale such as NH₃. The quality of other products and the capabilities to measure other pollutant concentrations are expected to increase in the coming years.

The overall goal of this project is to demonstrate the use of satellite observations of NO₂ for the estimation of NO_x (i.e., NO + NO₂) emissions in Germany at a national level. A software toolchain that is able to assess NO_x emissions from satellite data, for a selected region and time period is developed. This tool is designed to be flexible in its application and extendable to other countries and species. The software tool will be made publicly available to allow collaboration and achieve the envisioned generalizations.

At first a literature study on available methods and applications has been performed, to decide on an optimal approach for estimating NO_x emissions. The findings from this literature review are discussed in chapter 3.1. It became evident that on a country level usage of spaceborne data for emission inventory reporting and or verification is not common practice. However, in the scientific community methods have been developed but have not yet been implemented outside academia.

The methods reported in scientific literature were reviewed to identify the most viable candidates to be implemented in this project. Some approaches, like the Ensemble Kalman Filter (EnKF) and adjoint based methods (e.g., 4D-var), rely on a chemical transport models (CTMs) in combination with satellite products to assess the accuracy of emissions that served as input to the CTM. An ensemble of emissions or emissions as a variable are used respectively to make a comparison between synthetic and actual measurements to improve emission estimates. These methods do not function completely independently from the a-priori emissions that serve as input to the CTM. The usage of a CTM also requires a significant amount of data input next to satellite retrievals and the computational burden to run a CTM is usually high.

Other approaches do not necessarily rely on a CTM and estimate emissions based on satellite data and wind fields only. These methods rely on a plume fitting routine (Fioletov et al., 2011) or are mass balance based (Beirle et al., 2019). Avoidance of the use of a CTM comes at the expense of additional assumptions, e.g., steady-state situations and linear chemistry, but are much less computationally demanding. Hence, such methods were decided for as an initial application to estimate NO_x emissions over Germany.

The available data sources for satellite-based NO_x concentration measurements are discussed (3.2.5) and a suitable choice of data products was made based on the performed literature research and the selected methods. The individual emission estimation methods are cast into the aforementioned general framework emission tool and developed as an individual branch which will form a blueprint for future developments.

The NO₂ data products most extensively used in recent years in the scientific community are the Sentinel-5P NRTI NO₂ and Sentinel-5P OFFL NO₂ products which can be found on the TEMIS website (see section 3.2.3 for more details on these products). They are the official TROPOMI products and hence also accessible through the Copernicus data hub. They are continuously updated and available in the highest resolution currently achievable. The OFFL data has been checked for quality and in its current form becomes available a few days after acquisition, which is fast enough for the applications envisioned in this project.

To assure consistency, a logical choice of OMI data is a product available from the same data provider. For trend analysis the QA4ECV version 1.1 OFFLINE product is most suitable because it dates back to 2004. Hence the used products are the Sentinel-5P TROPOMI Tropospheric NO₂ 1-Orbit L2 5.5km x 3.5km V1 (S5P_L2_NO2__HiR) product (>2018) and the QA4ECV version OMI product for trends (2005 - 2019/2020).

A generic tool to assess emissions based on these selected datasets has been developed. This tool is cast into a framework that is extendable to other pollutants (NO_x, NH₃, SO₂, PM_{2.5}, etc) using a selection of methods presented in section 3.1.4. These selected methods (plume fitting routine (Fioletov *et al.*, 2011) or mass balance based (Beirle *et al.*, 2019)) have been applied to estimate NO_x and NH₃ emissions but can also be applied to specific other pollutants. The tool is designed to have global geographical coverage and temporal coverage that is dependent on the queried satellite(s) but for NO_x will span from 2004 till now.

Within the tool a user selects a region of interest, a period of interest and a pollutant of interest. Based on this choice, a list of available satellite products can be given, but generally it is not necessarily specified because these three inputs should be sufficient to determine the optimal choice of satellite product, which will normally be decided by the tool. Lastly a choice is made for the method to derive emissions of the selected pollutant within the region and time period of interest. Some methods will be more suitable for certain species and/or regions and hence an optimal choice will be suggested. This choice furthermore depends on the resolution and quality of the available satellite products.

A python based open-source tool is available through GitHub (<https://github.com/UBA-DE-Emissionsituation/space-emissions>). Currently scripts for the quantification of NO_x emissions from OMI and TROPOMI observations are developed, but extensions to other pollutants and satellites are possible within the framework. TROPOMI data is used to estimate NO_x emissions when this is available and OMI data when TROPOMI is not available (prior to October 2017).

The tool has functionality to download satellite data (both OMI from TEMIS and TROPOMI using the Sentinel API), ERA5 meteorological data using the CDS API (Climate Data Store) and derive emission estimates based on three different methods, called the naïve approach, Gaussian plume fitting routine (Fioletov *et al.*, 2017) and the divergence method (Beirle *et al.*, 2019, 2021).

When this tool is applied for various years a trend in emissions can be derived. The various functions can be run using exemplary Jupyter notebooks that are likewise available in the GitHub repository. These notebooks can be used to interactively launch parts of each module in a stepwise fashion and display intermediate results thereby giving an overview of the functionality of the tool.

The tool is subsequently applied to estimate emissions from TROPOMI data for 2019.

The estimation of emissions through direct integration of atmospheric concentrations over the vertical columns within a region (called the Naïve method) results in a NO_x emissions estimate from Germany of 1097.1 kton. The Gaussian plume-based fitting routine (Fioletov *et al.*, 2017)

led to an estimate of 1241.0 kton and a computation based on the divergence of the pollutant flux field (Beirle et al., 2019) resulted in an estimate of 1260.7 kton. These estimates are all within 15% of reported total emissions for (1108.82, NFR, Submission 2022 (europa.eu)).

To derive the trend in NO_x emissions within the past 15 years, the Fioletov method was applied to OMI observations between 2005 and 2019. This analysis shows an average decrease of around 25% between the 2005 and 2019 period, which is in agreement with the reduction reported in emission inventories (20% reduction between 2005-2007 and 2014-2016 period and 23% between 2005-2007 and 2017-2019 period found in the 2022 NFR reported totals based on fuel sold [Submission 2022]).

Zusammenfassung

Innerhalb der letzten 10 Jahre haben satellitengestützte Messungen von Luftschadstoffen an Qualität, Reichweite und Häufigkeit enorm zugenommen. Angesichts der Vielzahl geplanter Missionen mit Schwerpunkt Luftqualitätsüberwachung ist davon auszugehen, dass sich dieses Wachstum in den kommenden Jahren fortsetzen wird. Mit zunehmender Instrumentenempfindlichkeit, räumlicher und zeitlicher Auflösung sowie weiteren Datenprodukten, die sich auf die unteren Schichten der Atmosphäre konzentrieren, werden diese satellitengestützten Messungen immer attraktiver für die Überwachung der Luftqualität und Ableitung von Emissionsmengen.

Von den derzeit verfügbaren Satellitenprodukten haben troposphärische NO₂-Daten aufgrund ihrer guten Qualität im Vergleich zu Daten für andere Schadstoffe derzeit die meiste Anwendung in der Modellierung und Überwachung der Luftqualität gefunden. Die aktuellen Ansätze mit NO₂ können als Beispiele dienen, wie mit Instrumenten der neuesten Generation auf hoher räumlicher Skala auch weitere Schadstoffe, z. B. NH₃, beobachtet werden können. Die Qualität zusätzlicher Produkte und die Möglichkeiten zur Messung anderer Schadstoffkonzentrationen werden in den kommenden Jahren zunehmen.

Das Ziel dieses Projekts ist es, die Nutzung von NO₂-Satellitenbeobachtungen für die Abschätzung von NO_x (also NO + NO₂)-Emissionen in Deutschland auf nationaler Ebene zu demonstrieren. Dazu wird ein Softwarewerkzeug entwickelt, welches in der Lage ist, NO_x-Emissionen aus Satellitendaten für eine ausgewählte Region und einen ausgewählten Zeitraum zu quantifizieren. Dieses Tool ist so konzipiert, dass es in seiner Anwendung flexibel und auf andere Länder, Schadstoffe und Satelliteninstrumente erweiterbar ist. Das Softwaretool wird öffentlich zugänglich gemacht, um die internationale Zusammenarbeit und die Nachvollziehbarkeit der Ergebnisse zu fördern.

Begonnen wurde mit einer Literaturstudie zu verfügbaren Methoden und Anwendungen, die bestehende Ansätze zur Abschätzung von NO_x-Emissionen evaluiert. Die Ergebnisse dieser Literaturrecherche werden in Kapitel 3.1 diskutiert. Es wurde deutlich, dass die Verwendung weltraumgestützter Daten für die Berichterstattung und/oder Verifizierung von Emissionsinventaren auf Länderebene keine gängige Praxis ist. In der wissenschaftlichen Literatur wurden jedoch durchaus bereits Methoden entwickelt, die für die Zwecke dieses Projekt adaptierbar sind.

Die in der wissenschaftlichen Literatur beschriebenen Methoden wurden im Weiteren bewertet, um die geeignetsten Kandidaten für die Implementierung in diesem Projekt zu identifizieren. Einige Ansätze, wie der Ensemble-Kalman-Filter (EnKF) und adjointbasierte Methoden (z. B. 4D-var), stützen sich auf chemische Transportmodelle (CTMs) in Kombination mit Satellitenprodukten, um die wahrscheinliche Höhe von Emissionen zu bewerten. Diese Methoden funktionieren allerdings nicht unabhängig von den A-priori-Emissionen, die als Input für das CTM dienen. Zudem erfordert die Verwendung eines CTM erhebliche Datenmengen und eine hohe Rechenleistung, was für diese Projekt vermieden werden soll. Diese Methoden kamen daher hier nicht zum Einsatz.

Andere Ansätze beruhen nicht auf einem CTM und schätzen die Emissionen nur auf der Grundlage von Satellitendaten und Windfeldern. Diese Methoden beruhen auf einer Plume-Fitting-Routine (Fioletov et al., 2011) oder basieren auf Massenbilanzen (Beirle et al., 2019). Die Vermeidung der Verwendung von CTM resultiert in einer Reihe zusätzlicher, vereinfachender Annahmen, z. B. stationäre, atmosphärische Situationen und einer linearen Chemie, ist aber

deutlich weniger rechenintensiv. Im Projekt kommen solche Verfahren zur Abschätzung der NO_x-Emissionen über Deutschland zum Einsatz.

Als Eingabe für diese Methoden werden die verfügbaren Datenquellen für satellitengestützte NO_x-Konzentrationsmessungen diskutiert (Abschnitt 3.2.5) und eine geeignete Auswahl an Datenprodukten, basierend auf der durchgeführten Literaturrecherche und den ausgewählten Methoden getroffen. Die einzelnen Emissionsabschätzungsmethoden werden in das oben genannte allgemeine Softwarewerkzeug implementiert und entwickelt. Die Architektur der Software ist so gewählt, dass weitere Emissionsberechnungsverfahren später problemlos hinzufügbare sind.

Die NO₂-Datenprodukte, welche in den letzten Jahren am häufigsten verwendet wurden, sind die Produkte Sentinel-5P NRTI NO₂ und Sentinel-5P OFFL NO₂, die auf der TEMIS-Website zu finden sind (vergleiche Abschnitt 3.2.3). Dies sind auch die offiziellen TROPOMI-Produkte und daher zudem über den Copernicus-Datenhub zugänglich. Die Daten werden laufend aktualisiert und stehen in der höchsten derzeit erreichbaren Auflösung zur Verfügung. Die OFFL-Daten wurden qualitätsgeprüft und stehen in ihrer aktuellen Form wenige Tage nach der Erfassung zur Verfügung, was für die in diesem Projekt vorgesehene Anwendung völlig ausreichend ist.

Um die Konsistenz mit TROPOMI zu gewährleisten ist eine logische Auswahl von OMI-Daten ein Produkt, das von demselben Datenanbieter erhältlich ist. Für die Trendanalyse ist das Produkt QA4ECV Version 1.1 OFFLINE am besten geeignet, welches Daten zurück bis in das Jahr 2004 bietet. Vor diesem Hintergrund wurden für dieses Projekt die beiden Produkte Sentinel-5P TROPOMI Tropospheric NO₂ 1-Orbit L2 5.5km x 3.5km V1 (S5P_L2_NO2__HiR) (ab 2018) und die QA4ECV-Version OMI-Produkt für Trends (2005 - 2019/2020) ausgewählt.

Auf der Grundlage der ausgewählten Datensätze wurde ein generisches Softwarewerkzeug zur Abschätzung von Emissionsmengen entwickelt. Dieses Tool ist in ein Framework eingebettet, das auf andere Schadstoffe (NO_x, NH₃, SO₂, PM_{2.5} usw.) erweitert werden kann. Die ausgewählten Methoden „Plume-Fitting-Routine“ (Fioletov et al., 2011) oder „Massenbilanz“-basiert (Beirle et al., 2019) wurden zur Schätzung von NO_x- und NH₃-Emissionen verwendet, können aber perspektivisch auch auf andere Schadstoffe angewendet werden. Das Tool ist so konzipiert, dass es eine globale geografische Abdeckung erlaubt und bezüglich der zeitlichen Begrenzung lediglich von den verwendeten Satelliten und deren Start- bzw. Enddaten abhängt.

Bei der Verwendung des Werkzeugs wählt ein Benutzer eine Region, den gewünschten Zeitraum und den zu berechnenden Schadstoff aus. Basierend auf dieser Auswahl wird eine Liste verfügbarer Satellitenprodukte angeboten. Oft ergibt sich die optimale Wahl des Satellitenprodukts aber bereits aus den drei Eingaben, so dass durch das Werkzeug entschieden wird. Zuletzt wird eine Auswahl für die Methode getroffen, um die Emissionsmengen des ausgewählten Schadstoffs innerhalb der Region und des Zeitraums abzuleiten. Einige Methoden sind für bestimmte Schadstoffe und/oder Regionen besser geeignet, daher wird durch die Software eine optimale Auswahl vorgeschlagen. Diese Auswahl hängt zudem auch von der Auflösung und Qualität der verfügbaren Satellitenprodukte ab.

Im Ergebnis ist ein Python-basiertes Open-Source-Tool auf GitHub entstanden und unter <https://github.com/UBA-DE-Emissionssituation/space-emissions> abrufbar. Derzeit sind nur Skripte zur Quantifizierung von NO_x-Emissionen aus OMI- und TROPOMI-Beobachtungen vorhanden, Erweiterungen auf andere Schadstoffe und Instrumente sind aber möglich und erwünscht. Wie oben erläutert werden TROPOMI-Daten verwendet, wenn diese verfügbar sind, und OMI-Daten für Zeiträume zu denen TROPOMI noch nicht verfügbar war (vor Oktober 2017).

Das Tool verfügt über Funktionen zum Herunterladen von Satellitendaten (sowohl OMI von TEMIS als auch TROPOMI unter Verwendung der Sentinel-API), ERA5-Wetterdaten unter Verwendung der CDS-API (Climate Data Store) und zum Ableiten von Emissionsschätzungen auf der Grundlage von drei oben genannten Methoden, dem „naiven“ Ansatz, der „Gaussian Plume“-Anpassungsroutine (Fioletov et al., 2017) und der Divergenzmethode (Beirle et al., 2019, 2021).

Mittels der Anwendung des Werkzeugs über mehrere Jahre lässt sich auch der langjährige Trend der Emissionen ableiten. Die verschiedenen Funktionen der Software können über beispielhafte Jupyter-Notebooks getestet werden, die ebenfalls im GitHub-Repository verfügbar sind. Die Notebooks erläutern die Nutzung des Werkzeugs und zeigen wie schrittweise Teile jedes Moduls interaktiv zu starten sind und welche Zwischenergebnisse erzeugt werden.

Das Tool wird anschließend zur Schätzung der NO_x-Emissionen in Deutschland aus TROPOMI-Daten für das Jahr 2019 angewendet.

Die Schätzung der Emissionen durch direkte Addition der atmosphärischen Konzentrationen über die vertikalen Säulen innerhalb der Region (sogenannte „naive“ Methode) ergibt dabei eine Schätzung der NO_x-Emissionen aus Deutschland von 1097,1 kt für 2019. Die Anpassungsroutine auf Basis der „Gaussian Plumes“ (Fioletov et al., 2017) führte zu einer Schätzung von 1241,0 kt und eine Berechnung basierend auf der Divergenz des Schadstoffflussfeldes (Beirle et al., 2019) ergab 1260,7 kt. Alle diese Schätzungen liegen innerhalb eines 15%-Intervalls um die Inventar-Gesamtemissionen für 2019 von 1108,82kt (Submission 2022 (europa.eu)).

Um schließlich den Trend der NO_x-Emissionen für die letzten 15 Jahre abzuleiten, wurde die Fioletov-Methode auf OMI-Beobachtungen zwischen 2005 und 2019 angewendet. Diese Analyse zeigt einen Rückgang von etwa 25% in diesem Zeitraum, was gut mit der Reduktion übereinstimmt, die die Emissionsinventare verzeichnen (20% Verringerung zwischen 2005-2007 und 2014-2016 und 23% zwischen 2005-2007 und 2017-2019, vergleiche die NFR-Gesamtemissionen aus der Submission 2022).

1 Background

1.1 Introduction

Within the past decade the data availability of satellite-based air pollutant measurements has increased tremendously. The number of already planned missions with a focus on air quality shows this growth can be expected to continue in the forthcoming years. With an increase in instrument sensitivity, spatial and temporal resolution, and more products focusing on the lower layers of the atmosphere, these satellite-based measurements are becoming more and more attractive for air quality monitoring and emission studies.

Out of the currently available satellite products, tropospheric NO₂ data is one of the most used products in air quality applications. The NO₂ datasets are most commonly used for trend analysis but also for satellite product based emission estimates at both large point source and regional scale. The current standard practices with NO_x can function as examples for species that only the latest generation instruments were able to observe at high spatial scale such as NH₃.

The background to the project that is the foundation for the realization of this report is given in chapter 1. In chapter 2 the strategy on how this tool came into existence is explained. It all starts with an extensive literature research into various methods to derive emissions from satellite retrievals. From the results of this literature research, various viable approaches were identified that are described in chapter 3, from which two methods were selected to be developed further. Chapter 3 also includes the tool-development and -implementation. Details on the resulting emission estimates are elaborated and discussed.

1.2 Aim of the project

The overall goal of this project was to demonstrate the use of satellite observations of NO₂ for the verification of reported NO_x (i.e., NO + NO₂) emissions in Germany at a national level and to show how this approach can be extended to other trace gases and in more detail. The chemical lifetimes of NO₂ and NO are very short, while cycling between both states, therefore emissions are often reported in total NO_x. The atmospheric ratio NO_x:NO₂ is typically around 1.32 (Seinfeld, 1989; Beirle et al., 2019).

The following specific questions have been answered by the project:

- ▶ Which method for inverting emissions and/or deriving emission trends from the satellite products is most appropriate for meeting the needs of UBA in the verification of the reported NO_x emission inventory?
- ▶ To what geographical scale is the method able to provide NO_x emission estimates or trends in these emissions? The focus of the project was to the verification of national emissions.
- ▶ Is the method transferable to NH₃ and other pollutants (e.g. CH₄, CO₂, SO₂), and what possible additional methods are required for this translation?
- ▶ Is satellite data available to perform such analysis, and from whom?
- ▶ Can these methods be integrated in an easy to use toolchain for yearly repeated use by UBA, taking into account factors like: accuracy of each method, ease of repeated use.
- ▶ Is it possible to derive information for different source sectors?
- ▶ What are the uncertainties associated with the calculation of emissions estimates from satellite data?

The answers to these questions are used to create a software toolchain that is designed to produce estimates of NO_x emissions from satellite data, for a particular selected region and time period.

The developed toolchain will be tested for Germany to assess:

- ▶ The estimates of the NO_x emissions based on the identified satellite data country scale for the year of 2019, and how do they compare to the emissions submitted for the 2022 Informative Inventory Report (IIR) and the emission trend for the period of 2005-2019 (at NUTS 0).
- ▶ The structural differences between the satellite derived estimates and the official reported inventory data and how to account for these difference in the comparison.

The UBA envisages to make the tooling developed in this project publicly available (under properly selected licenses) to assist other countries in the independent verification of their inventories. The modular software design will allow country and or satellite specific adaptations to accommodate future improvements in resolution and observations for other species of air pollutants).

2 Approach

2.1 Introduction

The project started with a literature review, to identify suitable methods for deriving German national NO_x emissions from satellite observed concentrations. In this literature review several viable options were found. In this project, we looked for relatively simple methods which do not require inputs from a chemical transport model (CTM).

Based on the selection of the best applicable method a suitable source where satellite data can be collected was identified. For the chosen satellite product a processing pipeline (verification tool) was designed that produces an emission estimate for a given region (Germany) and specified time period.

The processing pipeline in which this method was implemented was designed to allow generalizations to other methods, regions and pollutants. It was set-up in a way to allow for future extensions without fundamental alterations to the computational framework itself and to enable easy collaboration with other interested parties.

In the next paragraphs the methodological structure of this study is presented and will further elaborate on each of the steps that led to the final choices for most suitable method and best applicable data sources and from there the development of the verification tool.

2.2 Methodological structure

2.2.1 Literature research

The results from the literature research are discussed in detail in chapter 3.1. There, several existing applications for the estimation and verification of emissions using satellite observations are explained in detail. The research includes scientific publications as well as current and past projects on this topic. The main focus was on publications and projects about satellite based emission estimates for NO_x and NH₃ species, mostly at the regional scale but other applications are also included.

A variety of applications exist that use various techniques to estimate emissions for a wide range of pollutants (NO₂, NH₃, SO₂, etc). The methods vary widely in terms of complexity and the computational burden involved.

Four main categories of approaches were identified:

1. Mass balance based methods (for more details see 3.1.4.1)

This method category relies on a direct estimation of emissions from satellite data. No model or fitting routines are involved in the simplest approaches and the estimate is based on the concentration fields (pollutant density seen by the satellite) or concentration fluxes (by combining the concentrations with wind fields). This simplified approach ignores many aspects of atmospheric chemistry and transport but has still shown to produce accurate emission estimates under certain conditions. Extended versions of this method include a model to help with the translation of observed satellite columns to estimated emissions.

2. Plume fitting based methods (for more details see 3.1.4.2)

These methods rely on a direct fit of satellite data. No chemical transport model and underlying emission inventory are involved, and the estimate is based on measured local

concentration fluxes. This fitting approach assumes that a (fixed) exponential lifetime of a species accurately describes the underlying chemistry. From its most basic form several adjustments can be made to add extra detail, for example improving the assumed lifetimes by using model-based estimates.

3. Kalman filter-based methods (for more details see 3.1.4.3)

These methods rely on a chemical transport model and its underlying emission inventory to estimate emission based on a comparison between modelled and measured concentration fields. An ensemble of models outputs with additively (for example using a method called DECSO (Mijling and Van Der A, 2012)) or multiplicatively (e.g. the Ensemble Kalman Filter) varied emissions is used to arrive at a best emission estimate.

4. Adjoint based methods (for more details see 3.1.4.4)

In this type of method an inverse version of a CTM (or an approximation thereof) is used to derive the emissions given a model output. Models are used to derive synthetic (satellite) measurements from computed concentrations fields to allow fitting of corresponding actual measurements.

A method of the second category that fits satellite data with Gaussian plumes (Fioletov et al., 2011) was deemed to be the most suitable choice for estimating NO_x emissions based on its relative simplicity, low computational cost, maturity and reported performance. Furthermore, it can act independently from emission inventories and does not rely on a CTM. The mass balance type approaches generally have lower computation demands but are more susceptible to noise induced errors because numerical derivatives have to be computed.

2.2.2 Data sources and Compatibility issues

In recent years more and more satellite data have become available and products based on satellite measurements are available from several data providers at a timely to near real time basis. A categorization of satellite products in various levels can be made based on the amount of processing that went into producing them. Level 2 TROPOMI NO₂ products were identified as the most suitable choice for the selected method. The TROPOMI instrument has the highest resolution currently available for NO₂.

The choice for a level 2 product allows control over the grid size and resolution but does not require translation from a spectrum (L0-L1 level products) into an observed atmospheric concentration, which is a computationally expensive task and in itself a field of research.

The most extensive validation reports and scientific work were performed on Sentinel-5P NRTI NO₂ and Sentinel-5P OFFL NO₂ products which can be found on the TEMIS website (see section 3.2.3 for more details on these products) and are also accessible through the Copernicus data hub (<https://scihub.copernicus.eu/>). Most importantly it is the official TROPOMI product and is continuously updated and improved.

With this choice for method and data product, there are a number of limitations and compatibility issues that have to be taken into account. These are:

- a) Spatial resolution
- b) Instrument sensitivity

- c) Uncertainty in satellite products
- d) Bias in satellite products
- e) Temporal resolution of satellite products and temporal variability in emissions
- f) Unavailability of data (for example due to clouds)
- g) Gaps in a-priori emission data

These compatibility issues are discussed in more detail in Section 3.2 and more specific in paragraphs 3.2.6 and 3.3.2, but we summarize how these can be mitigated for the application in this project (Gaussian plume-based NO_x emission estimation) in the next section on satellite data processing and method development.

2.2.3 Satellite data processing and method development

A tool to assess emissions based on satellite images is to be developed and is designed to be broadly applicable to assess emissions of various pollutants (NO_x, NH₃, SO₂, PM_{2.5}, etc) based on a choice of various methods. The tool is designed to have global coverage and to be extendable beyond what has been developed in this work.

Within the tool a user will be able to select a pollutant, period, and region of interest within the boundaries of available satellite products. These three inputs are sufficient to determine the optimal choice of satellite product. Lastly, a choice must be made on which method is used to derive emissions.

One particular branch (with a specific pollutant, satellite product and method) was fully developed within this project, but the design of the tool enables generalizations beyond this stream. The estimation of the German national total NO₂ emissions from TROPOMI images using the plume-based method was implemented within this project.

The tool hence starts with the TROPOMI product download as part of a bigger download tool that will be able to download data products from various satellites and sources. After the download the longitudes, latitudes and times of the retrievals are matched with wind fields collected from the ECMWF data storage at the Copernicus Climate Change Service (C3S) Climate Data Store (CDS, <https://cds.climate.copernicus.eu/>). This additional data stream is necessary for the Gaussian plume-based method but will also be required for other methods mentioned in the previous chapter. After additional pre-processing on the collected and merged data, like re-gridding and noise reduction, the data is fitted with a Gaussian plume model and emission estimates are produced and presented to the user.

The aforementioned compatibility issues are dealt with within the developed stream of the tool. The following approaches were implemented to deal with these compatibility issues:

- Spatial resolution

Coarse spatial resolutions of the satellite instrument can create a smearing effect in the estimated emissions. At the borders of regions of interest the resolution of the final emission fields can cause a partial overlap between multiple regions. Emissions for such regions need to be intelligently split between both sides of the border. In most cases this should be viable based on the dominant sources on either side of the border, but for regions with several overlapping sources, there can be remaining uncertainty due to attribution errors/uncertainty. In general this issue will have limited influence on results since regions are often much bigger than satellite footprints and will be mitigated by a minimal allowed size of the selected region.

- Instrument sensitivity

The sensitivity of the instrument determines the lowest observable concentration. Limited sensitivity of the instrument will directly lead to a lower overall fraction of emission totals that can be derived. Based on the (sometimes known) sensitivity and number of days and sources below the detection threshold the effect of such missed emissions can be derived. A potential drawback is that initial knowledge on the actual emissions and the instrument sensitivity is required. In Germany this effect is expected to be small because of a dominance of emissions from large sources. Applications to less industrialized regions could potentially miss a significant amount of the initial emissions, the fraction of which will be estimated by using the current emission inventories and expected instrument limits.

- Uncertainty in satellite products

Limitations to the precision of the satellite product will result in noisiness of the data which makes it more difficult to fit measurements with Gaussian plumes. The first strategy to reduce noise would be a reduction in resolution through spatial averaging and/or filtering if uncertainty introduces artefacts or complications. Secondly, temporal averaging can be used to reduce uncertainty. These strategies come at the cost of reduced spatial and temporal resolution respectively.

- Bias in satellite product

A bias in satellite products can result in a fixed or concentration dependent over or underestimation of measured pollutant concentrations. In the Gaussian plume-based method a few terms can be added to the linear system, for example a polynomial, to fit a potential bias (Fioletov et al., 2017). A large part of the bias in the TROPOMI- NO₂ product is induced by the coarse model used to calculate the length of the mean light path in the atmosphere which is a required input to produce an L2 product. Precomputation of this parameter at a higher resolution with a CTM (for example LOTOS-EUROS) can significantly reduce the bias. The bias corrections can be based on literature whenever this is available if CTMs have to be avoided. The polynomial solution is initially used, and the latter two options can be applied if shortcomings in the bias mitigation strategy remain.

- Temporal resolution of satellite product and temporal variability in emissions

The plume-based method assumes a steady state at the time of the overpass, which takes place in the afternoon (between 12:30 and 13:30). Estimates therefore need either an a-priori correction or posterior adjustment (Dammers et al., 2019) to account for temporal variations to the seasonal and diurnal cycles. Time profiles are required to make this posterior adjustment and translate the emissions at time of satellite overpass to annual totals.

Incidental emissions can significantly increase the atmospheric concentrations, for example contribution from plumes of wildfires can create large perturbations in the concentration field over a short period and will result in an overestimation of long-term anthropogenic emissions. The simplest mitigation strategy is the exclusion of periods in which the incidents occur, or adjust for it posteriori, by removing their plumes (when identifiable). This can be achieved by taking an additional data streams into account from for example wildfire monitoring services or by creating wildfire recognition functionality (based on time profiles, CO products, characteristic albedo changes or additional infrared observations).

- Missing data due to e.g., clouds

Missing data due to for example clouds and instrument outages can create gaps in the observation record. An adjustment to the final emission totals is needed using a similar approach as for mitigating the temporal variability of emissions. The times of the used retrievals enable the translation to annual total emissions at a later stage.

- Gaps in a-priori emission data

Missing emission locations in inventories do not have any effect on the Gaussian-plume methods because it operates independently from a-priori emissions fields. This is a strength compared to methods relying on CTMs. Misrepresentations of emission time profiles will introduce errors when a translation to annual totals are made. Weekly, monthly or yearly time profiles can be assessed with the Gaussian plume-based method and misrepresentations therein can be detected. Misrepresentations in daily time profiles are more difficult to mitigate because of the approximately fixed hour of the day of the overpass.

All above mentioned aspects are further elaborated in paragraph 3.3.

2.2.4 Development of a Verification Tool and its implementation

The insights gained from the work in the aforementioned paragraphs were the starting point for the tool development as presented in Section 3 of this report. In Paragraph 3.3 and 3.4. the development and the use of the tool is further elaborated. In section 3.5 the results of the implementation of the tool for the German inventory are presented.

2.2.5 Conclusion

Section 4 of this report draws conclusion of the preformed work and gives an outlook on the future development related to the use of satellite observations in emission estimates.

3 Results

3.1 Literature research

3.1.1 Satellite observations of atmospheric composition

In the early 1990s the first satellite products with a focus on atmospheric composition became available. Since then further scientific developments have brought a wealth of satellite products into the air quality market. Examples of widely known and used instruments are the GOME, SCIAMACHY and IASI on European (ESA and EUMETSAT) platforms, OMI, MOPITT, CrIS and MODIS on American (NASA and NOAA) platforms and the GOSAT instruments on Japanese (JAXA) platforms. In October 2018 the newest ESA earth observation mission Sentinel-5P has been successfully launched containing the TROPOMI instrument.

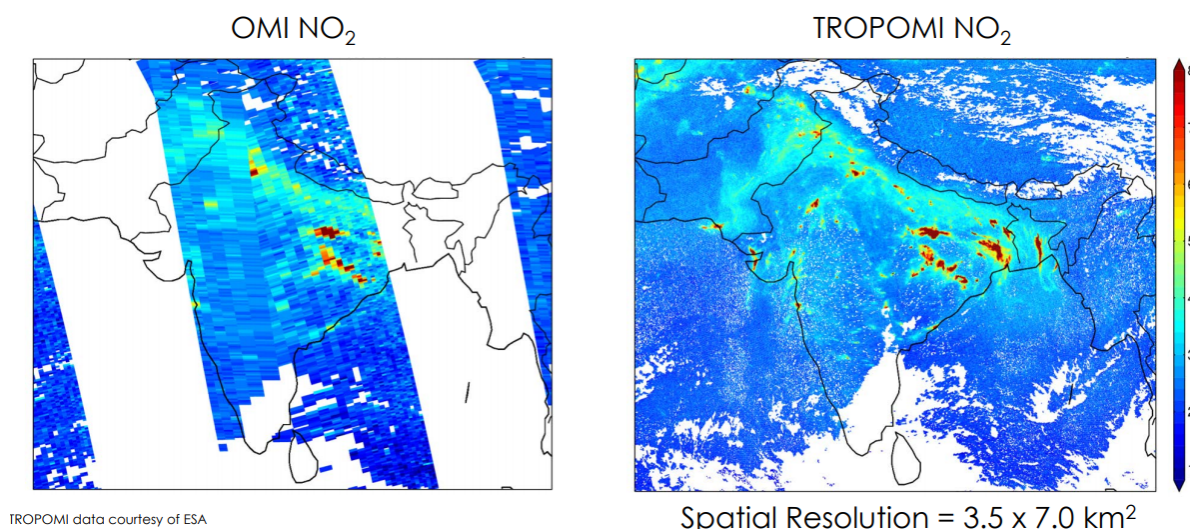
The atmospheric composition products that are currently available from satellite instruments encompass, among others: Nitrogen dioxide (NO_2), Ozone (O_3), Carbon Monoxide (CO), Aerosol Optical Depth (AOD), Dust, Ammonia (NH_3), Sulphur Dioxide (SO_2), specific Volatile Organic Compounds (VOCs), i.e. Formaldehyde (HCHO) and Glyoxal (CHCHO), Methane (CH_4) and carbon dioxide (CO_2), with more species becoming available with improving instrument capabilities.

The bulk of the satellite instruments that are relevant for air pollution are in so-called Lower-Earth Orbiting (LEO) orbits, circling the Earth and thereby providing global coverage within one or multiple days. The advantage of global coverage is then counteracted by the temporal resolution of at most once or twice per day per location. Alternatively, some products are now also becoming available from so-called Geostationary (GEO) satellites, which provide a high temporal resolution for a selected region of the Earth (usually covering only one continent). The planned GEMS (launched), TEMPO and Sentinel 4 missions are examples of such geostationary satellites producing atmospheric measurements at an hourly temporal resolution.

Satellite instruments detect atmospheric species by measuring the radiation emitted or reflected by the earth to retrieve information on the atmospheric composition. The sensitivity of the instrument to different layers in the atmosphere determines the amount of information that the instrument can provide about the vertical distribution of the atmospheric composition. In most cases it is only possible to retrieve vertically integrated information for the total or partial column of the atmosphere observed by the instrument. The absence of information on the vertical distribution of pollutants requires extra information from other sources to allow the conversion of column to surface concentrations. One example of this is the combination of the satellite data, including information on the sensitivity at different altitudes, with atmospheric chemistry models.

In recent years many developments took place that brought the satellite products closer to the needs of the users in the air quality field. Products with a focus on the lower layers of the atmosphere (such as lower tropospheric columns) try to close the gap between the observed quantities and the quantities of interest for the users. Another important example is the increase in spatial resolution of the satellite instruments. Images from the TROPOMI instrument with a spatial resolution of $3.5 \times 7 \text{ km}^2$ (see Figure 1 and since recently $3.5 \times 5.5 \text{ km}^2$) illustrate the potential to distinguish between different source regions within a country and even individual sources. Improvements to resolution and intelligent targeting capabilities, also benefit the amount of useable data through an increase of cloud free pixels.

Figure 1: Example of improved resolution of TROPOMI versus OMI tropospheric NO₂ data product over India.



Source: https://appliedsciences.nasa.gov/sites/default/files/NO2_Session_1_final.pdf

3.1.2 NO₂ satellite products

Satellite based measurements of NO₂ have been available since the late nineties (from the Global Ozone Monitoring Experiment, GOME). Over the last two decades the overall quality and resolution of the observations has drastically improved. For air-quality studies tropospheric NO₂ observations is one of the most relevant satellite products due to its negative health impacts and because it is a major precursor of several secondary air pollutants.

The GOME instrument was one of the first to provide a long timeseries that could be used for trend analysis of tropospheric NO₂ columns. The spatial resolution of these GOME observations was 40 by 320 km, except for specific days with smaller swath at 40 x 40 km resolution (reducing spatial coverage). Since then newer instruments have been developed with increasing spatial resolution: SCIAMACHY with 30 x 60 km, GOME-2 with 40 x 40 km, OMI with 13 x 24 km resolution and most recently TROPOMI with a 7 by 3.5 km resolution. In the near future the geostationary Sentinel 4 instrument will provide observations at a similar resolution as TROPOMI for the European region, as well as a high (hourly) temporal resolution. The hourly observations will, for the first time, allow the monitoring of the (daytime) NO₂ diurnal cycle.

The sensitivity of satellite instruments to boundary layer concentrations is strongly dependent on molecular scattering (in the UV) and thermal radiation (in the thermal infrared region). In the case of NO₂ it emits a strong signal in both the free troposphere/stratosphere and in the boundary layer (with more than two-thirds of the total NO₂ located in the boundary layer over heavily polluted regions). The relation between tropospheric column and surface concentrations is heavily influenced by the local sources due to the short lifetime of NO₂ and the dominance of the anthropogenic sources at ground level.

3.1.3 NH₃ satellite products

About twelve years ago, the first methodology was developed to retrieve ammonia distributions by use of a satellite instrument for the Tropospheric Emission Spectrometer (TES) (Beer *et al.*, 2008). A year later the Infrared Atmospheric Sounding Interferometer (IASI) provided the first global picture on the ammonia distribution across the world (Clarisse *et al.*, 2009; Coheur *et al.*, 2009). Since then the IASI satellite (van Damme, Clarisse, *et al.*, 2014; van Damme *et al.*, 2015;

Whitburn *et al.*, 2015), TES (Beer *et al.*, 2008; Shephard *et al.*, 2015), the Atmospheric Infrared Sounder (AIRS) (Warner *et al.*, 2016), the Cross-track Infrared Sounder (CrIS) (Shephard and Cady-Pereira, 2015; Shephard *et al.*, 2015, 2020) and the Greenhouse gases observing satellite (GOSAT) (Someya *et al.*, 2020) have provided bi-daily NH_3 distributions. IASI at ~ 12 km resolution and CrIS at ~ 14 km resolution, currently show the most promising results. IASI global retrievals are available on the web. CrIS, with a spectral resolution similar to IASI, and a 4 times lower spectral noise (~ 0.04 K at 280 K) in the ammonia spectral region, has the potential to detect smaller NH_3 concentrations than is currently possible with IASI (Shephard *et al.*, 2015, 2020), with global retrievals available on request. TES and GOSAT both have a less dense spatial coverage than the scanning satellites (IASI, CrIS), but have a higher spectral resolution, which are sampled at regular intervals. This provides a very sparse coverage of the globe. While the sensitivity is a big advantage of TES and GOSAT, the lack of coverage hampers their use in applications. AIRS currently has one of the longest temporal records, and while a recent study by Warner *et al.* (2017) reported on global trends, the relatively low sensitivity of the instrument and lack of open access data holds back further applications.

The biggest challenges in NH_3 observations are the strong spatial gradients and the fact that much of the NH_3 is close to the surface, which makes it difficult to detect from space. Under conditions with significant thermal contrast near Earth's surface and a large enough signal-to-noise ratio, satellite instruments can be sensitive to boundary-layer NH_3 concentrations (Clarisse *et al.*, 2010). The shape of the profiles retrieved by these instruments at the current signal-to-noise ratios and spectral resolutions are strongly influenced by the retrieval of a priori information, and the retrievals typically contain less than or around one degree of freedom for the signal. Due to the low signal to noise ratio of the current instruments the detection of ammonia outside the tropical regions is mostly bound to the spring and summer seasons with limited results for the late autumn and winter seasons. This can hamper the monitoring of ammonia, e.g., in Europe, as major emissions sometimes take place in the early spring. Compared to IASI, the CrIS instrument has improved sensitivity. However, their relatively large footprint will remain unchanged. From 2022 onwards geostationary satellite instruments such as IRS aboard MTG are expected. This instrument will enable the study of diurnal cycles of ammonia, but due to the increased distance to earth the signal to noise ratio and associated accuracy will be limited and is expected to reach IASI levels of performance for only a fraction of the scenes. Another challenge is validation of the products as a lack of dense and precise measurement networks exists. Globally, there are only a few measurement networks, with most consisting of only a small number (>5) of locations, most without a consistent measurement record and almost none providing any information on vertical profiles (Erisman *et al.*, 1988; Dammers *et al.*, 2017; Tevlin *et al.*, 2017). Furthermore, most measurements have coarse temporal resolutions. The most common instruments, the passive samplers, at best give bi-weekly concentrations for longer periods of time analysis, which all together make them suboptimal for validation (Shephard *et al.*, 2015; van Damme *et al.*, 2015; Sun *et al.*, 2017). A more recent approach is the use of Fourier transform infrared instruments which observe the full profile in the atmosphere (Dammers *et al.*, 2015) which enables a more representative validation of the satellite products. A drawback is that most of the current FTIR sites worldwide are in regions with low NH_3 concentrations, with only the station in Bremen, Germany being representative for a high NH_3 emission region.

3.1.4 Methods for satellite-based emission estimates

Traditionally emission inventories are constructed through a bottom-up methodology, i.e. by combination of two sets of data: activity data (such as the energy consumed, the industrial production or the number of animals in an agricultural area) and emission factors (the amount

of emission per unit of activity). Emission factors consider information on the technology level such as the installation of abatement measures in specific power or chemical plants. In Europe each country compiles its own emission inventory as required by the EU (National Emission Ceilings Directive) and the convention on Long-Range Transboundary Air Pollution (LRTAP). Each country is obliged to annually report its emissions in a prescribed format (annual emissions by sector and by pollutant), mostly for reporting compliance with and progress towards emission reduction commitments.

The derivation of emissions with satellite observations (also often referred to as top-down emissions but to avoid confusion here will be referred to as satellite derived emissions) is highly relevant as up-to-date emission information is often lacking. Emission inventories based on official reported emissions usually only become available after a delay of a few years and, depending on the species, can have high uncertainties associated with them. Emissions in some regions can show strong increases or decreases with each yearly iteration of the inventory. The availability of multiple years of data from single satellite instruments (or multiple similar instruments) offers the opportunity to create a consistent trend estimate of pollutant emissions. Furthermore it is hard to keep someone responsible for non-anthropogenic emissions and reporting thereof, which is reflected in the quality of information on these types of sources. Here again satellite derived emissions can be a solution.

Satellite observations have been used to monitor different types of emission sources: anthropogenic point sources (powerplants), natural point sources (volcanoes, lightning), anthropogenic area sources (energy extraction, shipping emissions, megacities) and natural area sources (biomass burning, soils, biogenic). Streets *et al.* (2013) provided an overview of capabilities in this field of work.

In a previous project for UBA (FKZ 3717 51 251 0), TNO identified the inversion of NO_x and NH₃ emissions as two of the most promising air quality management applications exploiting satellite data. This conclusion was based on a thorough literature study and expert consultations. So far, emission inversions for NO₂ have shown the most success for anthropogenic sources. The satellite derived relative emission trends for NO₂ on continental scales tend to be consistent to trends in emission inventories. On a more local urban to point source scale the uncertainties tend to increase and derivation of city or point source emissions have larger uncertainties for sources not isolated from other large sources or situations where the contrast between the polluted city centre and the background is insufficient (i.e. low wind speeds). The derived absolute emissions (except for point source estimates) currently mostly provide total emission estimates without any information on the distribution over different source sectors. This further complicates the usage of the estimates for improvement of emission inventories, which, in-turn, is further hampered by a lack of interaction with the emission community.

A wide variety of techniques are used within this type of application from simpler approaches such as mass balance techniques to sophisticated and computationally demanding techniques such as 4D variational or ensemble Kalman filter data assimilation. In the next four subchapters/paragraphs we give an overview of the commonly used methods found in literature. The quality of the inverted emissions depends on the quality of the applied model/method. Errors in the model are directly transferred into errors in the retrieved emissions. There have been only a few studies comparing different approaches (Arellano and Hess, 2006; de Foy *et al.*, 2014; Cooper *et al.*, 2017) and those studies will be referenced where applicable.

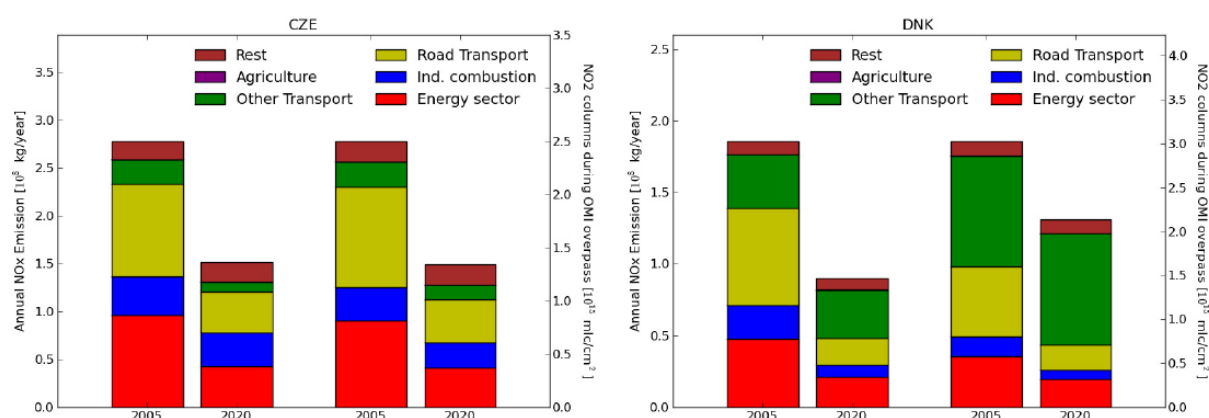
3.1.4.1 Mass balance

Introduction

Naively, one might assume that the total vertical column densities (VCD) of a particular species as estimated from satellite retrievals could be integrated, over a particular area of interest and time period, to give an estimate of the emissions in that area. This very simplified approach ignores several important aspects that contribute to what a satellite measures. For example transport to and from the area of interest is ignored, background concentrations are assumed to be negligible and chemical losses are not taken into account. The error introduced by these simplifications is dependent on, among other things, the size of the area of interest, the species under investigation and the meteorological conditions at the time of the retrievals. Nonetheless, this naïve approach might give reasonable estimates under certain conditions and can be seen as a first step towards a mass balance approach.

An illustration of the applicability of such a naïve approach is provided in (Schaap et al., 2013). In this paper the authors assessed whether emission changes were directly translated into tropospheric OMI- NO₂ changes. The results indicated that for many countries, this was the case but for medium- and small-sized coastal countries such as Denmark (see Figure 2), the contribution of the increasing shipping emissions in adjacent sea areas masked a significant part of national emission reductions.

Figure 2: Comparison of emission total, as well as the modelled OMI-NO₂ column in 2005 and 2020 for the Czech Republic (CZE) (left) and Denmark (DNK) (right). Both the emissions (left two) and modelled (right two) columns are separated into the major sectors.



Source: Schaap *et al.*, 2013)

If one takes into account all aspects that cause the creation and destruction of a species within a particular volume V , one could write a mass balance for this volume:

$$\frac{\partial m}{\partial t} = \sum sources + \sum sinks = Fl_{in} - Fl_{out} + E + P - L - D_{dep}. \quad (1)$$

In this equation $\frac{\partial m}{\partial t}$ described the temporal mass change of the species of interest within the volume V . This is equal to the difference between sources and sinks within that volume.

Fl_{in} and Fl_{out} describe the flow into and out of the volume respectively. E describes the emissions within V (anthropogenic or otherwise), P describes the chemical production, L respectively describe the losses due to chemistry and deposition. A similar relation can be derived for the concentration of a particular species by simply dividing equation 1 by a certain volume.

The very naïve approach described in the introduction of this section assumes that the emissions in a volume can be estimated by the total measured mass in this volume.

$$\int_V dv m \approx \int_V dv \int_t dt E \quad (2)$$

With this approach it is crucial to consider a loss term as well. For example, for NO_x, losses and production due to interactions with ozone. These interactions cause a steady state in the presence of solar radiation, known as the Leighton relationship. Extended versions of the naïve approach consider more terms of equation 1, which are used to assess emission from satellite data with a rather simple method.

Applications

The earliest studies typically focussed on large isolated point sources such as urban centres, large localized fires, energy plants and industrial complexes. Beirle et al., (2003) were one of the first to study signatures from point like sources using NO₂ satellite data. They used statistical analyses on GOME tropospheric NO₂ VCDs to identify weekly cycles for different regions and cities in the world, with the work mostly limited by the low spatial resolution of the GOME pixels. It was shown that for point sources dominated by the emission term, time profiles can be deduced purely from satellite data.

This was followed up by a study by Lamsal et al. (2014) which were one of the first to compare derived NO_x emissions trends with those in emission inventories. In this study a global atmospheric chemistry model is used (GEOS-Chem) to estimate the relation between emissions and VCD values. For a global estimate Fl_{in} and Fl_{out} in equation 1 are zero and the effect of D_{dep} , P and L are computed by the model allowing estimation of the emissions E from the measured mass distributions. This is a hybrid approach using a synergy between satellite data and chemical transport models (CTMs).

Only a few studies have also targeted line like sources such as shipping. Shipping emissions typically have large uncertainties and are often quite isolated which facilitates their inversion without interference from other sources. Vinken et al. (2014) used a synergetic approach using tropospheric NO₂ columns from OMI and the global GEOS-Chem model to produce a top-down ship NO_x emission inventory for the Baltic Sea, the North Sea, the Bay of Biscay and the Mediterranean Sea for 2005-2006 based on a mass-balance approach to constrain the ship emissions while accounting for nonlinear sensitivities to changing emissions in both model and

satellite retrieval. The results reported by Vinken et al., (2014) provided a first indication for errors in both the quantity as well as the location of the models a-priori emissions.

Estimates of NH₃ have only started to emerge in recent years, as satellites capable of observing NH₃ were only introduced recently. The first comparison studies of satellite NH₃ observations to surface observations and model simulations showed underestimations of the modelled NH₃ concentration levels, pointing to underestimated regional and national emissions (Clarisse *et al.*, 2009; Shephard *et al.*, 2011; Heald *et al.*, 2012; Nowak *et al.*, 2012; Zhu *et al.*, 2013; van Damme, Wichink Kruit, *et al.*, 2014; Schiferl *et al.*, 2016; Zondlo *et al.*, 2016; Lonsdale *et al.*, 2017).

Since the initial model comparisons, the first studies with direct emission estimates have recently been reported. These studies were initially mostly mass based inversions for large point sources (Van Damme *et al.*, 2018; Clarisse *et al.*, 2019) and at a regional level (Van Damme *et al.*, 2018).

The studies mentioned above rely on models to estimate the effect of terms in equation 1 that cannot be derived (easily) from satellite retrievals. A 'purely' satellite based approach to derive NO_x emissions from point sources was presented by Beirle et al. in 2019 (Beirle *et al.*, 2019). Here the Gauss' law:

The sum of all sources of the field in a region (with sinks regarded as negative sources) gives the net flux out of the region,

is used to estimate emission sources. The net flow into a volume, $Fl_{in} - Fl_{out}$, is computed from the divergence of the flux of a species. To compute this flux, meteorological data, i.e. wind field, is required. The following description is used to estimate emissions.

$$D = E - S \rightarrow E = \frac{rV}{\tau} + \nabla(rV\vec{w}) \quad (3)$$

Here D is the divergence of the flux field $\vec{F} = rV\vec{w}$, which is the product of the ratio r of NO_x and NO₂, the VCD V and the wind field \vec{w} . S is the sink term due to chemical removal and deposition which is assumed to be proportional to the concentration of the species, i.e. $\frac{rV}{\tau}$.

This method was shown to allow estimation of NO_x emissions from large point sources in South Africa and Germany, with a detection limit down to 0.03 kg/s for ideal conditions.

Estimation of SO₂ emissions using mass balance based methods are possible (Beirle et al., 2014) despite the fact that satellite products are less developed/accurate than for example for NO₂. The methods described in this section have not been used to estimate PM2.5 emissions for multiple reasons. Next to the difficulty of deriving PM2.5 concentrations from satellite retrievals the most fundamental reason is the underlying complicated chemistry (dominated by secondary production rather than primary emission) that makes it impossible to derive emissions from observed concentrations.

Uncertainty

Mass balance techniques assume a direct relation between surface emissions and the observed total column density. By using a large enough domain, transport and diffusion can typically be ignored for short lived species. Remaining is the emission of the species in question which is balanced by the loss of the species to a set of sinks, typically chemical conversion and deposition. The methods can be simple, using an assumed fixed lifetime, or more complex, using iteratively finite mass balance (iteratively running a chemistry transport model until the model matches the observations). Cooper et al. (2017) showed that an iterative finite mass balance approach for NO₂ provides similar accuracy as an approach using an adjoint (discussed in section 3.1.4.4),

which is significantly more computationally demanding) but fully accounts for nonlocal sources and nonlinearities in the NO_x chemistry.

Mass balance techniques based on the divergence of flux fields are sensitive to noise in these fields owing to the numerical computation of the divergence. Furthermore, the assumption of a linear relation between concentration and loss term can be a cause for uncertainty as well as the reliability of the used wind fields.

3.1.4.2 Gaussian plume models

Introduction

The next step in complexity is the addition of advection and diffusion to represent the transport of molecules throughout the domain. The algorithms typically use a form of a Gaussian plume model to present the flow downwind of a point source, and include both the advection and diffusion of a pollutant plume. Fits can be made on a 1d plane using the line density with a fixed cross-wind width, or 2d using the full plume shape. The methods are typically more precise in estimating emissions from point sources than basic mass-balances, as they allow a more accurate representation of the plume while also allowing for a fit of the lifetime. Depending on the quality of the satellite information and emission source shape and size, either the line or full 2d fit can give more accurate results. Over the years these plume models have evolved with additional complexity, the newest models allowing fits of several sources at the same time, which enables emission estimates for larger regions, while better constraining other sources.

Applications

The first studies by Beirle et al. (2011) and Pommier et al. (2013) only used a basic dependence on wind direction, to determine the NO_x emissions and lifetime for 7 (mega)cities and one large point source around the world. This evolved further into methods taking into account diffusion and plume shape such as those first used in studies by Fioletov et al., (2011). McLinden et al. (2016) for SO₂ multiple industrial sources, Goldberg et al. (2019) for NO₂ and CO₂ from industrial sources and cities. Multiple strategies exist to model plumes in various levels of complexity. For some applications one-dimensional line representations of plumes as a column average aligned with the wind direction can be sufficient to accurately estimate emissions of localized sources. This method was used to determine the strength and distribution of NO_x emissions from Paris (Lorente *et al.*, 2019) facilitated by the high signal to noise ratio (SNR) and spatial resolution of TROPOMI. In this study CAMS global near-real time atmospheric composition reanalysis was used to estimate the lifetimes or equivalently the chemical loss term under the conditions at the time of the TROPOMI retrieval, thereby introducing (external) computational burden into the method. Estimates for urban sources and most of the larger industrial sources and powerplants typically show good comparison to conventional gridded emission inventories such as EDGAR, TNO-MACC and its successor CAMS. For regions with only a few strong emission sources the method can be highly accurate as shown by Zhang et al. (2018) who used a fast Gaussian fitting method for the detection of NO_x sources using OMI observations for the China North Plain and found 94 individual NO_x emission sources. The weakest source that they were able to detect was Zhangjiakou city, with a NO_x emission rate of 0.4 Gg N year⁻¹. The derived NO_x emission rates at the level of cities and provinces show a good agreement with former studies.

Application to other species (short lived)

While OMI-NO₂ observations were the focus of the initial studies, the methods were quickly applied to SO₂. Similar to NO₂, the initial studies aim was to better constrain emissions from large industrial sources and volcanoes (Fioletov *et al.*, 2011; McLinden *et al.*, 2016). These

estimates were used to create the first SO₂ satellite-based emission inventories. Recently with the launch of TROPOMI this effort was repeated by Fioletov et al. (2020) showcasing that using only one year of TROPOMI SO₂ observations are already enough to accurately derive SO₂ emissions. Fioletov et al. (2017) was also the first to take the method a step further and estimate emissions at a country/regional level by extending the method to derive emissions for multiple point sources at once. Besides NO₂ and SO₂, the same methods can be applied to other short-lived species. Compared to NO_x, emission estimates for NH₃ are still in the early research stages, but with the availability of NH₃ observations, the first few studies have looked at NH₃ emissions from larger point like sources such as fires (Adams et al., 2019), and industrial and agricultural sources (Dammers et al., 2019).

Gaussian plume-based methods have not been applied to estimate PM emission from satellite data. The reasons are similar to those mentioned before. The most fundamental reason being the complex underlying chemistry, which is dominated by secondary production rather than primary emission, that makes it hard to describe PM 'plumes' with a Gaussian (or other) models.

Uncertainty

While the Gaussian plume-based methods are typically fast, computationally cheap, and applicable to any strong localized source. The ability to get accurate results as referenced above relies on single source methods, which can usually not be used in regions where the source is not isolated from other large sources or produce results with a higher uncertainty. The method is also very dependent on a well-described flow-field and any misrepresentation of the daily wind fields and/or large variations in orography can create large uncertainties as shown in the model evaluation of the method by de Foy *et al.*, (2014). The study also indicated that in regions with other sources, the lifetimes fitted with the often used Exponentially-Modified Gaussian (EMG) method are typically biased low. Because of the direct relation of lifetime to the estimated emissions this is a large source of uncertainty. Whereas for NO_x in-stack measurements of emissions exist for NH₃ this is not the case, which makes direct validation of the satellite based estimates challenging, but Dammers *et al.* (2019) reported the uncertainty of individual sources of error, based on a set of Monte-Carlo simulations. The largest two sources of error were lifetime and plume spread (width of the plume), with both contributing around 40%, which is dependent on the strength of the source. The uncertainty of the satellite observations is the third largest cause of uncertainty. The combined uncertainty was reported to be between ~20-50% of the total emissions, with the upper limit largely driven by uncertainties in assumed lifetimes and the source strength. With more accurate sensors, with higher spatial resolution, and model-based estimates of lifetime (Lorente *et al.*, 2019), this uncertainty can strongly be reduced. Another factor to keep in mind is that the satellite instruments footprint/ground pixel puts a lower limit on the detectable sources.

3.1.4.3 (Ensemble / Adjustment) Kalman Filter-based studies

Introduction

The current state of the art methods typically used for NO_x emission estimates from satellites either use a Kalman filter like variational approach or 4Dvar within a chemistry transport model (CTM) and are typically capable of either splitting between sectors while sacrificing precision on the spatial distribution or resolving emissions at higher spatial scales while losing information on sector specific emission attribution (see references in the application section below).

Typically one or more types of parameters such as emissions are perturbed throughout the domain to create a model state. Doing this several times per timestep creates an ensemble of model states, which can be analysed in comparison to a set of observations. In this analysis step the parameter is optimized so that the model state closely matches the observations. The cost of

such a method typically increases linearly with the number of ensemble members and/or perturbed model parameters.

The methods discussed in this section do not require an adjoint model and can be run at moderate amounts of CPU cost even though they are computationally more expensive than mass balance and plume-based methods.

Applications

On a regional scale a few examples stand out, the DECSO (Daily Emission estimates Constrained by Satellite Observation) algorithm developed by KNMI, typically run within the Chimere CTM, and the Ensemble Kalman filter-based approach developed by TNO, that uses the LOTOS-EUROS CTM. Both approaches have been applied to NO₂ and are currently being tailored for application to NH₃.

Mijling & van der A (2012) developed the relatively fast algorithm, called DECSO, for estimating daily emissions of short lived pollutants. The algorithm has been successfully applied to several regions around the world, producing emission inventories for regions such as Eastern Asia (Miyazaki *et al.*, 2016), at a resolution of ~25km and with the addition of the TROPOMI satellite down to ~10km (van der A *et al.*, 2020). Ding *et al.*, (2018) used the DECSO algorithm to produce a ten-year timeseries of shipping NO_x emissions over the Chinese seas using OMI data. The results were in good agreement with shipping emissions from the STEAM model. The DECSO algorithm uses an inversion method based on an extended Kalman filter that only requires one forward model run of a chemical transport model (CTM) to calculate all local and non-local emission/concentration relations. It updates emissions additive, not multiplicative, which makes it capable of detecting unaccounted emission sources, and thus very effective in regions where inventories have high uncertainties or missing emissions. The capabilities of the algorithm were further showcased in a recent paper by Ding *et al.* (2020), showing that the method is very capable in picking up NO_x emission changes following the COVID lockdowns, and a paper by Van der A (2020), illustrating that in combination with TROPOMI it is possible to constrain NO_x emissions of compressor stations, power stations and cities over Siberia.

TNO developed the Ensemble Kalman filter-based approach (EnKF) within the LOTOS-EUROS chemistry transport model. The approach has been applied to several species such as O₃ (Curier *et al.*, 2012), SO₂ (Barbu *et al.*, 2009; Fu *et al.*, 2017), particulate matter (Timmermans *et al.*, 2009; Segers *et al.*, 2010) and NO₂ (Eskes *et al.*, 2013; Timmermans *et al.*, 2019) using in-situ and satellite observations. The most recent study for NO₂ analysed the impact of Sentinel 5P and 4 observations on NO₂ analysis (Timmermans *et al.*, 2019). Most of these applications have focused on the improvement of modelled surface concentrations while updating the emissions using the EnKF data assimilation of (satellite) observations. The EnKF method has been used in the Globemission project to derive emission estimates over Europe (see section 0). Here it was found that the method was very dependent on the accuracy of the satellite product. One of the drawbacks of the method is the fact that the emissions can only be updated at locations with already existing emission sources (although the addition of a 'ghost' source in the entire domain has been shown to circumvent this drawback).

Application to other species (short lived)

To our knowledge the DECSO method has only been applied to estimate NO_x emissions. However, with adjustments it may be applicable to any species that is part of the used model, and for which a continuous set of satellite observations is available. The method is currently already being tested for estimates of NH₃ based on CrIS-NH₃ satellite observations. Similarly the EnFK method in LOTOS-EUROS can essentially be adopted to any species already included in the chemistry model for which observations are available. This has been indicated by the studies on

SO₂ (Barbu *et al.*, 2009; Fu *et al.*, 2017), O₃ (Curier *et al.*, 2012), and particulate matter (Timmermans *et al.*, 2009; Segers *et al.*, 2010). The algorithm has already been adjusted for NH₃ estimates for which the publication is in preparation (van der Graaf *et al.*, 2021 in prep).

Uncertainty

Kalman filter-based methods are more accurate than plume models but naturally limited by the uncertainty and biases in the observations, although this can be accounted for by giving a robust (expected) distribution of the error. Similarly the quality of the emission estimates are directly bound to the skill of the model to properly simulate the state of the species. Misrepresentation of the lifetime of a species can especially have a strong impact due to its direct relation to the emissions. Furthermore, the satellite temporal and footprint resolution form a major source of uncertainty to the derived columns concentrations and emissions, and a continuous stream of observations are needed for accurate estimates. A study by Liu *et al.* (Liu *et al.*, 2017) showed the potential of higher resolution (both spatial and temporal) NO₂ satellite observations for emission estimates. They showed that the assimilation of the 3km resolution (TEMPO-NO₂) columns can locally reduce the errors in the predicted NO₂ column concentration by up to 50%, which has a proportional effect on the emission estimates. The coarse resolution of the footprint hampers the discrimination of urban and rural sources at smaller spatial scales. Typically higher uncertainties are found for regions with limited ship traffic and thus lower emissions that are not captured by the inversion algorithm because of the limited resolution of the satellite and biases in the data product. Furthermore, the uncertainty in the lifetime of NO₂ and smaller number of observations in winter also lead to larger uncertainties in the allocation of emissions.

There are also more method specific limitations depending on the assimilation approach. For example an ensemble Kalman filter approach is typically not very sensitive to temporal changes and thus needs accurate information on the temporal emission distribution. In case of the EnKF method, a-priori knowledge on the emission patterns (temporal and spatial), the typical reach (correlation length) and lifetime of the species are essential for the overall quality of the inversion. Besides these limitations, with proper accounting for biases and uncertainties in the observations, the uncertainties in emission estimates using the DECSO method are found to typically be of the order of 20% (Ding *et al.*, 2018; van der A *et al.*, 2020) per grid cell (between 0.125-0.25 degrees).

One of our current development projects is aimed at deriving emissions for several sectors at moderate spatial scales using the EnKF method in combination with a source attribution routine (Kranenburg *et al.*, 2013) in the LOTOS-EUROS model. Results should be more precise for this method than with a plume model due to more precise constraints and the possibility to track and follow emissions using a labelling routine for source attribution. It is possible to increase accuracy in source sectors at national and provincial levels by using information from regions with high sensitivity to specific source sectors. Deriving emissions at NUTS 3 level is expected to be out of reach for now until satellites with multiple overpasses per day and/or higher spatial resolutions (~1km²) become available.

3.1.4.4 Adjoint based methods

Introduction

Adjoint based methods rely on an interplay between CTMs and (satellite) observations to improve model performance or emission estimates. A model that is used to describe a physical system in general receives input (e.g. emission inventories, meteorological data, landcover data, etc) to produce an output (e.g. surface concentrations of pollutants, synthetic measurements, etc). An adjoint model is aimed at inverting (part of) the physical system to be able to discern

what input would have been necessary to generate a given output. A variational approach with the adjoint model can be used to minimize the difference between model predicted and actual observations. Here a distinction is made between 3Dvar and 4Dvar approaches with adjoint models depending on the dimensionality of the adjoint model. Because (part of) the physical system is inverted an adjoint model is also quite commonly referred to as an inverse model.

In the applications of interest in this study, the model is a CTM, the input that is allowed to vary is the emission inventory and the output is the VCD a satellite would observe. So, given a particular emission inventory the CTM can predict what a satellite would observe. Contrarily, given a particular set of satellite observations the adjoint CTM tries to estimate what emissions could have produced these retrievals. Making an adjoint model is usually complex and computationally demanding and often simplifications are required, nonetheless applications of the described principle (or derivations thereof) are widely used to constrain emissions.

Applications

There have been several studies aimed at complete global inversions to estimate worldwide NO_x emissions. One of the first global estimate was derived by Stavrakou *et al.* (2008), using GOME and SCIAMACHY observations in combination with a global CTM, called IMAGES, to derive emissions for 1997-2006. The emission changes that follow from this adjoint approach are geographically specified (with a coarse resolution due to the computational demand of the method). Therefore, they allow regional assessment of the under- and overestimations of NO_x emissions.

In recent years, similar assessments have been repeated in several other studies for different regions, either assimilating NO₂ observations on its own or in combination with other species to capture more parts of the NO_x chemistry (e.g. Miyazaki *et al.*, 2012; Miyazaki *et al.*, 2017). An example of such multi-species assimilation methods is the hybrid estimation of NO_x and SO₂ emissions in China and India for the period 2005–2012 (Qu, *et al.*, 2019). The joint assimilation was shown to outperform single-species inversions. In these studies, a multitude of satellite products is used, each selected for optimal performance for the species of interest. We will not elaborate too much on the details of this type of method and the applications found in literature as adjoint based methods are not suited for the envisioned application in this work.

Application to other species

The application of data assimilation techniques with adjoint models is not limited to the estimation of NO_x emissions. For long-lived species such as CO₂ (Babenhauserheide *et al.*, 2015; Zheng, French and Baxter, 2016), CO (Jiang *et al.*, 2017) and CH₄ (Krol *et al.*, 2005; Bergamaschi, Alexe and Segers, 2014; Houweling *et al.*, 2017) a plethora of examples exist where satellite data and adjoint modelling is used to improve emission estimates. Likewise, for other short lived species many other applications exist.

Next to the aforementioned estimation of SO₂ emissions (jointly with NO_x) by Qu *et al.*, (2019) the same author published an application of SO₂ only inversions (Qu, Henze, Li, *et al.*, 2019). In general noisiness of the satellite retrievals hampers the applicability of SO₂ inversion methods and the relevance of SO₂ monitoring is reduced for applications in Europe due to the strong reductions in (anthropogenic) emission sources.

For NH₃, very recently high resolution (36 km²) inversion of IASI ammonia columns were used to estimate ammonia emissions in the United States (Chen *et al.*, 2020). Flexibility was given to the adjoint model in modifying the emissions, because of the high uncertainty in bottom-up emission inventories, which resulted in predicting the inventory totals with an error of up to 32%.

An earlier study shows that in the US estimates of NH_3 emissions by assimilating TES observations with an adjoint-based inversion resulted in heterogeneous adjustments showing an increase in California throughout the year, an increase in different regions of the West depending upon season, and exhibit smaller increases and occasional decreases in the Eastern U.S (Zhu et al., 2013). Inversions on CrIS observations of NH_3 in the US showed similar summer-/winter contrast, but generally higher adjustments (Cao et al., 2020). CrIS was also used recently in combination with IASI to estimate NH_3 emissions on a global scale for the period 2008–2017 with inversions using the Eulerian global CTM LMDz-OR-INCA (Evangeliou et al., 2020).

Another application was the estimation of volcanic ash emissions from Eyjafjallajökull in 2010 by assimilating satellite data and ground-based observations (Lu et al., 2016). Here the focus was on a single source instead of a region or sector. A so-called modified trajectory-based 4D-Var (Trj4DVar) approach is used, which combines 4D-Var with trajectory-matching. An optimal linear combination of trajectories (with different injection heights etc.) generated with different inputs (emission) is used to fit observation data which results in improved volcanic emission estimations.

Adjoint based assimilation of satellite AOD measurements have been used to improve PM concentration predictions of CTMs (Schwartz et al., 2012; Zhang et al., 2016; Pang et al., 2018). The difficulty of deriving PM concentrations from AOD retrievals should be noted and most often ground based measurements are required to make this translation. Furthermore, a step towards improving emissions estimates instead of ground concentrations predictions has not been attempted.

Uncertainty

Improper incorporation of the local chemistry, may have a large impact on the derived emissions. For example, Stavrou et al. (2008) found that taking into account the influence of the emission updates on the chemical lifetime of NO_x has a significant impact on the results.

The starting point of the variational approach should be chosen with care (Lorenc and Payne, 2007; Zhang et al., 2008). It is not uncommon for a multidimensional optimization problem, such as the 3Dvar and 4Dvar assimilation schemes, to have local minima that make it more difficult to reach the global optimum (Zheng, French and Baxter, 2016). In general, making inversion problems bigger, by including, for example more species, more emissions sources, more measurement data to assimilate, increases the complexity of the optimization landscape and makes it more challenging to reach optimal solutions. Nevertheless the inclusion of more data will generally improve estimates (Qu, et al., 2019) thereby creating a trade-off between numerical burden and inversion system complexity.

The performance of the adjoint approach is also dependent on the quality of the input of the model. For example emission inventories have both a space- and a time-dependent component. If either of these components does not align well enough with the actual physical situation the chance exists of adjoint based methods to inflate or deflate emissions unrealistically to force better alignment, although mitigation strategies exist to reduce the propagation of errors (Janjić et al., 2018).

3.1.4.5 Trend estimates

Introduction

Long term satellite observations can be used for the detection of changing emissions, which aid in the verification of pollution control strategies and compliance to emission control requirements. In addition, satellite observations can provide latest information on changes in emissions, which is not yet available from bottom-up inventories. Satellite based emission trend

estimates have been used to show the reduction in NO_x emissions due the economic recession (Russell, Valin and Cohen, 2012), emission controls (Duncan et al., 2013; Lu et al., 2015) and the COVID pandemic (Bauwens et al., 2020; Biswal et al., 2020).

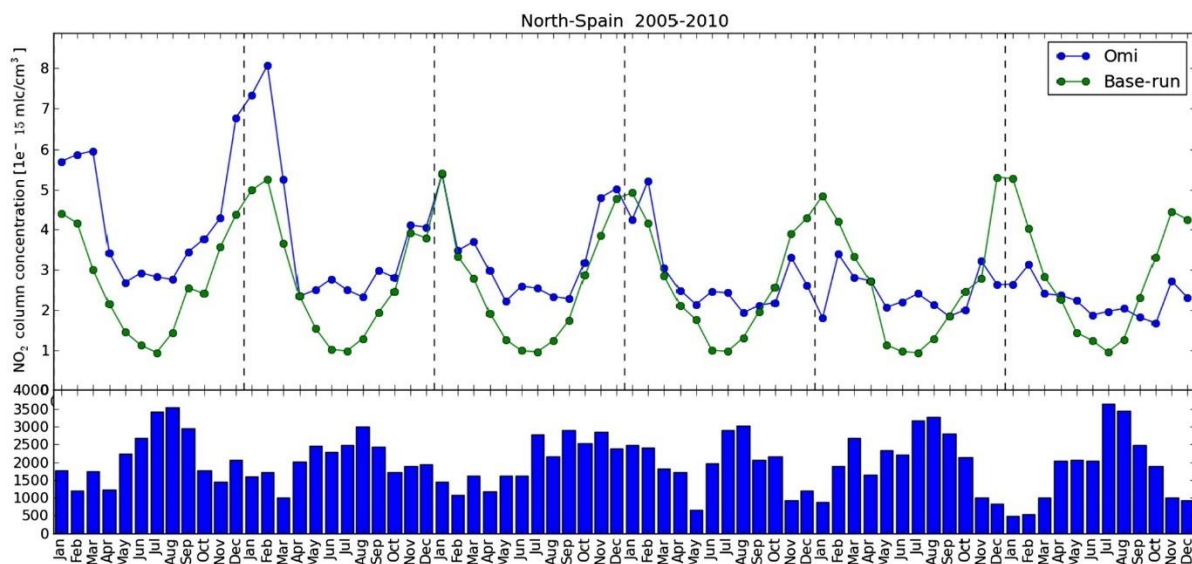
As with the estimation of emissions, trends may be determined by using only the satellite observations and assuming a direct relationship between the tropospheric (NO₂) column and the surface NO_x-emissions, or by using a CTM to account for the variations due to transport, meteorology and chemistry, in combination with the satellite observations. In the latter case usually, the emissions for each year/month/day are derived (see methods in sections 3.1.4). Based on these emissions trend analysis is performed.

Applications

Initial studies mostly focussed on trends in tropospheric OMI columns at a regional scale (Castellanos and Boersma, 2012; Zhou *et al.*, 2012; Curier *et al.*, 2014; Lamsal *et al.*, 2015) or on large point sources (Hilboll, Richter and Burrows, 2013; Schneider, Lahoz and Van Der A, 2015; Huang *et al.*, 2017; Paraschiv and Paraschiv, 2019).

Castellanos and Boersma (2012) for example used a spectral analysis on the OMI data to isolate the low frequency variations from higher frequency variations in the data and thereby determine regional trends over Europe. This method however does not account for low frequency variations caused by e.g. differences in meteorology. This impact of differences due to meteorological changes is taken into account in a study using the synergy between a CTM and satellite observations by Curier *et al.*, (2014). They estimated trends across Europe between 2005 and 2010 based on the OMI NO₂ tropospheric columns observations (blue line in in Figure 3) and the CTM LOTOS–EUROS. The model with fixed emissions (see green line in Figure 3) was used to capture a large fraction of the variability in NO₂ with a high temporal resolution, representing changes in tropospheric NO₂ columns not related to emission changes (e.g. because of meteorological changes) although a seasonal signal in the bias between the modelled and retrieved column data remained. This bias was then used to estimate the changes in tropospheric NO₂ originating from changes in emissions. This work was performed within the Globemission project described in section 0. In the same project also trends were derived based on the data assimilation of OMI observations with an EnKF in the LOTOS-EUROS model (Curier *et al.*, 2011, 2014; Schaap *et al.*, 2013) . The system was able to identify areas with major emission reductions (e.g. northern Spain which was confirmed by earlier studies). The study also pointed out the large uncertainty associated to uncertainties in the satellite products. The results changed considerably when going from version 1 OMI product to a newer version 2 OMI product.

Figure 3: Monthly time series for northern Spain for OMI-NO₂ and LOTOS–EUROS NO₂ columns for the period 2005–2010. Histograms provide the number of data points included in the average.



Source: (Curier *et al.*, 2014)

The studies focused on regional and point source trends were followed by trends derived for shipping emissions (de Ruyter de Wildt *et al.*, 2012), and city scale (Konovalov *et al.*, 2010; Tong *et al.*, 2015).

An example of a study performing trend analysis without relying heavily on CTMs showed that bottom up emission inventories during the recession underestimated NO_x emission reductions by about 25% for large cities in the US based on satellite data together with ground observations (Tong *et al.*, 2015). The translation of observed VCDs into NO₂ surface concentrations requires modelling but is in this study precomputed and stored in a look-up table. OMI data from 2005 till 2012 was used over the US with a focus on the 8 largest cities. Also assimilation based methods (Miyazaki *et al.*, 2017) are employed to estimate NO_x trends on the global scale.

Application to other species

In case of NH₃ only a small number of studies report on trends in tropospheric columns and emissions. The trend studies are currently mostly limited by the short measurement records and quality of the satellite products that are currently in a more experimental phase. Only the TES and AIRS instruments had measurement records long enough for trend analysis (e.g. at least 8–10 years), with recently IASI-A joining this small group of instruments (with first observations at end of 2017). Warner *et al.*, (2017) reported on regional trends in NH₃ concentrations using AIRS tropospheric columns. More recently, this was followed by the first studies reporting emission and column trends for strong point and area sources (Van Damme *et al.*, 2018, 2020; Dammers *et al.*, 2019).

Trends in surface PM_{2.5} concentration have been estimated from satellite observations on both the global (van Donkelaar *et al.*, 2010), country and city scale (Gui *et al.*, 2019). Similarly for SO₂ trends in the surface concentration have been determined from space on national (Qu, Henze, Li, *et al.*, 2019) and global scales (Wang and Wang, 2020). These methods usually focus on reporting surface concentrations and contrarily to the work presented here do not necessarily make a translation to underlying emissions.

Uncertainty

The current and future monitoring capabilities of trends are limited by the quality of both the observations, models and the relatively short instrument measurement records. Errors in the observations can be due to several factors such as the presence of high aerosols loadings, limited resolution of a priori profiles, constant a priori profiles in time. In addition, long-term emission estimates may be affected by discontinuities in the measurements and retrieval inputs.

Errors in the models are for example the uncertainties in the chemistry, the vertical mixing, and the limited resolution. Another typical problem is a lack of knowledge on the temporal emission variability. With the advent of geostationary satellites, capable of measuring trace gasses at high temporal resolution, the detection of the diurnal cycle will become available. The availability of higher temporal resolution observations will also allow the detection of daytime emissions that are now missed when they do not take place in the few hours before overpass. By using observations from various times of the day, it should become possible to derive information on emissions from different sources, as the sensitivity to different sources will change during the day.

3.1.4.6 Overview of relevant research projects

The ESA - GlobEmission project

The GlobEmission project was a consortium between the KNMI (The Netherlands), BIRA-IASB (Belgium), FMI (Finland), TNO (The Netherlands), and VITO (Belgium) in which global and regional trends in NO_x, SO₂, and VOC emissions were quantified. In addition, inverse modelling was applied based on OMI and GOME2 satellite data to improve emission estimates. In the project 5 algorithms have been developed and applied, each for a specific type of emission estimate (species) and temporal/spatial scale (https://www.temis.nl/emissions/docs/GE_ATBD_03_04.pdf). Shorter assimilation intervals ask for fast data assimilation algorithms, while transport issues become important for high spatial resolution. The methods differ in their emission domain (global or regional), the used satellite data, and the used chemical transport model, and sensitivity derivation. The performance of the algorithms in combination with the available satellite data has been tested. An error estimation based on theoretical calculations has been performed and tested with real satellite data.

The five algorithms and their application in GlobEmission are:

- ▶ Adjoint based method in global IMAGES model for global emission estimates of HCHO and SO₂. Description of method in section 3.1.4.4.
- ▶ DECSO method with CHIMERE CTM for NO_x emission estimates over East Asia, Middle East, South Africa, and India. Description of method in section 3.1.4.3.
- ▶ Remnant approach using the LOTOS-EUROS CTM to fit the bias between modelled (with fixed emissions) and retrieved NO₂ tropospheric column. This approach applied for estimation of NO_x emission trends in Europe. Description of the method and results is provided in section 3.1.4.5. The methods provide a scaling of fixed emissions and is therefore particularly suitable to compare trends in relative terms, i.e. percentage increase or decrease within a region of interest.
- ▶ Ensemble Kalman Filter in LOTOS-EUROS CTM to derive NO_x emissions over Europe. Description of method in section 3.1.4.3.
- ▶ 4-D Var assimilation approach in SILAM CTM to derive aerosol and fire emissions over Europe. Description of method in section 3.1.4.4.

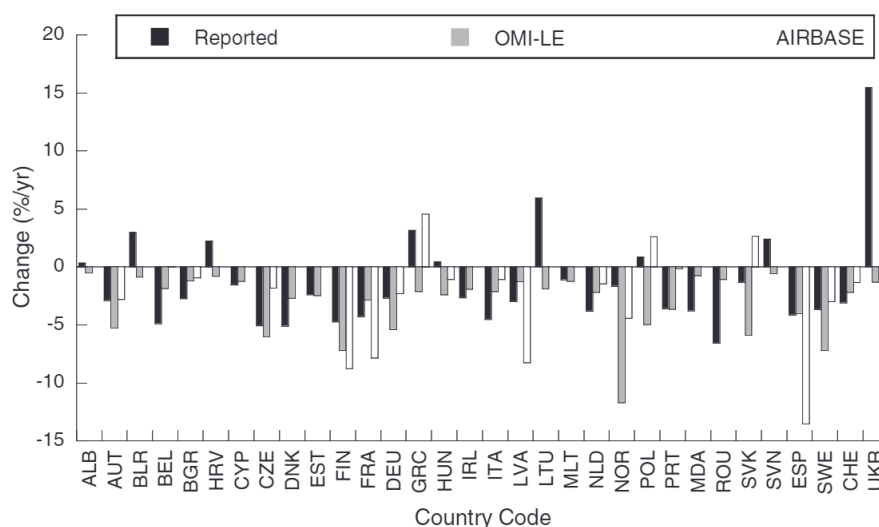
In addition to the descriptions of the methods in the indicated sections and the descriptions in the subsequent sections, a more detailed technical description of the used methods can be found online (https://www.temis.nl/emissions/docs/GE_ATBD_03_04.pdf).

With approach 1, otherwise poorly registered, effects and interannual variability of crop residue burning in China from the long-term record of OMI satellite observations of formaldehyde were estimated. Furthermore, a top-down approach that constrains the emissions with satellite observations was shown to increase the quality of emission data for isoprene, the most abundantly produced biogenic VOC. The GlobEmission dataset generally showed the best performance in comparison with other isoprene inventories. The results for this compound indicated the importance of including meteorological variability.

Approach 2 was applied for amongst others estimates of NO_x emissions from power plants in South Africa, and SO₂ point source detection in India, South-Africa, the Middle East and Europe.

Approach 3 has been used for calculations of European NO_x emission trends to check national emission reporting. The results from the application of this method are presented in Figure 4. The reported and estimated NO_x emissions tend to compare better over Western Europe than over Central and Eastern Europe. This may illustrate the differences between countries in updating their emission inventories but may also reflect that the dominant NO_x source in Western Europe is road transport which, is rather well-documented and gradually decreasing in emissions due to the implementation of new technologies. In eastern Europe emissions are dominated by large point sources from the power sector and secondary contributions from households and transport which are less well documented. The comparison between trends based on the AIRBASE stations differs more from the reported emission strengths than the values derived from OMI, which we attribute to the impact of local sources on the trends at in-situ stations.

Figure 4: Comparison of reported emission trend per year and the derived trends from OMI and AIRBASE in-situ data for European countries. The total national NO_x emissions reported in July 2012 for 2005-2010 were used and the changes relative to 2005 were computed (Curier *et al.*, 2014).

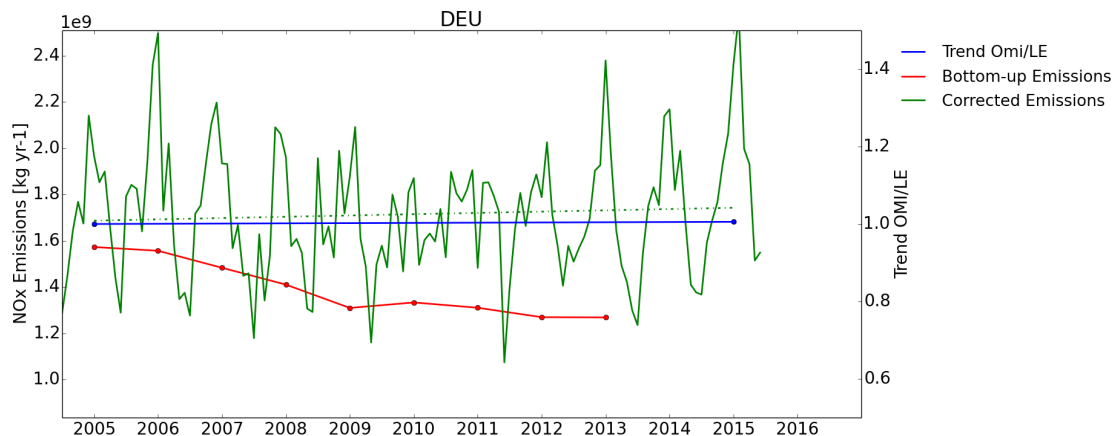


Source: this study

Approach 4 has been described in section 3.1.4.5 and was applied in addition to approach 3 within the project to detect NO_x trend over Europe. In Figure 5 the satellite-derived emissions with approach 4 for Germany and the trend in these are plotted against the officially reported

emissions and the trend as derived with approach 3. Unfortunately, the linear trends from approach 3 and 4 (blue line and dashed green line) are largely influenced by the higher emissions in 2014 and 2015, which were not yet available at the time of the project from the official reports. It can be seen that both approaches provide similar trends. It must be noted that uncertainties associated with the OMI product impacts the results. Two different versions of the product led to considerably different results.

Figure 5: Comparison of trend for Germany derived with approach 3 (blue), with emissions from official reports (red) and satellite-derived emissions with approach 4 (green) and the trend in those (dashed green).



Source: this study

Approach 5 is based on the satellite measurement of aerosol optical depth (AOD) in an 4D-Var type data assimilation method described in (Vira and Sofiev, 2012).

The resulting emission datasets from the GlobEmission project have been used worldwide, and for many users it is the only reliable information on the emissions in their area. The data has led to numerous publications. The development and usage of the DECSO algorithm for NO_x inversion was mentioned as one of the outlooks for future improvements. We have seen that since the Globemission project the DECSO algorithm has indeed been developed further, resulting in numerous publications as mentioned in section 3.1.4.3.

EU- MarcoPolo project

The objective of MarcoPolo (Monitoring and Assessment of Regional air quality in China using space Observations. Project Of Long-term sino-european co-Operation) was to provide air quality information for China using satellite observations and CTMs. The project builds upon the work performed in the Globemission project described above and mostly uses the same methods to improve emission estimates.

The DECSO Ensemble Kalman filter emission estimation algorithm (Mijling and Van Der A, 2012) is used to generate a monthly NO_x emission inventory for East China over the period 2005-2015 using VCDs retrieved by OMI and GOME-2. For PM the SILAM 4d-Var data assimilation system is used to derive top-down multi-annual aerosol emission estimates over Asia based on the MODIS 550 nm aerosol optical depth (AOD). Isoprene concentrations and anthropogenic VOC fluxes are computed using HCHO column densities observed by OMI and a source inversion system built on the CTM IMAGESv2 in a similar way as was done in the GlobEmission project. For SO₂, a mass-balance method, based on the Chinese bottom-up inventory (MEIC), together with an inversion

using the CTM CHIMERE and OMI SO₂ columns, is used to provide updated monthly SO₂ emission estimates of various point sources (Koukouli *et al.*, 2018).

An uncertainty estimation of the thus derived inventory data is based on comparison of satellite observations, emission estimates and model results to ground observations in urban, rural and forest environments. The validated data is made freely available at the MarcoPolo website (<http://www.marcopolo-panda.eu/products/toolbox/emission-data>) with the aim to improve existing air quality modelling and forecasts.

MEaSURES

An example of a large non-European project with a focus on the derivation of emissions is the “Multi-Decadal Sulfur Dioxide Climatology from Satellite Instruments” within the NASA MEaSURES program (<https://earthdata.nasa.gov/esds/competitive-programs/measures/multi-decadal-sulfur-dioxide>). The aim of the project was creating and archiving of a long-term consistent SO₂ record, covering SO₂ measurements and emissions (Fioletov *et al.*, 2019).

Within the project emissions and trends were derived for all major SO₂ sources such as volcanoes and anthropogenic sources such as smelters, refineries and coal power plants.

The project can function as a template for this project as the methodology used within the project is in many aspects applicable to other species like NO₂ and NH₃. Especially the methods using plume models (both for single (Fioletov *et al.*, 2013), and multiple point sources to entire regions (Fioletov *et al.*, 2017)), with typical uncertainties of 20% (regional estimates, (Fioletov *et al.*, 2017))-50% (small single sources, Fioletov *et al.*, 2013, de Foy *et al.*, 2014), can easily be applied to NO₂. Lifetimes of both species are of the same order (1-10hours) and the major emitters are relatively static in location and of anthropogenic origin. Exact source locations for many large industrial complexes, power plants and refineries are available through the European Pollutant Release and Transfer Register (E-PRTR), but the magnitude of the emissions and their characteristics such as stack heights may be unknown or uncertain. Instead of checking by hand if the reporting of large point source emissions is consistent with their productivity as well as technology standard, one can use remote sensing data of SO₂, NO₂ and NH₃ to estimate their emission strength and evaluate their reported numbers (Fioletov *et al.*, 2013, 2017; Beirle *et al.*, 2019; Dammers *et al.*, 2019). Such techniques offer a cost-effective way to identify which point sources require a closer look.

3.1.5 Use of satellite data in official national emission reporting

So far there is no known use of imaging spectroscopy/ spaceborne spectrometer data for the emission inventory reports. Some countries use spaceborne data for localization of source areas:

- ▶ The US uses updates of Emission Factors/Activity by spaceborne detection/ characterization of burnt areas via multispectral instruments and use Google Earth for location checking of emission source (e.g. chimney location).
- ▶ The UK uses ship tracking via GNSS for activity data and data on the expanse and area of airports for area sources determination.

3.1.6 Summary of methods and characteristics

In this section the methods that are used in literature and that have been discussed in the previous section are summarized (see Table 1). The methods are ordered by increasing level of (computational) complexity, which corresponds to the order in which they were introduced in this chapter. The details in the table refer to application of the mentioned method in combination with satellite data to derive or improve emission and pollutant concentration

estimates. It should be noted that EnKF and Adjoint methods were initially applied to assimilate ground based measurements but have since been applied to satellite data as well.

For all methods unaccounted biases in the satellite products that are used will reduce the accuracy of the results. In the first two methods these effects will most likely be strongest because no information from a CTM is used that can potentially identify unrealistic biases. Hence these two methods are labelled as most inaccurate.

The mass balance method (Beirle et al., 2019) is most straightforward. Calculation of the divergence of acquired VCDs that are translated into a flux field through multiplication with a corresponding wind field at the time of the satellite retrieval is computationally cheap. The uncertainty is caused by taking a numerical derivative (divergence) on noisy satellite data. Accuracy of this method can furthermore be negatively influenced by the simplified approach of a sink term through a fixed lifetime. This constant lifetime and sink term together with the steady state assumption and the Gaussian description of point sources are the most important implicit assumptions in this method. Source sector distinction is only possible (if at all) based on timing and spatial differentiation of the identified sources.

The Gaussian plume-based method is less noise sensitive, because no numerical derivatives are required, and the plumes seen in the satellite images are fitted directly. Still uncertainty is introduced by numerical challenges. Neighboring plumes can shift emissions in case they are hard to distinguish through the fitting routine. This is a result of the sometimes poorly conditioned linear least squares problem that is solved. Accuracy of this method can once again be negatively influenced by the simplified implicit assumption of dealing with the sink term through a fixed lifetime and presence of a steady state with respect to decay. Also sector distinction is only possible based on timing and spatial differentiation of the identified sources.

The more accurate inclusion of the sink terms and other nonlinearities in the chemistry of the investigated species in the EnKF and adjoint based methods improves the accuracy of these methods compared to the methods without a CTM. The assumption of a steady state is relaxed and no longer implicitly present in the model. This comes at the expense of rapidly increasing computational costs. Also, the inclusion of (a numerical version of) physical laws makes their uncertainty lower and accuracy higher. A drawback is that these methods do not operate independently from CTMs and their underlying emission inventories. Methods such as EnKF and most adjoint based methods will not be able to identify emissions that are not in this inventory, contrary to the mass balance and Gaussian plume-based methods (this is different for methods such as DECSO which use additive instead of multiplicative functions for changes to the emissions, which means they can add to locations with missing emissions).

Table 1: Methods to derive emission estimates from satellite data.

Method	Species for which applications have been demonstrated	Seminal publication(s)	CTM usage required	Required input data	Computational burden	Uncertainty*** and accuracy****	Source-category distinction
Mass Balance	SO _x , NO _x , NH ₃	(Beirle <i>et al.</i> , 2011)	no	VCD, Windspeed, species lifetime	Low (~hour, several CPU cores)	High uncertainty and very accurate (~40-65%, (Beirle <i>et al.</i> , 2019))	Limited
Gaussian plume	CO ₂ , SO _x , NO _x , NH ₃	(Fioletov <i>et al.</i> , 2011, 2020)	no	VCD, Windspeed, species lifetime	Moderate (~hours, several CPU cores)	Medium uncertainty and accuracy (~30-40%, (Dammers <i>et al.</i> , 2019))	Limited
(Ensemble / Adjustment) Kalman Filter	Chlorofluorocarbons, isoprene, O ₃ , CO, CO ₂ , SO _x , PM _{2.5} , NO _x , NH ₃ ,	(Mijling and Van Der A, 2012; Ding <i>et al.</i> , 2020)	yes	VCD, CTM input*	High (~days to weeks using many CPU cores)	Low uncertainty and accurate (~20%, (Ding <i>et al.</i> , 2020))	Yes
Adjoint based methods	PM _{2.5} , CH ₄ , O ₃ , CO, CO ₂ , SO _x , NO _x , NH ₃	(Bergamaschi <i>et al.</i> , 2000, 2010)	yes	VCD, CTM input*	High (weeks using many CPU cores)	Low uncertainty (~10-15%, (Cooper <i>et al.</i> , 2017)) Highly accurate (~10-15%, (Cooper <i>et al.</i> , 2017))	Yes

*CTM input refers to data that is required to run a simulation with a CTM, which includes meteorological data, emission data, orographic data and climatological data. **The method described in the 2019 paper seems most promising, but mass balance methods have a longer history. ***Uncertainty independent of uncertainties in the satellite products or lack of model skill. ****Accuracy independent of uncertainties in the satellite products or lack of model skill.

Various satellite products are used in combination with the methods listed in Table 1, which include GOME, OMI, CrIS, TROPOMI, MOPITT. More information on these satellite products can be found in section 3.2.

The main focus of EnKF and Adjoint based method is usually improvement of CTM performance which is determined from its agreement with measurements. These methods are in general not used to improve emission estimates even though they generally automatically produce updated emission estimates alongside the improved model performance. To avoid the necessity of CTMs the focus of further discussions will lie on the mass balance and Gaussian plume-based emission estimates.

3.1.7 Overview and recommendation of most appropriate methods

Based on the review of literature and past projects on the use of satellite observations for emission estimates, as reported in above sections, the following two methods are expected to be the most suitable for the development of a tool for emission verification over Germany, also considering the requirements and vision set by UBA and the possibilities within this project:

Method 1: NO₂ sources based on the method by (Beirle et al., 2019)

Where OMI allowed the study of larger point sources and regions, TROPOMI's superior footprint and sensor capabilities enable the study of intermediate to small point sources (emissions ~0.5 tonnes /hour) and rough estimates of city level emissions. Beirle et al showed an example of this in their 2019 study. The method describes the concentration field as a combination of emissions and sinks.

The NO₂ VCDs, V as seen by TROPOMI are translated in a flux field, \vec{F} , by giving the column a direction based on the wind direction, \vec{w} , at the time of the overpass. The divergence of this flux field is equal to the net flow into a volume, i.e. $Fl_{in} - Fl_{out}$ in equation 1. Equation 3 is used to compute the emissions. These emissions are simply the sum of the (negative) sources and the divergence of the flux field, $\vec{F} = rV\vec{w}$, with r being the ratio of NO_x and NO₂. The sink term due to chemical removal and deposition, S , is assumed to be proportional to the concentration of the species, i.e. $\frac{rV}{\tau}$.

During TROPOMI's overpass time (daytime) the dominating sink is the rapid chemical loss reaction of NO₂ and OH. By iteratively fitting all the major plume sources and calculating the divergence of the concentration fluxes it is possible to derive emissions from point sources as weak as 0.03 kg/s under the best conditions. This method can be applied to cities as well as large point sources.

The chemical lifetime is an important parameter within the emission estimates and is usually a parameter that's assumed (fixed) and thus one of the largest sources of uncertainty. By directly fitting the lifetime this source of uncertainty can be reduced, which will lead to the most significant improvements when regional variations in the lifetime exist. One could derive a first order spatial distribution of the lifetime by iteratively fitting the lifetimes of the largest sources in the domain and improve the overall emission estimate. Alternatively, a set of CTM modelled concentration fields of NO₂, NO, and OH can be used to calculate a representative lifetime. For larger regions this method can give reasonably robust estimates, because the numerical computation of the divergence tends to underestimate strong emissions from point sources through shifting them partly to lower background regions but keeping them in the region of interest if it is sufficiently large.

Method 2: Regional constraints of SO₂ sources, Fioletov et al., 2017.

Similar to NO₂, SO₂ concentration fields are dominated by large point sources with a mix of smaller sources in the background. Quite similar to the approach used in Beirle et al. (2019), Fioletov et al. (2017) fit clusters of SO₂ sources using several years of OMI observations. Instead of iterative fits applied to a mass balance, Fioletov et al (2017) constrained SO₂ emissions by using a superposition of Gaussian plumes, each originating from a separate source. By describing each observation as a combination of contributions from each source a simple linear mathematical system can be set up:

$$Ax = B \quad (4)$$

in which, B are the satellite observed VCD/concentrations, x the emissions sources and parameters constraining the bias, and A the Gaussian plume function that links each emission source with each observation. The novel approach that Fioletov et al (2017) took, was applying the method for SO₂ at a 0.5x0.5 degree scale for the entire European region. Fioletov et al. (2017), showed that using a complete grid of possible source locations, it's possible to find missing sources and quantitatively derive and update emissions of individual sources, as well as regional totals, which were found to closely match those reported in the inventories.

We foresee that for NO₂ an increased spatial scale is needed, which is possible due to the higher resolution of TROPOMI observations. With the higher resolution the computational cost will rise proportionally, which is something to be analysed in detail. One of the more important assumptions in this method is the chemical lifetime, and similar to Beirle et al (2019) method, isn't directly fitted and thus has to be derived using another method. Possible methods are using a CTM to derive the lifetime using a labelling routine, fits to large point sources (Beirle et al., 2019; Fioletov et al., 2011/2013), or using concentration fields from the species that NO₂ reacts with (similar to Lorente et al., 2020).

Compared to Beirle et al's (2019) mass balance method the multiple Gaussian plume approach should be more accurate for point sources and less sensitive to artefacts in the advection fields. Large scale biases remain something to be resolved. Fioletov (2017) fit a smoothly varying function to approximate the spatial variations in the bias of the satellite product but did so with knowledge of earlier validation studies. For TROPOMI-NO₂ there have been several validation studies, which will be studied in detail in the next phase of this project.

In combination with the outcome of the work in the next two work-packages, a proposal will be made and discussed with UBA to decide on the exact method to be used. We foresee that the most appropriate product for the emission estimates will be the TROPOMI NO₂ product, together with the OMI product for the trend estimates.

3.2 Data sources and Compatibility issues

3.2.1 Introduction

Satellite remote sensing of the atmospheric composition for air quality applications has a rich history. A comprehensive overview of this history up to 2007 is provided by Randall Martin (Randall V. Martin, 2008) and an overview of the capabilities around 2013 is provided by David Streets (Streets et al., 2013). Around the end of 2018 an up-to-date overview of (planned) satellite missions for different species was provided by TNO in the report of the FKZ 3717 51 251 0 project. Since then, this information is partially out-of-date due to e.g. changed launch dates, loss of instruments or instruments taken out of operation. We will therefore start by

giving an updated overview of the currently available satellite products and their characteristics with a focus on NO₂ and NH₃.

Within satellite products, a categorization is made between various levels based on the amount of processing (steps) that went into producing them. Sometimes a subdivision of these levels is made. Level 0 refers to unprocessed instrument and payload data. Level 1 refers to the spectra that are acquired by the satellite after time-referencing, annotation with ancillary information and georeferencing (Level 1A) and processed to sensor units (level 1B). If these spectra are used to derive geophysical variables (like vertical column densities) one speaks of level 2 data. When these variables are regridded to a uniform spatial and temporal grid they are called level 3 data. Results from analysis on (combinations of) these variables (i.e. by taking the divergence and computing the emission) are called level 4 data.

We will start this chapter with summarizing the recommendations on which satellite products are currently considered most suitable for producing satellite-based emission estimates. After that we will provide more detail on the various available satellite products and also discuss options for NH₃ estimates. The recommendations are based on the information that is provided in the subsequent sections (i.e. sections 3.2.3-3.2.6).

3.2.2 Recommendations for satellite data used to estimate NO₂ emission

For emission verification within this project there is a preference for level 2 satellite products because keeping control over the relatively computationally inexpensive step of regridding of the satellite data allows for customizing this grid and investigating the effect resolution has on the performance of the various methods. Basically the lowest level data will have been manipulated less making anomalies in data much more interpretable.

The lowest level data (L0-L1) will however still require a translation from a spectrum into an observed VCD, which is a computationally expensive task and in itself is a field of research. This holds to a much lesser extend for the translation from level 2 to level 3 data which often comes down to regridding, interpolating, filtering and averaging of data.

Among level 2 TROPOMI NO₂ products, most extensive validation reports and scientific work is done on Sentinel-5P NRTI NO₂ and Sentinel-5P OFFL NO₂ products which can be found on the TEMIS website (see section 3.2.3 for more details on these products). This furthermore is the official product also accessible through the Copernicus data hub. It is continuously updated and available in the highest resolution currently achievable. The NRTI data becomes available within 3 hours after data acquisition and is intended for users that need quick access to the data and for rapid use in operational processing. This high release speed comes at the cost of reduced data completeness and a slightly lower data quality as compared to the other data streams. The OFFL data becomes available within a few days after acquisition, which is fast enough for the applications envisioned in this project.

To assure consistency, a logical choice of OMI data would be a product available from the same data provider. For trends analysis the QA4ECV version 1.1 OFFLINE product is most suitable because it dates back to 2004. The OMI DOMINO version 2.0 NRT product is only available from 2018 onwards and despite bearing most similarities to the TROPOMI products of choice, it is less useful due to the limited time range for which it is available.

Hence the suggested product choice for this project is the Sentinel-5P TROPOMI Tropospheric NO₂ 1-Orbit L2 5.5km x 3.5km V1 (S5P_L2_NO2__HiR) product and the QA4ECV version OMI product for trends and DOMINO version 2.0 product if a validation or separate measurement of TROPOMI retrieved NO₂ concentrations for recent years (>2018) should be required.

The DOMINO product relies on relatively coarse Air Mass Factors (AMFs) from the TM4 model (or in updates the TM5/TMP5-MP model) to compute VCDs. TM5 is also used to produce the look-up table (LUT) used in the TROPOMI product of choice. The inaccuracies introduced by using these rather coarse AMFs should be kept in mind when working with the chosen satellite products. A non-trivial improvement can be made by using higher resolution AMF (derived from for example the lotos-euros CTM). This will be discussed in more detail at the end of the next section.

3.2.3 NO₂ Satellite products

With the reviews and project reports mentioned in the introduction as starting point and extensions to include more recent information, Table 2 and Figure 6 with available products for NO₂ was produced.

It should be noted that the so-called Ultraviolet and Visible Atmospheric Sounder (UVAS) an instrument planned to be operational by April 2021, but was lost upon launch on 17 November 2020, is present in Figure 6 but will not be discussed further here.

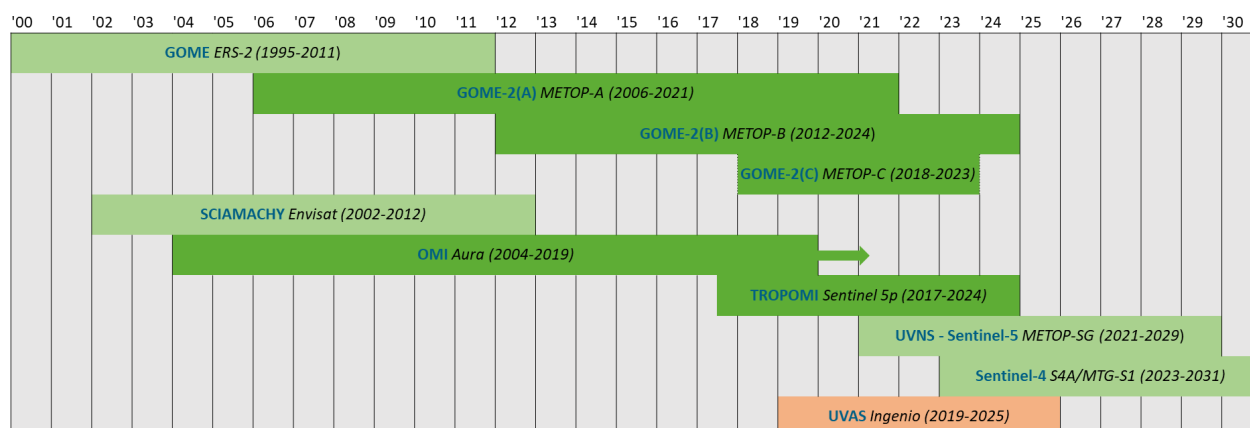
Table 2: Overview satellite instruments capable of NO₂ observations.

Instrument	Spectral Range (nm)	Spatial resolution (km x km)	Operational	Global coverage (days)	Observable species
GOME	240-790	320 × 40	1995-2011	3	NO ₂ , SO ₂ , O ₃ , NMVOC/ HCHO, AOD
SCIAMACHY	240-2400	30 × 215	2002-2012	6	NO ₂ , HCHO, SO ₂ , CO, CH ₄ , O ₃
OMI	270-500	13 × 24	2004-operational	1	NO ₂ , AOD, HCHO, SO ₂ , O ₃
GOME-2 A,B,C†	240-790	80 × 40	2006-operational	1	NO ₂ , HCHO, SO ₂ , O ₃
TROPOMI	270 – 2385	3.5 × 7*	2017-operational	1	NO ₂ , HCHO, SO ₂ , O ₃
SENTINEL-4	305- 775	8 × 8	Launch scheduled for 2023	Stat.	NO ₂ , AOD, SO ₂ , O ₃ , HCHO
SENTINEL-5	270 – 2385	7 × 7	Launch scheduled for 2021	1	NO ₂ , AOD, SO ₂ , HCHO, CO, O ₃

†GOME-2A, 2B and 2C are equipped on METOP-A, B and C respectively which are all currently operational. *

The resolution of TROPOMI has increased to 5.5 km×3.5 km since 6 August 2019.

Figure 6: Overview of past, current and future approved tropospheric NO₂ missions over Europe. The currently operational systems are in dark green. UVAS is in orange because this mission was unable to provide any retrievals due to a launch failure.



Source: this study

In the satellites listed in the table above it is common for the entire spectral range that is listed not to be acquired, but rather a discrete set of bands within it. The mentioned spatial resolution can vary between the different spectral bands acquired by the same satellite. Furthermore, it should be noted that the list of species that are 'observed' can grow after a satellite is already in operational for some time due to advances in retrieval algorithms.

The only currently operational satellites that measure atmospheric NO₂ concentrations are OMI, GOME-2 and TROPOMI. These satellite products, their availability, characteristics and limitations will be discussed in more detail in this chapter and Appendix A.1.

Because of the coarse resolution of GOME-2, observed pollutant concentrations are averages over a relatively large domain making it hard to pinpoint sources. Within one GOME-2 satellite retrieval 'point' lie respectively 10 and 130 OMI and TROPOMI retrievals. Because down-sampling to a coarser resolution is always possible and the operational period of OMI exceeds the operational period of GOME-2 the focus in this project will lie on the usage of TROPOMI and OMI satellite data for estimating NO₂ emissions. At a later stage GOME-2 could be used to validate concentrations measured by TROPOMI but combining satellite products is not always trivial as will be further discussed in section 3.2.6.

In the near future, instruments similar to TROPOMI will be launched on the Sentinel-4 and 5 missions. The Sentinel-5 mission will complement the TROPOMI observations but with an overpass time in the morning as opposed to the early afternoon overpass time of TROPOMI. The Sentinel-4 mission is a geostationary satellite which will provide observations with a high temporal resolution (30-60 minutes). The additional information this provides will allow to track emissions through time and improve the time profiles that are now usually based on statistical activity data.

3.2.4 NH₃ Satellite products

Currently there are eight (operational) satellite instruments capable of measuring NH₃ in the boundary layer, IASI-A (-B & -C, Van Damme et al., 2014; 2020), GOSAT (1&2, Someya et al., 2020), CrIS (1,2, Shephard and Cady Pereira 2015), and AIRS (Warner et al., 2016). Of these instruments, only IASI and CrIS give global coverage at high enough resolution and with high enough sensitivity for the study of emissions. Both TES and the GOSAT satellite instruments have large gaps (>50km) between observations or a limited swath which makes mass-balance or

plume model inversions impossible for NH₃. The AIRS instrument is capable of NH₃ observations in the boundary layer but has a lower spectral resolution and currently the product is only available in the form of monthly NH₃ averages for specific pressure layers.

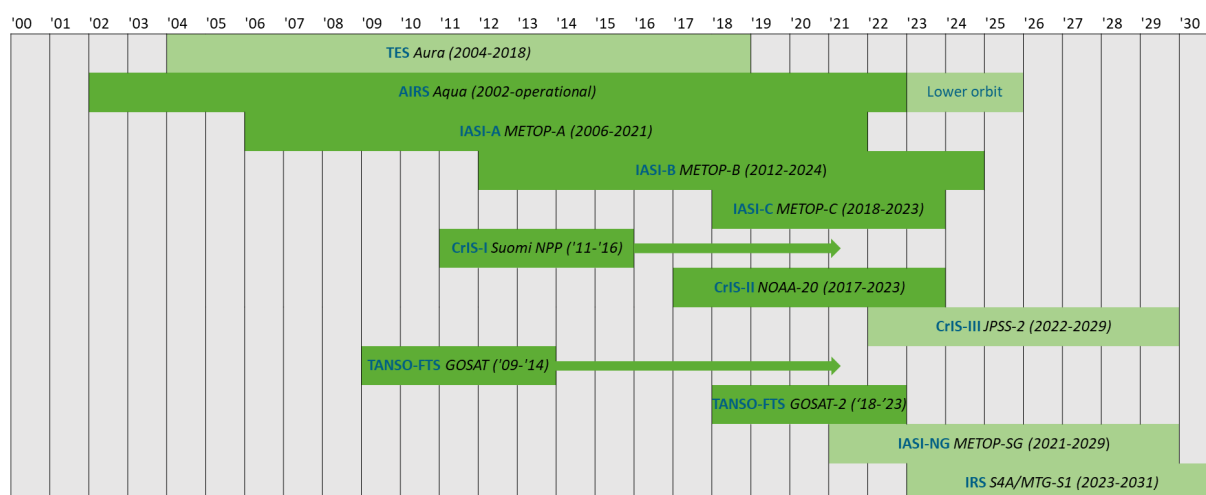
Table 3 and Figure 7 provide an overview of the instruments, their characteristics and (expected) lifetimes.

Table 3: Overview satellite instruments capable of observing NH₃. D stands for diameter in case of round pixels.

Instrument	Spectral Range (nm)	Spatial resolution (km x km)	Operational	Global coverage (days)	Observable species
TES	3300-15400	8 × 5	2004-2018	-	a.o. NH ₃ , CO, O ₃
AIRS	3800-15300	13 D [‡]	2002-operational	1	a.o. NH ₃ , CO
IASI-A	3600-15500	12 D [‡]	2006-operational (B&C launched later)	1	a.o. NH ₃ , CO, O ₃
CrIS-1	3920-15380	14 D [‡]	2011-operational (CrIS-2 launched in 2017, 3 more planned)	1	a.o. NH ₃ , isoprene
GOSAT-1	5500-14300	10.5 D [‡]	2009-operational (2 launched later)	-	a.o. NH ₃ , CH ₄ , CO ₂
IASI-NG*	3600-15500	12 D [‡]	Launch scheduled for 2021 (with Sentinel 5)	1	a.o. NH ₃
IRS**	4440-6250 8260-14700	4 x 4	Launch scheduled for 2023 (with Sentinel 4)	Geostationary	a.o. NH ₃

‡D stand for diameter, applicable for satellites with circular footprints. *<https://www.eumetsat.int/eps-sg-iasi-ng>, **<https://www.eumetsat.int/mtg-infrared-sounder>

Figure 7: Overview of past, current and future approved tropospheric NH₃ missions over Europe. The currently operational systems are in dark green. Specific satellites are operational beyond their expected mission duration which is denoted by arrows for the extended periods.



Source: this study

3.2.5 Data providers

Both the L2 and L3 data can be used for emission inversions. Once again, L2 data allows for more freedom, and the ability to apply different data criteria, while L3 data can be more accurate and is more easily used due to the aggregated nature of the data. None of the proposed methods in section 3.1.7 however, can viably use monthly aggregated concentrations which limits the options of L3 data, which is commonly provided as a monthly mean. It is not uncommon to see several groups in different continents provide similar satellite products for a single satellite instrument. Typically, the approaches use slightly different assumptions throughout the retrieval process, for example using a different Radiative transfer algorithm or choosing an a-priori vertical profile from one model or another. Because of these choices the performance of the products can be significantly different over for example source and background regions.

In the next section the most used products and performance/quality indicators will be described for both the NO_x satellite instruments and the NH₃ instruments. After giving examples for both species, the possibility of merging several satellite products will be discussed, for example combining the OMI and TROPOMI products into a single product. Finally, a summary will be given of the different products and the pros and cons of each when used for the proposed methods.

3.2.5.1 NO_x data

One source that provides data products for many different satellites and species (including NO₂) is TEMIS (Tropospheric Emission Monitoring Internet Service). For NO₂, level-2 products based on TROPOMI, OMI, GOME-2, SCIAMACHY, GOME and combination thereof are available.

Another data provider with a wide range of data products is NASA's Earth Science Data Systems (ESDS). Here level-2 and level-3 NO₂ product for OMI and TROPOMI are provided. This product is thus produced using a different retrieval algorithm than the one available from TEMIS.

For TROPOMI, OMI and GOME-2, the GeoPortal of the Deutsches Zentrum für Luft- und Raumfahrt (DLR) and the Copernicus Open Access Hub are additional data providers. The details of the different satellite products offered by above mentioned providers and other openly

available datasets that are relevant for this project are summarized in Table 6 (level-2) and Table 7 (level-3), which can be found in the appendix.

Other sources like for example Caeli (<https://www.caeli.nl/nitrogen-dioxide---no2.html>) provide commercial NO₂ products which are not discussed further because the added benefit of using these sources compared to openly available ones for this project is unclear.

An inter-comparison of all the OMI and TROPOMI LEVEL 2 products from different providers is not readily available. However comparisons of satellite products with ground based observations to assess the quality of the products have been made.

In one comparison (Wang et al., 2020) between OMI (QA4ECV Level 2 data compiled by KNMI/TEMIS), TROPOMI (both RPRO and OFFL Level 2 products compiled by the KNMI/TEMIS) and ground based measurements (using a Multi-axis differential optical absorption spectroscopy, MAX-DOAS) underestimations of ground observations, ranging from 30% to 50%, with OMI being less biased than TROPOMI, were found over China. Despite the negative drift, the temporal variability of OMI and TROPOMI closely match the ground-based records, since correlation coefficients are above 0.8 and 0.95 for daily and monthly scales, respectively. In this comparison TROPOMI retrievals were considered better suited due to its higher spatial resolution.

For assessment of the global performance of TROPOMI products (a combination of RPRO and OFFL Level 2 products compiled by the KNMI/TEMIS) a comparison (Verhoelst et al., 2021) has been made with an extensive ground based measurement network composed of 19 MAX-DOAS instruments, 26 Network for the Detection of Atmospheric Composition Change (NDACC) Zenith-Scattered-Light DOAS (ZSL-DOAS), and 25 Pandonia Global Network (PGN)/Pandora instruments distributed globally. This showed a negative bias for the tropospheric concentration, of -23% to -37% in clean to slightly polluted conditions but reaching values as high as -51% over highly polluted areas., in agreement with the results found over China. Errors in the TROPOMI tropospheric columns are known to originate from shortcomings in the (horizontally coarse) a priori profile representation in the TM5-MP chemical transport model used in the S5P retrieval and, to a lesser extent, to the treatment of cloud effects and aerosols.

The effect of improved AMFs by using regional high-resolution models has been investigated for TROPOMI (Griffin et al., 2019). Using the 'regular' product (S5P_L2_NO2___HiR from KNMI/TEMIS) a bias of -15% to -30% of the TROPOMI tropospheric NO₂ columns with ground-based in situ and remote sensing (plane) measurements in the (often covered in snow) Athabasca Oil Sands Region of Canada was found. Using the alternative tropospheric NO₂ VCDs, with a high-resolution AMF computed with the CTM GEOS-Chem, this bias is reduced to between 0% and -25%.

Recently, around Belgium also airborne NO₂ measurements from APEX (Airborne Prism EXperiment) have been compared to TROPOMI retrievals (OFFL Level 2 product compiled by the KNMI/TEMIS) (Tack et al., 2021). Again, a negative bias for TROPOMI with respect to the validation measurements was found (-14±12%) which was reduced (to -1±12%) by using a priori NO₂ profiles at a higher resolution, with AMFs computed using the Copernicus Atmospheric Monitoring Service (CAMS) regional chemistry transport model (CTM) ensemble. This shows the relevance of wisely choosing how to incorporate AMF, Surface albedo, cloud cover, pressure, temperature and orography.

3.2.5.2 NH₃ data

As described above there are currently two satellite instruments series capable of accurately measuring ammonia concentrations at both high spatial and temporal resolution and with

satellite products available as either open-access or on request. These two instruments are the IASI and CrIS instruments. Table 8 that is found in the appendix gives a summary of the available products, with a summary of the provider, period of soundings, and where to get the data.

The only operational product available for IASI is the ANNiv3 product (Van Damme *et al.*, 2020), which was built using the ANNI (Artificial Neural Network for IASI) retrieval framework which was developed by the Université libre de Bruxelles (ULB), and L'ATMOS/IPSL institute (Sorbonne University, Paris). The retrieval framework is applied to all three IASI satellites (A, B-, C-) and available for download at, <https://iasi.aeris-data.fr/nh3/>. A monthly aggregated level-3 dataset is also provided and can be found under <https://iasi.aeris-data.fr/catalog/>. The long measurement record of IASI (A, 2008 -now, B, 2013-now, and C, 2018-now) makes it an excellent product for emission estimate applications although it is hampered by its lack of an averaging kernel (sensitivity of the product to concentrations at different altitudes), which make model inversions complicated as no profile information nor estimate of sensitivity is available. Validation is also limited with the latest validation studies either looking at individual pixels (Guo *et al.*, 2021), using only ground data (Van Damme *et al.*, 2015), or looking at previous versions of the satellite product (Dammers *et al.*, 2016). The general outcome however, is that the product shows average to good correlations with in-situ and airplane data (Guo *et al.*, 2021), general overestimations for background regions while underestimating concentrations for regions with high concentrations (Dammers *et al.*, 2017). The main limitations of the product are the high uncertainty in background regions, which limit the use for emissions estimates. Similarly, the large footprint and lack of observations under cloudy conditions limit the spatial resolvability and temporal representativity, although the second can be adjusted for by taking into account diurnal and yearly emission cycles typically used in air quality models/part of emission inventories.

The most commonly used product of the CrIS-NH₃ instrument is the CrIS-FPR product (v1.5, Shephard 2020; Shephard and Cady-Pereira *et al.*, 2015) produced by Environment and Climate Change Canada. The product is a scientific development product and available on request. The product is to be produced operationally by NASA/AER but as of yet is not available to the public. The CrIS instrument was launched at the end of 2011 but the first data became available after May 2012. A second instrument has been launched in 2017 but as of yet no ammonia product has been produced for the second satellite. Three more instruments are planned over the next decades, so a continuous set of data will remain available. The product shows a good correlation with both in-situ surface data and FTIR-NH₃ data, overestimating concentrations in regions with lower concentrations while only showing a very small negative bias for larger concentrations. The product both provides the concentration profile and vertical column density data, but as the degrees of freedom (DOF, amount of information) is limited, only the VCD or complete profile should be used for inversions. The bottom profile concentrations can typically be interpreted as an average over several retrieval layers and will at best show a correlative relation with surface data. As the retrieval is performed in log-space the averaging kernels, which are provided in the product, require additional work to be used in Kalman filter and 4d-var based model inversions. Similarly to IASI, the uncertainty at low concentrations, the satellite pixel footprint with a diameter of 15km and temporal coverage are the limiting factors for emission inversions. No level 3 data are currently being produced operationally. Alternatively to the CrIS-FPR product two other groups (JPL, USA and RAL Space, UK) are working on their own retrieval algorithms but as of yet nothing is available operationally.

3.2.5.3 Combinations of data sources

Combination of NO₂ products

For NO_x a merged product (Georgoulias et al., 2019) based on GOME/SCIAMACHY/GOME2 is available from the TEMIS web portal. This product is created by scaling to SCIAMACHY derived concentrations. The set is available till 2017 and not provided at the resolutions of OMI or TROPOMI.

Combinations of OMI and TROPOMI and/or other satellite products to a unified satellite product is currently not done and a scientific endeavour in itself. The separate products are difficult to compare or merge because a coincidence in time and space is needed and in the best case an application of the same retrieval algorithm to the spectral datasets that are compared. This effort to merge datasets may take over a year and requires serious investments. Currently, in the scientific community the focus lies on comparing satellite products (He et al., 2019; Compernelle et al., 2020; Wang et al., 2020) rather than merging them into a single product. The lack of interest and investment in a merged product is understandable since this combination is unlikely to outperform the best option among the available products for any given application.

Combination of NH₃ instruments

As of yet there has not been an attempt to actively merge the measurement records of both the CrIS and IASI satellites. Initial comparisons have been done but the differences between the retrievals and instrument detectors hamper an easy combination. The combination of the several IASI instruments measurement records has not yet been performed, but recent studies do show differences between the products, which might be overcome through a detailed study (Dammers et al., 2019; Van Damme et al., 2020). A combination of the CrIS and IASI records is complicated by several factors, such as the difference in instrument detectors, overpass time, and retrieval strategy. The individual products produce similar temporal and spatial patterns and the main differences can be attributed to the difference in overpass times, the instrument limitations/sensitivities and the retrieval strategies. A solution would be the application of a single (or both current) retrieval to both spectral datasets which would remove any instrument specific bias/uncertainties. Such an effort, however, can take multiple years and is not expected to occur in the next few years, mostly due to lack of funding and other more immediate priorities.

3.2.6 Limitations and compatibility issues

There are a number of limitations and compatibility issues that affect the applicability of the methods for emission estimation discussed in section 3.1.4. These are:

- ▶ Spatial resolution
- ▶ Instrument sensitivity
- ▶ Uncertainty in satellite products
- ▶ Bias in satellite products
- ▶ Temporal resolution of satellite products and temporal variability in emissions
- ▶ Unavailability of data (for example due to clouds)
- ▶ Gaps in a-priori emission data

Below, we will explain these compatibility issues in more detail, but we will describe how they are planned to be mitigated in this project in the next chapter.

3.2.6.1 Spatial resolution

The footprint of the satellite determines the resolution to which the tropospheric concentration of the species of interest can be resolved. Clearly, if the resolution becomes coarser than for example the average separation between sources resolving these sources becomes extremely challenging. For regional total estimates similar effects will occur at the edges of the region of interest, as it is uncertain if the emissions originate past the edge of the defined domain or within the overall domain. Furthermore, if source attribution of emissions is based on spatial and temporal differentiation of the various sources (which is the case for the Mass balance and Gaussian plume-based method) attribution capabilities will likewise reduce with increasing footprint size.

3.2.6.2 Instrument sensitivity

The sensitivity of your satellite directly determines the overall smallest emission source detectable by your satellite product. Sensitivity can be increased through averaging over longer periods of time, at the cost of a reduction in temporal resolution. For the mass balanced and Gaussian plume-based methods the missed emission sources due to a limited sensitivity will be directly reflected in the overall emission totals. For Kalman filter and adjoint based methods the effect is reduced because the sensitivity of the satellite can be incorporated in the description of the synthetic/model-based observations. Only emissions that are missing in the a-priori emission inventory can still be missed.

3.2.6.3 Product uncertainty

Higher product uncertainties result in noise that cause increased granularity of the derived concentration fields. This will most strongly affect the mass balance method due to the sensitivity to noise of the numerical derivative, which is necessary for computing the divergence. The plume, Kalman filter and adjoint based methods will be rather insensitive to noise because the plume and CTM output fields will be relatively smoothly varying and generally reduce the influence of the noise. For the Gaussian plume and adjoint based method it might become more difficult to fit measurements with higher noise.

3.2.6.4 Product biases

A bias in the satellite product will reduce the accuracy of all four methods as described in section 3.1.4. The methods including a CTM will result in an emission estimate based on interplay between a priori emissions, the uncertainty assigned to them and the observations. Hence the effect of a bias can be reduced by assigning a variable set of uncertainties to a priori emissions and observations dependent on concentration and emissions strengths, but this will make the exercise to improve emission estimates much less impactful as the applied emission inventory will in relative terms have lower uncertainties than before. The methods without a CTM will be affected directly, albeit in a different way. The divergence methods are sensitive only to concentration dependent biases whereas the Gaussian plume-bases method will also be influenced by fixed offsets.

It should be noted that each available product is compared to results from alternative NO_x measurements (both ground-based and air borne) to estimate the quality of the product. These validations often expose structural and sometimes regionally varying biases and help pinpoint shortcomings and improve interpretation of the products. Surface albedo, cloud cover and the air mass factor (AMF) are crucial in translating observed spectra (L1) into VCDs (L2) and it is not surprising that various strategies exist for making this translation. Furthermore, physical quantities like pressure, temperature and orography influence this translation. The different L2

and L3 products each make the translation from the L1 data to (gridded) VCD in a slightly different way.

Next to these four satellite characteristics, three other issues can arise from potentially missing emissions in the inventory, unaccounted temporal variability of the emissions and gaps in the measurement records.

3.2.6.5 Temporal resolution of satellite product and temporal variability in emissions

Temporal variability in the emissions can be another cause of incompatibility/uncertainty. Emissions of most sources typically change throughout the day. While most observations are only available once a day at overpass time. CTM based inversions typically correct for such variations intrinsically adding temporal emission multiplication factors to handle seasonal, day-to-day and diurnal variations. Mass-balance and plume-based methods however typically assume steady states for the overpass times and need to either introduce an a-priori correction or posterior adjustment (Dammers et al., 2019) to account for such variations to the seasonal and diurnal cycles.

3.2.6.6 Unavailability of data

Another cause of compatibility issues is the unavailability of data. Be it due to clouds, or operational problems of the instruments, gaps can occur in the measurement record. If large event like emissions occur during such measurement gaps it can have a direct impact on the emission estimate and result in the misestimation of the emissions in a similar fashion to the detection threshold. CTM based methods are less impacted than methods without a CTM by such changes as previous timesteps are used to continue running the model and continue latter updates to the emissions, and in the 4Dvar example future and past observations are used to optimize emissions instead.

3.2.6.7 Gaps in a-priori emission data

Missing emissions in the reported emission inventories do not have any effect on the mass-balance and Gaussian-plume methods that do not make use a-priori emissions fields. Kalman filter methods, that use a scaling function to adjust the emissions, and most 3d and 4d var algorithms by design have problems to move away from (near zero) emissions as this usually rapidly increases the cost function. In many cases this is by design as a-priori knowledge of most emissions is assumed. Furthermore, emissions can potentially be misattributed to nearby (strong) point and area source, instead of the new location or one with weak a-priori emissions, due to the lower overall cost in increasing such emissions over (new) locations that need to be scaled by several factors. As such, short term emissions are the bane of such methods and typically adjustments have to be made for such systems to cope with event like emissions, such as volcanoes (Lu et al., 2016; Fu et al., 2017).

3.2.7 Outlook on future satellite instruments

With the launch of the most recent satellite instruments (TROPOMI) it is now for the first time possible to accurately measure daily emissions from cities such as Paris. With the first geostationary satellites (MTG-IRS/Sentinel 4/TEMPO (North America)/GEMS (South East Asia)) to be launched in 2023 applications like emission estimates will only improve further. With observations for the same area available every 30-60 minutes it will for the first time be possible to constrain the diurnal emission cycle, potentially reducing a large fraction of uncertainty coming from the description of temporal emissions. The increased load of observations will also increase the accuracy of monthly to yearly averaged emission estimates. Spatial resolution of

satellites is also expected to improve which will enhance the number of detectable sources and more accurately constrain already visible sources. A potential drawback could be the area covered (swath) by single satellites with ultra-high resolutions (200-300m scale) where a single satellite instrument only has limited coverage. A larger constellation of several instruments could remove such a limitation. An example of this are the several micro-satellites from GHGsat which can be used to pinpoint observations of specific emission sources. MTG-IRS will be a major step forward as for the first time it will be possible to produce very high-resolution observations for any species measured with such an infrared imager, e.g. NH_3 .

With the increased number of observations and its time coverage, validation capabilities can improve, since it will be easier to match measurements with a satellite overpass instead of the hassle of missed overpasses/wrong observations times encountered in current networks. Higher resolution footprints can also partially remove the current NO_2 bias as a large fraction still seems to follow from the very sharp concentration gradients and the differences in a-priori profiles. Improved modelling capabilities are however needed to get the most out of the new observations. Geostationary satellites can also help in linking the products of several current satellites with slightly different overpasses, as the new geostationary system can bridge the gap on the temporal changes in emissions/concentrations.

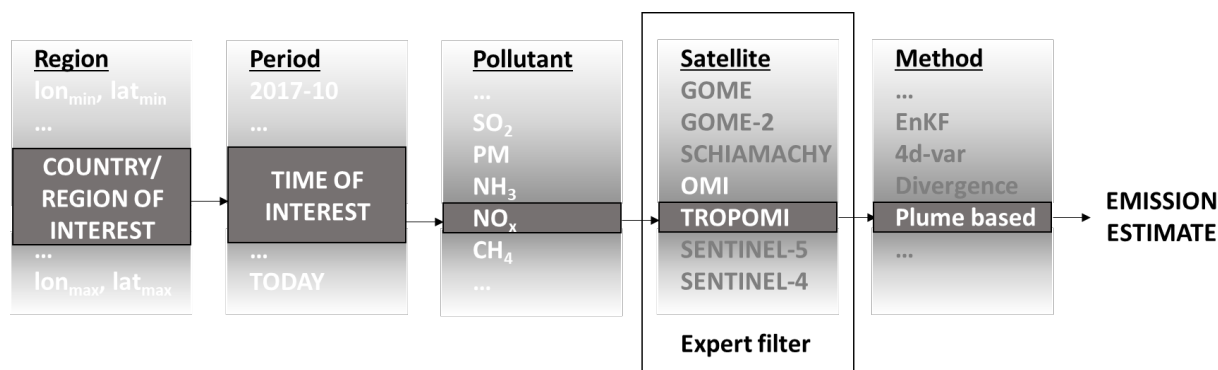
3.3 Satellite data processing and method development

3.3.1 Tool description

A generic tool to assess emissions based on satellite images has been developed. This tool is cast into a framework that is designed to be broadly applicable to assess emissions of various pollutants (NO_x , NH_3 , SO_2 , $\text{PM}_{2.5}$, etc) using a selection of methods discussed in the previous chapters. The methods mentioned in previous sections mainly focus on the estimation of NO_x and NH_3 emissions but can be applied to other species. The tool is designed to have global coverage and be extendable beyond what has been developed in this work.

Within the tool a user selects a region and period of interest. Subsequently the pollutant for which the emissions should be estimated is chosen. Based on this choice, a list of available satellite products can be given, but generally is not necessarily specified because these three inputs should be sufficient to determine the optimal choice of satellite product, which will normally be decided by the tool. Lastly a choice is made for the method to derive emissions of the selected pollutant within the region and time period of interest. Some methods will be more suitable for certain species and/or regions and hence an optimal choice will be suggested. This choice furthermore depends on the resolution and quality of the available satellite products.

Figure 8: General framework for the developed tool. The tool should eventually work for a multitude of pollutants, for which available satellite products will be selected based on the query of a user.



Source: this study

One particular stream (the one highlighted in Figure 8) in this workflow is fully developed in this project: the estimation of NO_x from TROPOMI and/or OMI images using various methods.

We will in this chapter elaborate on how this part of the tool is designed, but many of the components will be similar or will have counterparts with similar functionality in other applications. The developed part of the tool is initially designed to be able to derive German/national annual total NO₂ emissions from satellite imagery. It is intended to be flexible in target region and will hence be applicable to other countries. Furthermore, emission estimates for shorter time periods and spatial intra-country distributions of emissions are discernible.

Extensions to incorporate other methods, which have been presented in section 3.1, into the workflow should be possible, as well as extensions to other pollutants. With this type of flexibility, interest from and collaboration with other users is expected.

Taking the aims of public availability and easy collaboration into account a widely used and open-source language like python and a distributed version control system like git are suitable choices. Since the developed tools are to be operated on an online platform, this platform requires sufficient memory to store and handle satellite data and computational power to perform required optimizations.

3.3.1.1 Workflow – an example for NO_x emission estimates based on the Gaussian plume method

A graphical representation of the envisioned workflow with the stream that is developed for estimating NO_x emissions is shown in Figure 9. In this figure the solid grey lines refer to the optional components that can be added to this branch of the workflow. Solid connections refer to transfer of complete datasets while dashed connections refer to transfer of information to query selected parts of datasets.

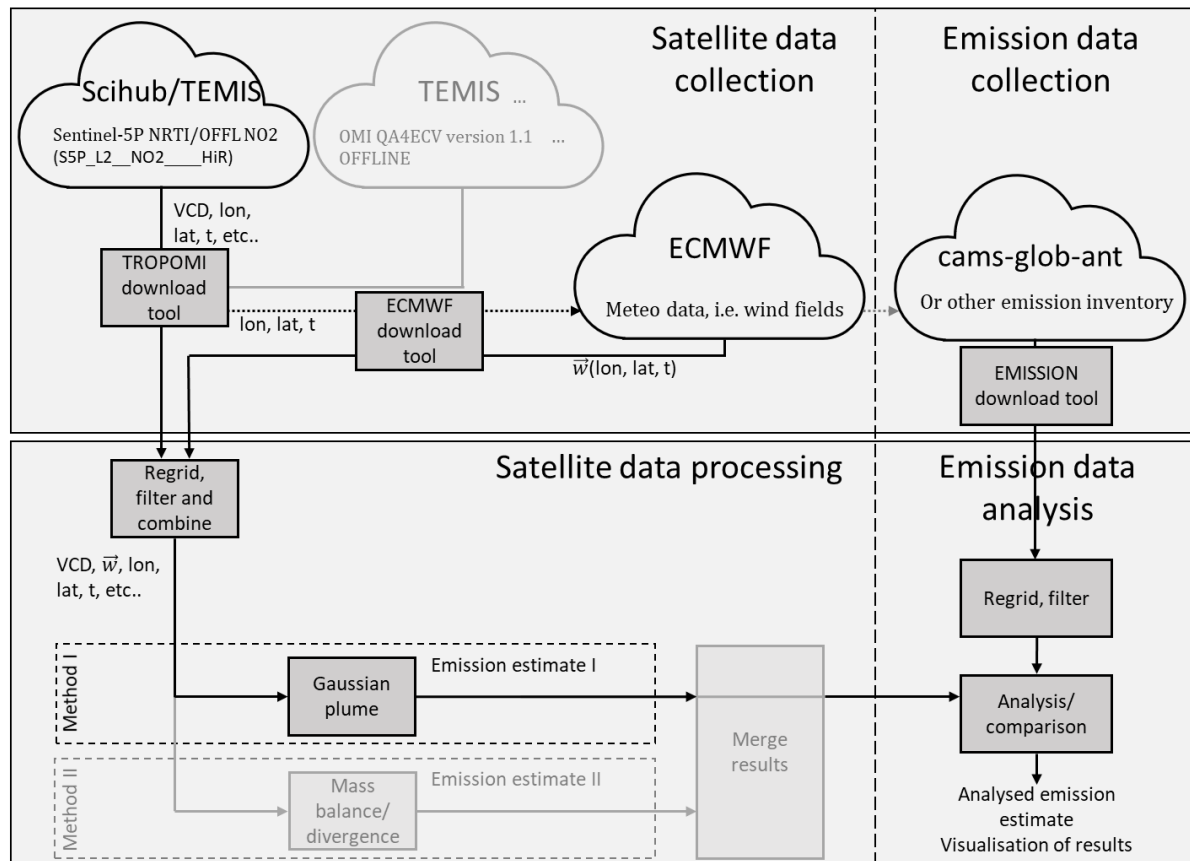
Scripts or functionalities are shown as dark grey rectangles. The data collection phase starts with a script (in this example NO_x case via a TROPOMI download tool) that is aimed at downloading data given a specific region of interest, time of interest and quality and cloud cover thresholds. Initially this script will be designed to download NRTI and OFFL L2 data from the SciHub open access datahub, but ideally should be extendable to other products and data providers with optimized regional products. Therefore, the TROPOMI download tool is incorporable into a bigger download tool that will eventually be able to download data from

various satellites and sources for different products, but currently has capabilities to download OMI, TROPOMI and ERA5 meteorological data.

After the satellite data is downloaded, wind fields matched with the longitudes, latitudes and times of the retrievals are downloaded from the ECMWF available at the Copernicus Climate Change Service (C3S) Climate Data Store (CDS) (this additional data stream is necessary for both the Gaussian plume-based method and the divergence method). Preselection of data to download based on longitude (lon), latitude (lat) and time (t) and/or only querying data at pixel level (potentially via the toolbox at CDS) could tremendously reduce the amount of data that needs to be collected.

Once both sources are queried and data is downloaded, the data collection phase is done. The next phase concerns the pre-processing of the data. The first step in the data processing phase will merge the acquired datasets. In this stage choices on how to deal with missing datapoints and what is a practical grid size and resolution should be made. Either in this step or the next smoothening (Gaussian, $1/r$ filtering or creating super observations) dealing with noise might be required dependent on the applied method. After this step the actual computation of the emissions takes place. In Figure 9 the method that is used is the Gaussian plume method. For this method the choice on what satellite product to use has been explained in the previous chapter. We will now elaborate further on which criteria to apply to select the observations from this product to use for computing emissions. The selection process is generalized and for most other emission estimation methods a similar approach should be used.

Figure 9: Graphical representation of the workflow(s) that has been developed in this project. The main workflow is displayed in black. (As an example, the Gaussian plume method is chosen, but the divergence method is likewise developed. Emissions derived from satellite data are compared to inventory data.



Source: this study

3.3.1.2 Data selection

In general satellite data products come with a quality indicator for each individual observation. This indicator can be used to select data that is considered reliable, accurate and/or meeting certain criteria. Here we give an example for the TROPOMI-NO₂ and OMI-NO₂ products, to be used with the Gaussian plume method.

TROPOMI

For each observation in the recommended TROPOMI-NO₂ product a quality indicator is provided, the so-called qa_value (f_{QA}), describing the status and quality of the retrieval result. This quality assurance value is a continuous variable ranging from 0 (low quality) to 1 (high quality) (also sometimes represented in percentage from 0 to 100). This is the main quality indicator for pixel selection, and all applications should use this to remove measurements with a qa_value smaller than the required threshold.

The qa_value is set to 0 if anywhere in the processing an error occurred. If this happens the record of the particular event that led to the underlying processing failure is stored in the processing quality flag. Removing pixels with a qa_value of 0 will be called validity thresholding.

Apart from warnings and errors, the qa_value depends on the solar zenith angle, tropospheric air-mass factor, quality of the DOAS fit, and filters unrealistic albedo values, which all influence the quality of the final tropospheric column total. Different values of the non-zero qa_value

indicate whether the footprint for example meets a maximum level of cloud cover, and whether there is snow or ice on the earth's surface below the retrieval. Higher surface albedos can hamper accurate determination of VCDs.

For advanced air quality applications a filter on $qa_value > 0.75$ is recommended. This removes cloud-covered scenes (cloud radiance fraction > 0.5), part of the scenes covered by snow/ice, errors and problematic retrievals. This so-called qa -thresholding will also immediately remove 'invalid' pixels.

An additional option to ensure high quality observations is selecting only a subset of pixels within the TROPOMI swath. At the edge of the TROPOMI swath the instrument uses a shorter integration time, resulting in smaller pixels but this also increases the overall noise level of the spectra, which affects the final retrieval. A study by Fioletov using the TROPOMI-SO₂ product illustrated the higher measurement uncertainties for the first and last 20 pixels and recommends to not use those edge observations (Fioletov *et al.*, 2020).

OMI

Like the recommended TROPOMI product the OMI product has an overall processing flag which together with several processing flags can help select the most optimal set of observations for a specific goal.

The first flag would be the processing flag, which indicates if any irregularities took place during the retrieval. By setting the `processing_error_flag` to 0, only valid observations are allowed. The second criterium is based on the Solar Zenith Angle (SZA). The assimilation scheme behind the slant columns has difficulties for observations under wintertime conditions in the high and very low latitudes, when the sun is very low near the horizon and sunlight hits the earth surface at relatively large SZAs. By filtering observations with a $SZA > 80$ degrees, this problem is removed. Similarly as described above for TROPOMI, OMI observations with cloud cover and observations with suspected snow/ice landcover can be filtered by setting the `snow_ice_flag` < 10 for snow free land pixels and the `snow_ice_flag` to 255 for ice free ocean pixels, and `cloud_radiance_fraction_no2` < 0.5 to ensure low cloud fractions. The next filter is based on the ratio between the tropospheric and total air mass factor. Conditions where the ratio is very large (> 0.2) typically happen under highly polluted conditions, where large amounts of surface NO₂ is potentially covered by aerosols/clouds which is hard to observe and potentially creates artificially large NO₂ columns.

When deriving trends one should also pay attention to use the same sampling conditions for the entire period. During recent years OMI's row anomaly has reduced the viewing capabilities (http://projects.knmi.nl/omi/research/calibration/instrument_status_v3/index.html) of the instrument to about 60% of the initial total. The problem varies over time and can introduce biases for long term analysis if not accounted for.

3.3.2 Mitigation of compatibility issues

For each method different compatibility issues can play a role and different mitigation strategies will be suitable. Here these issues (mentioned in section 3.2.6) and mitigation strategies will be discussed for each method for TROPOMI and OMI NO_x satellite data. For other pollutants other compatibility issues can play, or the extent to which these issues cause problems can differ.

3.3.2.1 Mass-balance methods

Spatial resolution

For the divergence methods the smearing effect of a coarse resolution will play a similar role at borders of regions and in general will have limited influence on results since regions of interest are likely much bigger than satellite footprints. Secondly smearing will cause a decrease in the divergence which can hamper the detection or accurate assessment of emissions. This resolution based smearing will be assumed negligible compared to the actual gradients around emission sources when these are detectable, but care has to be taken when smearing becomes large with respect to the actual gradients in the emission sources.

Instrument sensitivity

For the mass-balance methods the missed emission sources due to a limited sensitivity will again be directly reflected in the overall estimated emission totals. Based on the estimated sensitivity and number of days below the detection threshold the effect of such missed (and potentially overestimated) emissions can be estimated. A potential drawback is that initial knowledge on the actual emission is required and assumptions need to be made on the satellite product uncertainties to make an initial estimate of missed emissions. While over the German domain this effect is expected to be small, future applications to, less industrialized, regions could potentially miss an unacceptable amount of the emissions.

Uncertainty in satellite products

Limitations to the precision of the satellite products will make it more difficult to compute the divergence of the concentration fields. The same ways to reduce the effect of observations with high uncertainty/noise can be used as mentioned previously. Averaging several observations together either in time or in space into a single super observation as well as smoothening can be applied. These strategies again come at the cost of reduced temporal or spatial resolution or increased smearing of sources respectively.

Bias in satellite product

When the bias (accuracy) in the satellite product comes in the form of a fixed offset the mass balance method will not be affected because the divergence of this fixed term will vanish. However, if the bias is dependent on the concentration (as is the case for TROPOMI NO₂ with a positive bias for columns below $6 \cdot 10^{15}$ molecules cm⁻² and negative values above it (Verhoelst *et al.*, 2021)) corrections have to be made. Because of comparisons with ground based measurements these required corrections are sometimes available or the effect of the bias can be reduced by for example removing the lowest 5% of the observations to approximate the bias (Beirle *et al.*, 2019).

Temporal resolution of satellite product and temporal variability in emissions

Like the plume-based method the mass balance based methods assume a steady state at the time of the retrieval and a translation to annual totals or other time integrated periods can be made in the same way using posteriori time profiles at the cost of accuracy, especially in regions with non-linear chemistry.

Incidental emissions that create large perturbations in the concentration field will result in an overestimation of anthropogenic emissions, especially in regions where there are otherwise virtually no emissions. They will probably be easily discernible by the underlying time profile.

Missing data due to e.g. clouds

Gaps in the observation record will again need an adjustment to estimate final emission totals based on knowledge on the underlying time profiles. Hence it is important to consider the (average) time of the used retrievals to be able to make the translation to annual total emissions at a later stage.

Gaps in a-priori emission data

Missing emission locations in inventories do not have any effect on the mass-balance and Gaussian-plume methods because they operate independent of a-priori emissions fields. This is a strongpoint of both methods compared to relying on CTMs. Missing or misrepresented emission time profiles will introduce errors in these methods when these temporal distributions are used to scale emissions at satellite overpass times into time integrated totals. Most of the adjustments can be performed posteriori and thus can be replaced by any updated emission inventory.

3.3.2.2 Gaussian plume-based method

Spatial resolution

Coarse spatial resolutions can create a smearing effect in the estimated emissions. While for TROPOMI the spatial resolution is $\sim 7 \times 7 \text{ km}^2$ (with measurements since August 2019 having an improved resolution of $5.5 \times 3.5 \text{ km}^2$) at the border of countries pixels and the resolution of the final emission fields can cause partial overlap between multiple regions. Emissions for such regions need to be intelligently split between both sides of the border. In most cases this should be viable based on the dominant sources on either side of the border, but for regions with several overlapping sources, there can be remaining uncertainty due to attribution errors. In general this issue will have limited influence on results since regions are much bigger than satellite footprints. As the Gaussian plume method has not yet been applied to TROPOMI retrievals it is complicated to estimate the limits to the spatial resolution and regional size requirement. Throughout the development and usage of the methods these limits will become clearer, but Beirle et al's (2019) limits for the divergence method ($3 \times 3 \text{ km}^2$, 1 year data) are used as a first estimate.

Instrument sensitivity

For the Gaussian plume-based methods the missed emission sources due to a limited sensitivity will be directly reflected in the overall estimated emission totals. Based on the estimated sensitivity and number of days below the detection threshold the effect of such missed (and potentially overestimated) emissions can be estimated. A potential drawback is that initial knowledge on the actual emission is required and assumptions need to be made on the satellite product uncertainties to make an initial estimate of missed emissions. While over the German domain this effect is expected to be small, application to other, less industrialized, regions could potentially miss an unacceptable amount of the initial emissions.

Uncertainty in satellite products

Limitations to the precision of the satellite products will make it more difficult for the Gaussian plume method to fit measurements and introduce anomalous/artefact patterns in the fit. There are several ways to reduce the effect of the observations with high uncertainty. A common way to reduce the effect is averaging several observations together into a single super observation, which also coarsens the spatial resolution of the footprint. Another way is to increase the number of observations used for each potential source location, either by coarsening the target resolution for the emissions grid, lengthening the timespan, or subdividing the observations into smaller chunks. Another option is smoothening the final result (e.g. using Gaussian filters) which

comes at the cost of increased smearing of sources, and largens the effects of misattribution of emissions between nearby cells. If uncertainty turns out to introduce artefacts/problems, the first strategy to reduce noise would be a reduction in resolution through spatial averaging or filtering. Secondly, temporal averaging can be used to reduce uncertainty. If oscillations occur within the system due to under-constraining the problem, an additional basic dampening term will be added to the system.

Bias in satellite product

In the Gaussian plume-based method a few terms can be added to the linear system, for example a polynomial, to fit a potential bias (Fioletov et al., 2017). A large part of the bias in the TROPOMI-NO₂ product is induced by the coarse model input used to calculate the AMF factors. By recomputing AMFs with a CTM (for example LOTOS-EUROS) running at a higher resolution the bias can be significantly reduced. If we want to avoid relying on CTMs the AMF effects can be approximated based on literature whenever this is available. A high-resolution AMF will initially not be used but can be kept in mind if biases are found to introduce problematic errors that cannot be resolved by an additional polynomial fit or literature based bias corrections. High resolution AMFs are not usually a focus for data providers, and it will be challenging to find high resolution simulation runs to calculate the AMFs for the entire time period of interest.

Temporal resolution of satellite product and temporal variability in emissions

The plume-based method assumes a steady state at the time of the retrieval and needs to either introduce an a-priori correction or posterior adjustment (Dammers et al., 2019) to account for temporal variations to the seasonal and diurnal cycles. Since at the time of the overpass (fixed around a local time between 12:30 and 13:30) emissions are estimated, time profiles are required to make this posterior adjustment and translate the emissions at this point in time to annual totals. Similarly, incidental emissions and the higher resultant atmospheric concentrations, such as fires/biomass burning and plumes thereof, create large perturbations in the concentration field over a short period, but usually remain visible in the emission estimates for a long time. Depending on the plume shape and period of burning such emissions will either be approximated well (when using the Gaussian plume method) or create an overestimation of the emission field, especially in regions where there are otherwise virtually no emissions. The best way to cope with such observations is by excluding the periods in which the fires take place, or adjust for its posteriori, by removing the plumes or attributed emissions from the concentration/ divergence/emission fields. This can be achieved by taking an additional data stream into account from wildfire monitoring services or by creating wildfire recognition functionality (based on time profiles, CO products, characteristic albedo changes or additional infrared observations).

Missing data due to e.g. clouds

Missing data due to for example clouds and instrument outages can create gaps in the observation record. Plume-based methods will need an adjustment to the final emission totals using a similar approach as those proposed in the section on temporal variability. Hence it is important to consider the (average) time of the used retrievals to be able to make the translation to annual total emissions at a later stage.

Gaps in a-priori emission data

Missing emission locations in inventories do not have any effect on the Gaussian-plume methods because it operates independently from a-priori emissions fields. This is a strongpoint compared to methods relying on CTMs. Missing or misrepresented emission time profiles will introduce errors in these methods when these temporal distributions are used to scale emissions at

satellite overpass times into time integrated totals. Most of the adjustments can be performed posteriori and thus can be replaced by any updated emission inventory.

3.3.2.3 (Ensemble / Adjustment) Kalman Filter-based studies

Spatial resolution

For the KF based methods the spatial resolution does not necessarily hamper the capabilities to estimate emissions. The spatial resolution can be taken into account by the method when matching CTM output with measurements. It is known how to translate the atmospheric column concentrations discretized to the resolution of the CTM to the resolution of the satellite footprint.

Hence, a coarse resolutions will only hamper the method because high concentrations might be poorly discernible or when the model meteorology does not match the real life counterpart, but this is a general and fundamental concern when dealing with low resolutions and/or model comparisons. If the effect of smearing due to the coarse resolution makes it hard to decide which members of the ensemble better matches with the satellite retrieval the KF based methods will have a hard time to produce accurate emission estimates. This however would simultaneously mean that the quality of the retrieval is too poor to use for accurate emission estimates.

Instrument sensitivity

The incorporation of a CTM in KF based methods in combination with the expected uncertainties in the satellite products effects of missed emissions due to limited sensitivity can be estimated. If the sensitivity is known, which is usually the case, it can be taken into account in a similar way as the spatial resolution and will influence the synthetic measurement. In cases where the apriori emission fields have missing emissions, the instrument sensitivity will still play a role, but this will be the same with any of the other methods.

Uncertainty in satellite products

Limitations to the precision of the satellite products will make it more difficult to select or weight the ensemble members based on how well they reflect observation. However, since the noise is random and they will not hamper the weighted averaging as long as noise is small compared to variability in concentration fields. It is therefore likely that no mitigation strategy will be required. If necessary the averaging and smoothening can be applied to reduce noise.

Bias in satellite product

Both fixed and concentration dependent offsets will affect results from the KF based method. The former will lead to a corresponding mistake in all emission estimates while the latter will result in concentration dependent miscalculation. Either the synthetic measurements or the satellite observations can be adjusted to account for the biases. These corrections can be literature based when available.

If the bias is unknown, which is usually the case, another way to reduce its effect is by accounting for areas where biases are often most pronounced by introducing a larger observation uncertainty. Contrarily to the Gaussian plume or mass balance methods the time of the omitted retrievals will have a reduced effect on the overall emission estimates.

Temporal resolution of satellite product and temporal variability in emissions

Contrarily to the Gaussian plume and the mass balance based methods no steady state assumption is made and the time of the retrieval is intrinsically incorporated in the method. Any updated time averaged totals will be scaled based on a match between the synthetic and actual retrievals that were matched in time. It should however be noted that the overpass time of for

example TROPOMI is at an approximately fixed time of day and estimates will be particularly sensitive to a corresponding part of the time profile (a couple of hours prior to overpass time until the actual overpass time) used in the CTM. A structural misrepresentation of the emissions at this moment in time will have a stronger effect on the resulting emissions. Incidental emissions that create large perturbations in the concentration field that are not in the a-prior inventory will result in an overestimation of anthropogenic emissions similar to effect of the gaps that is mentioned at the end of this section. In both cases, emission results should be carefully analysed for large deviations in the diurnal and seasonal cycles.

Missing data due to e.g. clouds

Missing data due to for example clouds will simply reduce the amount of data that can be used to produce an emission estimate. The method will not be hampered in any other way by removal of data than reduced weighting of measurements in produced emission estimate or an increased weighting of the remaining measurements. Incidental emission can however completely be missed if observations are missing for a prolonged period, which can be corrected for posteriori using a similar method as with the Gaussian and mass balance methods.

Gaps in a-priori emission data

Since this method uses a CTM its crucial to have an accurate a-priori emissions dataset. Most Kalman Filter-based methods will scale the inputted emissions to match synthetic with actual observations. Missing emission locations in inventories will introduce errors in the KF based methods because neighbouring emissions will be scaled to account for the reduced pollutant concentrations seen in the model output. Similarly emissions in the inventory that are not actually present will lead to a reduction in the emission estimate of neighbouring emission sources. One can think of DECSO type of approaches (Mijling and Van Der A, 2012) that allow addition instead of scaling of emission sources in the update to mitigate the issue of gaps in a-priori emission.

3.3.2.4 Adjoint based methods

Spatial resolution

Like with the EnKF based method a synthetic measurement is computed in which the size of the satellite footprint is taken into account. Fundamentally the method will work with coarser resolutions, but logically the potential to fit very localized emissions is reduced due to the smearing effect of a coarse resolution.

Instrument sensitivity

In adjoint based methods a CTM is used and known uncertainties in the satellite sensitivities can again be used to estimate effects of missed emissions. Secondly, the sensitivity will influence the synthetic measurement and a reduced weight can be given to these measurements in the fitting routine. If this weight is reduced it simply results in less freedom for the model to deviate from the emissions that served as input to the CTM.

Uncertainty in satellite products

Limitations to the precision of the satellite products will make it more difficult to fit measurements with synthetic equivalents. This will be reflected by a poorer conditioning of the optimization problem that is solved in the adjoint based methods which can hamper the emission estimate. If necessary the averaging and smoothening can be applied to reduce noise.

Bias in satellite product

Also the adjoint based methods will be perturbed by both fixed and concentration dependent offsets. The same mitigation strategies as mentioned for the KF based method can be applied. Omission of outliers will probably be the most suitable strategy. The downside clearly will be the inclusion of less data and the potential of missing over- or underestimations of emissions if these particularly reveal themselves at the low or high end atmospheric concentrations.

Temporal resolution of satellite product and temporal variability in emissions

Like the KF based method, a CTM is required for adjoint based emission estimates. Hence temporal profiles of emissions are already incorporated in the model and the used optimization routine merely tries to match actual and synthetic retrievals that are coinciding in time. The update of the eventual time averaged emissions will hence account for the timing of the retrievals.

Similarly as mentioned for the KF based method, for retrievals at an approximately fixed overpass time will be more sensitive to a particular portion of the day.

Missing data due to e.g. clouds

Missing data has a similar effect on the adjoint based methods as mentioned for the KF based methods. Less synthetic data is matched to actual measurements in the optimization problem which results in reduced weighting of measurements in produced emission estimates. Enough data points should remain for the optimization to find a scaling for all parameters that are allowed to vary in the fit. This will however will quickly be the case since usually many retrievals are included in 3d and 4d var based methods.

Gaps in a-priori emission data

Since these methods are CTM based the same issues as encountered by the KF based methods will to an extent also apply here, as neighbouring emissions will be scaled to account for the reduced pollutant concentrations seen in the model output. Similarly emissions in the inventory that are not actually present will lead to a reduction in the emission estimate of neighbouring emission sources. In case of 4d var methods typically more observations will be used to adjust a single (emissions) parameter, therefore effect of missing a-priori data will be reduced compared to EnKF/3dVar methods.

3.3.3 Other openly available software

There are toolboxes that allow the computation of level 3 products based on the level 2 products mentioned in the previous chapter. For example, the Atmospheric toolbox (<https://atmospherictoolbox.org/>, an open-source software for scientific analysis of atmospheric earth observation data) provides useful tooling for downloading and handling of satellite data and allows for 'inhouse' production of level 3 data. In this toolbox other functionalities focussed on for example data visualisation and model comparison are available.

The Atmospheric toolbox is part of the broader Sentinel toolbox which also incorporates functionality for handling of Sentinel-1, Sentinel-2 and Sentinel-3 data. Many other openly available toolboxes exist, but their focus usually mainly lies on image recognition and segmentation rather than assessment of the atmospheric composition. Specifically, for TROPOMI tools are listed on <http://www.tropomi.eu/tools>. Two visualisation tools (Panoply and ADAGUC) are listed as well as a tool for inter-comparing satellite or model (Harp) and a tool to perform checks on L2 data (PyCAMA).

Often the capabilities of the available tools do not exactly fit the demands to answer a specific question or perform a particular task and it can be challenging to add to or alter these capabilities. These functionalities will hence be developed within this project and made online available.

3.3.4 Potential role of a CTM

There are three important gains that the inclusion of a CTM or basic output from a CTM can have in the workflow.

- ▶ Method validation and uncertainty/sensitivity estimation.
- ▶ Improvement of the methods currently mentioned in Figure 9.
- ▶ Ability to extend to methods that require CTMs

For a CTM the emission fed as input to the model run are known and hence can be used to see how close the derived emission estimate comes to the truth. This comparison can also shed light on the type of emissions that are missed or not estimated correctly (if any) because a CTM makes it possible to assess where concentrations originated from. Furthermore, noise and biases can be introduced at various steps in the processing pipeline to investigate how errors propagate through the system.

The mass based and Gaussian plume-based methods generally use fixed values for the lifetime (τ) of NO₂ and for the NO/NO₂ fraction (r). These parameters are in reality varying in space and time. How much this variation is and taking this variability into account becomes possible when a CTM is included. The error introduced with the introduction of a fixed lifetime can also be assessed.

The other two methods described in section 3.1.4, e.g. adjoint based and EnKF based method, have the usage of a CTM as a prerequisite. These methods will not be discussed further, but it should be noted that extensions to incorporate them into the tool can eventually only be achieved by using a CTM.

There are also clear drawbacks of incorporating a CTM. The most severe ones are the increased complexity, increased data demand, and increased computational burden. Dealing with these drawbacks will require an enormous effort, which is beyond the work presented here.

3.4 Development of the tool

3.4.1 General Description

A python based open-source toolset with the functionality described in previous sections has been developed and is available through GitHub (<https://github.com/UBA-DE-Emissionsituation/space-emissions>). Figure 10 shows an overview of the tools in this repository. It should be noted that the framework this tool is cast into is designed to be flexible with respect to the choice of pollutant and satellite. Currently the quantification of NO_x emissions from OMI and TROPOMI observations is developed, but extensions to other pollutants and satellites are possible within the framework. The expert filter shown in Figure 8 that allows a user to choose a satellite is currently not developed since from the choice of current satellites the only logical choice for most users will be to derive emissions from TROPOMI data, when this is available and to only resort to OMI when TROPOMI is not available (prior to October 2017).

The GitHub repository contains modules that can be used to download satellite data (both OMI from TEMIS and TROPOMI using the Sentinel API), ERA5 meteorological data using the CDS API

(Climate Data Store) and derive emission estimates based on several methods, such as the naïve approach, Gaussian plume fitting routine (Fioletov et al., 2017) and the divergence method (Beirle et al., 2019, 2021). A trend in emissions can be derived by application of this tool for various years. The functions can be run using exemplary Jupyter notebooks that are likewise available in the GitHub repository. These notebooks can be used to interactive launch (parts) of each module in a stepwise fashion and display intermediate results thereby giving an overview of the functionality of the tool.

A webapp to easily use the tools in this repository and accompanying tools to visualize results has also been developed (space-emissions.net). This webapp runs on the CODE-DE Cloud, which offers extensive computing resources for processing and generous storage space. On this platform, the satellite data of both TROPOMI and OMI is available for long periods. Furthermore, the corresponding ERA5 wind fields have been downloaded with the download module and pre-processed into subsets for easy reading and further operations (combined and re-gridded wind- and VCD fields stored as patch-based aggregated datasets to be ready for calculations of emissions). This availability of the data in smaller chunks saves the time it takes to download and pre-process data that will be required when running the tool for the first time. If a region or period is selected for which the data is not available yet on the CODE-DE server, the download tools will run to collect the missing datasets.

In the next sections we will describe in more detail the composition of the verification tool in the GitHub repository and how the webapp works in practice.

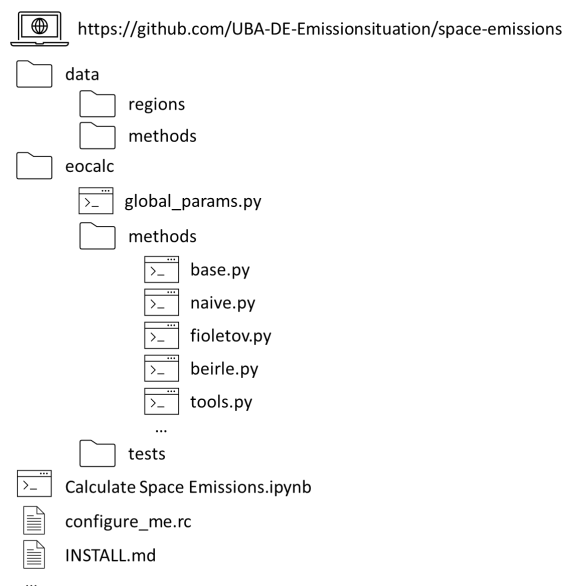
3.4.2 Open Source version

The tool that is available through the GitHub repository is composed of several components. These components are shown in the repository overview in Figure 10. The essence of the tool is found in the eocalc folder. This folder contains the emission estimator package, with all relevant scripts and functions to estimate emissions from satellite observations.

The core routines of the naïve summation, Gaussian plume fitting (Fioletov et al., 2011) and divergence based methods (Beirle et al., 2019) can be found within this folder in respectively `naive.py`, `fioletov.py` and `beirle.py`. Each of these methods comes with an accompanying set of tests, which can be found in the eponymous files in the tests folder. The tests are used to check if the functions used within the various methods work as intended and produce the expected output for a given input.

The eocalc/methods folder furthermore contains `tools.py` which is a collection of functions that have an application more general than a single specific method, for example functions that compute windspeeds, wind directions, plumes fields, combine satellite and meteorological data etc. The eocalc/methods folder furthermore contains `binas.py` which contains a basic selection of natural constants and other standard parameters, for example the radius of the earth and various atomic weights. Furthermore, `download.py` can be found in the eocalc/methods folder, which contains the required functionality to download TROPOMI, OMI and ERA5 data.

Figure 10: An overview of the tool components in the GitHub repository.



Source: this study

To enable direct out of the box utilization, initial instructions are written in the `INSTALL.md` file to create a python environment with all the required packages. Besides the python environment a data folder accompanies the repository that contains small data files used in the exemplary Jupyter notebooks (.ipynb) which will enable users to familiarize themselves with the various functionalities the tool offers.

The repository comes with a runtime configuration (.rc) file called `configure_me.rc`. This file contains settings that a user needs to modify for the tool to function properly. It contains information on where data is stored locally after collection, user specific login information for the Copernicus data store and for the Sentinel API, platform specific settings on memory usage and method specific settings like resolution and other tweakable parameters. The exemplary Jupyter notebooks work without modifications to `configure_me.rc`, but collection of data that is not available in the repository will require setting changes. The script `global_params.py` reads this configuration file and changes setting into global variables that can be used within other scripts.

The subfolder `regions` within the `data` folder contains sample regions in geojson format that are used in the exemplary Jupyter notebooks and tests. The `data/methods` folder contains sample satellite data likewise used in notebooks and tests for the respective methods. Only sample data files are provided because complete satellite data files when downloaded directly are too heavy (for example ~25Mb per day for OMI) to be added to the repository.

In the method modules (`fioletov.py`, `beirle.py`, `naive.py`) initial settings are used that can (should) be adjusted for the local machine/server by making changes to the configuration file. Examples of these are the pathways to the required L2 datafiles and the meteorological data, satellite names, data-product versions and global variable names.

In the `fioletov.py` module the Tikhonov/Dampening parameter, `mem_limit`, and target resolution of the grid are the three important parameters. The resolution is set to 0.2x0.2 degrees, mostly to limit the load on the server. The `obs_to_mem_limit` is also set to a fixed number of 2x10⁹ values and is used to limit the memory load of the $Ax=B$ problem that the algorithm is trying to solve. Further parameters are pollutant dependent, such as the lifetime (decay rate) and the plume width (diffusion + footprint). The dampening parameter is currently set to 0.009 based on

tests with simulated concentration and emission fields for a region similarly sized to a combination of Germany and the Netherlands (Chemistry Transport Model, LOTOS-EUROS).

In the `beirle.py` method a much higher resolution of 0.027×0.027 ($\sim 2.5 \times 2.5 \text{ km}^2$) is used, but dampening plays no role because no optimization is performed. The divergence of the flux field is computed with numerical derivative as the fourth-order central-finite difference approximation. This choice was based on the original publication but other differentiation schemes are also available for further testing.

A trade-off between what should be tweakable by a user and user friendliness is always made. Addition of more tuneable parameters also creates more opportunities to try and solve ill posed problems or arrive at nonphysical solutions for the emission estimates. Therefore the choice was made to hardcode the aforementioned parameters in the configuration file after an analysis showed what the optimal choices are (based on the results for simulated emission and concentration fields).

It should be mentioned that the dampening in the Fioletov method is related to the number of grid cells in the domain and thus the resolution of choice. Allowing a user to freely set these parameters would potentially lead to the computation of nonsensical solutions. However when an expert user knows what he or she is doing the parameters are easily tuneable within scripts associated with the various routines.

Besides the tool description provided in this report, further information can be found in the wiki that is attached to the GitHub repository. The wiki contains a description of the tool in a Nutshell that explains what is found in the various folder in the GitHub repository, a simple web app mock-up to show how the web app functions, and a description of methods used for deriving emissions. Furthermore, within the python files further documentation can be found, with extensive descriptions of the input and output parameters.

3.5 Tool results

3.5.1 The German 2019 National Emission data

The tool was applied to collect and process L2 OFFLINE TROPOMI data for the year 2019 as well as matched ERA5 wind fields. On this dataset the various tools were applied to estimate 2019 annual total NO_x emissions for Germany as a whole.

The output from the Naïve method, i.e. from `naive.py`, has been divided by the lifetime of NO_2 ($\sim 4\text{h}$) to account for the chemical losses in a similar way as is done in the other methods. All results are multiplied by 1.32 to convert the satellite measured NO_2 into NO_x . Results are by default presented for the selected pollutant, thereby corresponding to the specie in the satellite product (i.e. in this case NO_2). The average $(\text{NO}_2 + \text{NO})/\text{NO}_2$ ratio is reported to be around 1.32 (Beirle *et al.*, 2019). The outcomes of these computations together with the national bottom-up reported emissions from the gridded NFR emissions inventory (for 2019, gridded NFR (GNFR), CLRTAP, [Submission 2021 \(europa.eu\)](#)) are shown in Figure 11. Due to reporting guidelines a number of sources, such as Natural sources of NO_x emissions (for example lightning and biological decay), are not included in the reported National total for compliance with the CLRTAP for Germany. These emissions are reported as so-called memo items in the NFR While the total emissions of these memo items are estimated at 207 Kton (2021 submission) the contributions of the emissions within Germany are expected to be small compared (up to a few %) to the emissions with anthropogenic origin. The memo items, and a back of the envelope estimate of each of their contributions, are discussed in more detail in section 3.5.3.

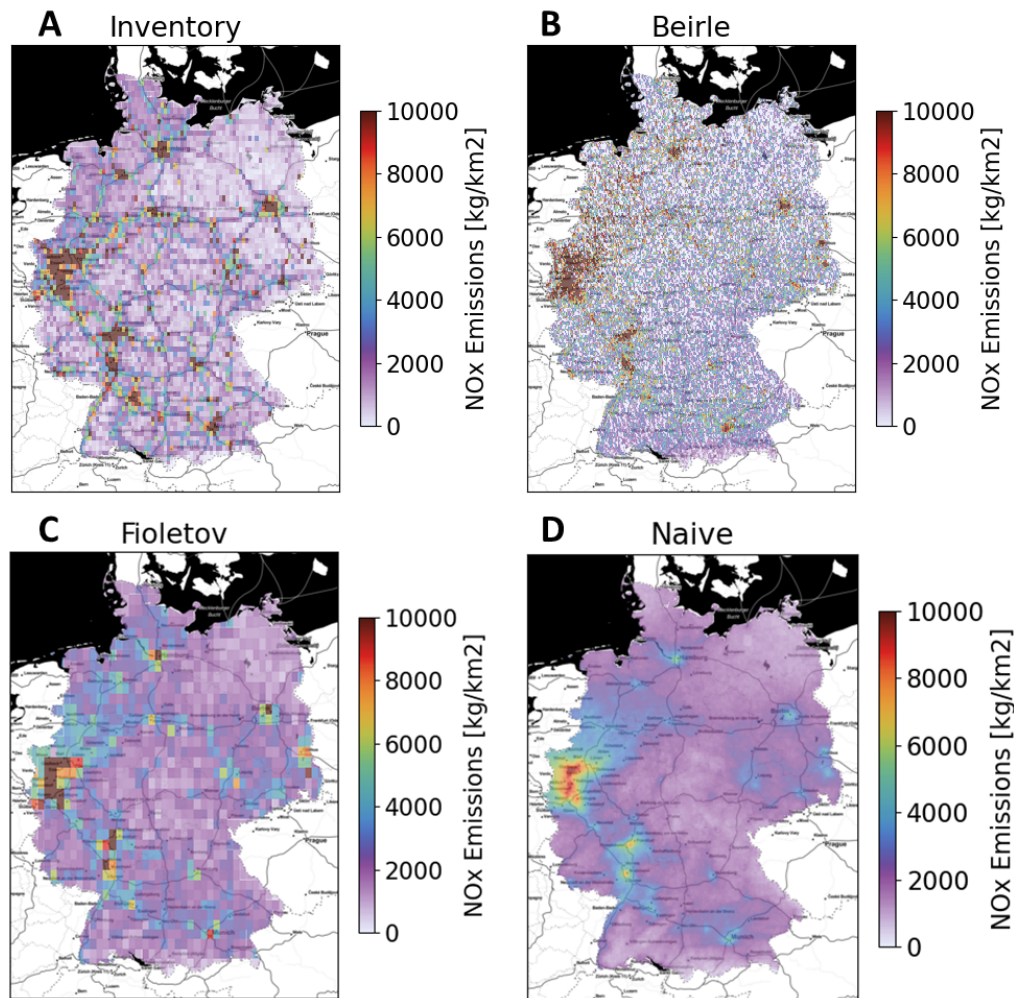
The spatial distribution found in the gridded inventory (Figure 11A) is captured well by all three methods (Figure 11). The largest pollutant concentrations are observed by TROPOMI over the largest source areas (highways, cities, industrial sites), such as the Ruhr valley and major cities such as Hamburg, Munich and Berlin. and all three methods give high emissions for these source regions.

The divergence method (Beirle *et al.*, 2019) shows a high-resolution distribution with large spatial gradients in the emissions as seen in Figure 11B. This is due to the computation of a derivative on noisy data. This can mostly be explained by the relatively high resolution (0.027 degrees) at which this method is applied (following the same resolution as the original publication by Beirle *et al.* (2019) as well as by the resolution of the (meteorological and satellite) input data. Nevertheless it seems that regions of high emissions are captured and the magnitude of the emissions is in agreement with the bottom-up emission inventory. Large point sources and larger industrial areas around cities show smearing of the emissions, due to the effects of diffusion and the limitations of the satellite footprints. The regional emission totals however are more comparable to the inventory.

The Gaussian Plume fitting routine (Figure 11C) (Fioletov *et al.*, 2017) and Naïve method (Figure 11D) show a much smoother emission distribution than the divergence method. For the former it is inherent to the method since Tikhonov regularisation is applied. It is also a consequence of the difference in resolutions since the Divergence method is applied on data with a resolution of 0.027 degrees while Fioletov is applied at a resolution of 0.2 degrees. The naïve method does not incorporate any method to account for transport and diffusion and will simply show the smooth average of the TROPOMI-NO₂ fields.

Results from the Gaussian Plume fitting method shows good agreement with the inventory with large point sources at corresponding locations and even busy highways seemingly appearing in the emissions estimate. The Naïve method is also able to retrieve the main distribution of emission sources, although the gradients over the domain are less pronounced. The emission estimates over the heavily emitting source regions are lower than the inventory and lower than the estimates from other methods. The underestimation can be explained by the fact that the Naïve method does not account for transport. Plumes will not be traced back to the location they originated from and hence will be misattributed to the underlying cells instead of the original source. Looking at higher resolutions, in general source regions with high emissions will thus be underestimated and adjacent regions will be overestimated due to this smearing effect.

Figure 11: Maps of Germany with yearly total NO_x emissions in kg/m². A) Emissions according to the gridded NFR (GNFR) inventory (CLRTAP) for 2019 B) Estimate using the divergence method for 2019 (Beirle et al., 2019) C) Estimate using the Gaussian plume-based fitting routine for 2019 (Fioletov et al., 2017) D) Estimate using the Naïve method(direct VCD summation) for 2019.



Source: this study

The results in Figure 11 are also evaluated grouped at the various administrative levels such as the German Bundesländer/federal states. By comparing emission estimates at various regional scales, a light can be shed on the quality and limitations of each method to determine emissions for the smaller administrative levels. The data is aggregated to 4 different administrative (ADM0-3, NUTS0-3) levels. The first is the German national total (ADM0), the second, the totals of the German federal states (ADM1), third, governmental regions (*Regierungsbezirk*, ADM2), and lastly the district level (*Kreis*, ADM3). In the total emissions for 2019 summed per federal state (Bundesländer) are given.

Figure 12 shows scatterplots comparing the inventory totals to the satellite based estimates at ADM1 to ADM3 levels, and gives an overview of the corresponding statistics.

The total national (Administrative level 0) German NO_x emissions in 2019 are 1136.5 kton according to the 2019 GNFR inventory used for comparison (gridded NFR, CLRTAP, [Submission 2021 \(europa.eu\)](#)), which is in close agreement with results for 2019 from the divergence method (1260.7±51.6%kton) the Gaussian plume fitting method (1241.0±50.5%kton) and surprisingly similar to the estimate using the naïve approach (1097.1 kton ±40.6%). Note, that

gridding effects can lead to small differences in the summed totals which here result in the inventory emissions as presented in Table 4².

The city states of Berlin, Bremen and Hamburg are not included in Table 4 as the surface area of these states is a lot smaller than average, and at the limit of the methods to produce accurate estimates. The fact that the national emissions are captured well by the naïve method is an indication that the difference between the NO_x that is emitted outside Germany but ends up in Germany and the NO_x that is emitted inside Germany but ends up abroad is small compared to the total national emissions.

Table 4: The annual emission totals of German federal states (in kt/yr and excluding city states) according to the GNFR inventory, the divergence method, the Gaussian plume fitting method and the naïve summation method.

Region	Area (km ²)	Inventory (GNFR, kt)	Beirle estimate (kt)	Fioletov estimate (kt)	Naïve estimate (kt)
Baden-Württemberg	35.752	113.1	123.6	117.0	103.5
Bavaria/Bayern	70.552	162.4	212.7	204.9	185.9
Brandenburg	29.479	68.5	81.4	87.4	82.6
Hesse	21.115	73.9	75.9	74.7	69.4
Lower Saxony/Niedersachsen	47.609	123.3	163.1	170.3	152.3
Mecklenburg-Western Pomerania	23.180	25.3	43.5	48.3	45.4
North Rhine-Westphalia	34.085	266.7	228.5	221.7	181.3
Rhineland-Palatinate	19.853	56.9	81.8	69.9	67.1
Saarland	2.569	12.0	10.3	9.9	8.2
Saxony	47.609	60.0	71.1	68.7	56.6
Saxony-Anhalt	23.180	48.4	66.3	63.4	59.4
Schleswig-Holstein	34.085	42.4	43.2	48.9	40.1
Thuringia	19.853	26.2	43.1	39.3	37.5
Germany TOTAL incl. city-states	357.022	1119.1*	1260.7 (±51.6%)	1241.0 (±50.5%)	1097.1 (±40.6%†)

² Please note that since the analysis a revised estimate for the National NO_x emission in Germany came available. The NO_x emissions amounts to 1108.8 kton for 2019 which is 27.7 Kton (about 2%) less than the estimate from the former submission used in the above analysis.

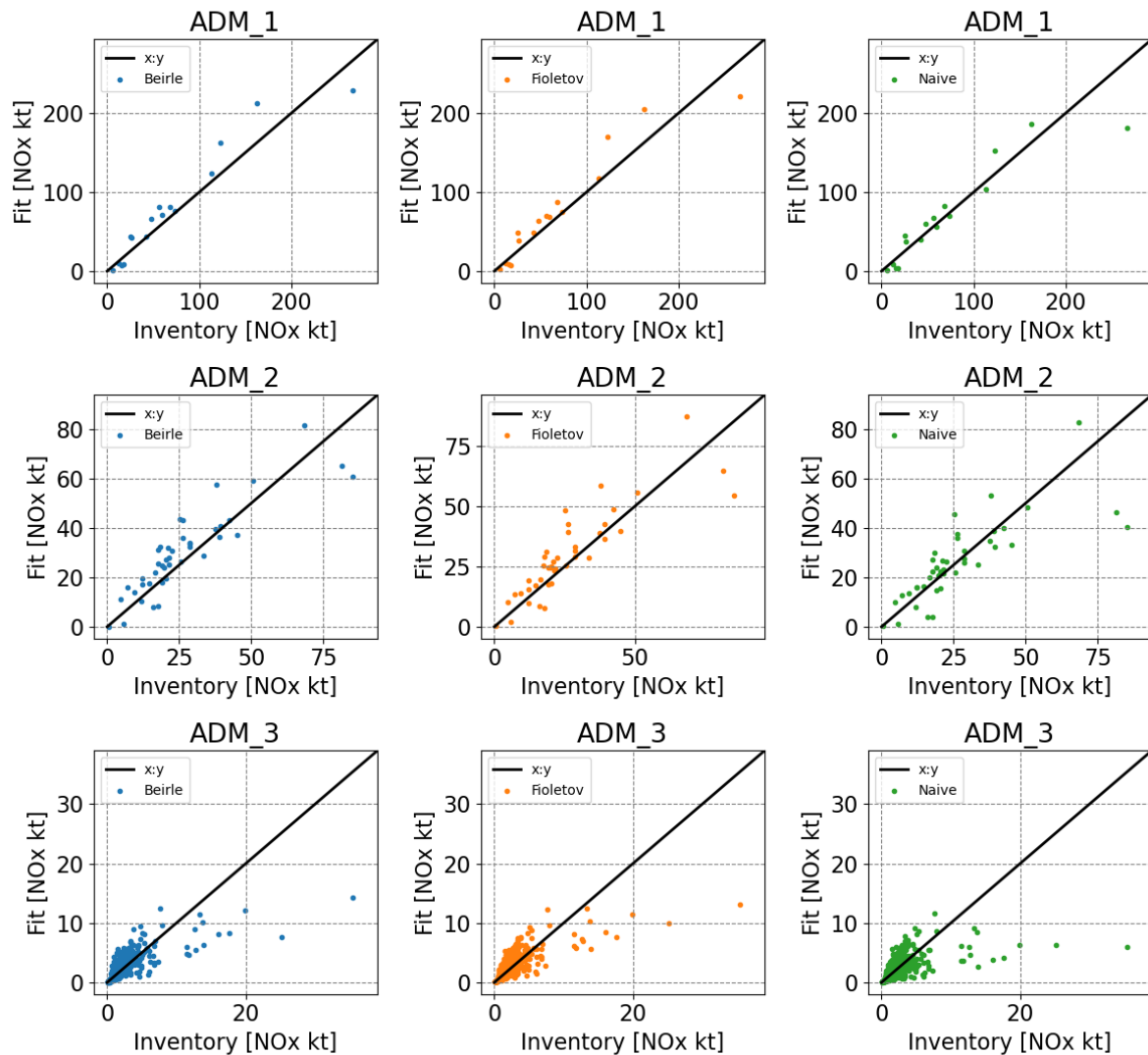
The uncertainties are based on the estimated variability of the individual terms and should be seen as the upper limit.

*Note that this reported inventory total is after cut off by the administrative borders polygon used in this study. ‡It should be noted that this reported uncertainty is lower than that of other methods because it is purely based on statistical uncertainties in VCD values, lifetime and structural uncertainties, due to e.g. advection/diffusion are ignored.

If the estimates from the various methods for each federal state (ADM1) are plotted against the inventory totals the plots in the top row of Figure 12 are produced. Overall, it shows that the satellite-based emissions are well correlated to the inventory, as can also be seen by the statistics in Table 5. At this high level of aggregation there is already (limited) visible misattribution of emissions. For example the estimated emissions of North Rhine Westphalia are too low compared to the inventory, due to misattribution of emissions to the Netherlands and the surrounding provinces (e.g. Lower Saxony, Rhineland-Palatinate). A solution could be to first fit and subtract the stronger individual point sources (with a Gaussian function, similarly performed by Beirle et al., 2019) and then aggregating to a lower spatial level, which could reduce the smearing effects for all methods.

Adding more details by computing the emission per governmental region (ADM2) or district (ADM3) produces the second and third row. At ADM3 level it is clear that the differences between the estimated emissions and the GNFR inventory increase for several locations, which for most can be linked to the misattribution of the emissions by each of the methods, due to not accounting for transport (naïve), not accounting for diffusion (Beirle), and the dampening factor (Gaussian plume method). An example of this is the datapoint with the highest emissions in the inventory, which corresponds to the region Rhein-Erft-Kreis which contains the huge point source emissions from two power plants (Neurath and Niederaußem). Its emissions are smeared out over large regions by each of the methods which consequently leads to an underestimation of the estimated emissions. As mentioned above for the Naïve method specifically ignoring transport will cause an additional smearing effect and subsequent additional underestimation of local emissions.

Figure 12: Scatter plot of the inventory vs estimated emissions for the various methods applied at various scales.



Source: this study

The statistics between estimated emissions and emissions reported in the inventory (Table 5) clearly show that the correlations and fitted slopes at the Bundesländer administrative level are close to one and intercepts are small (<10 kton) implying the methods are able to accurately estimate emissions at Bundesländer scale (if we assume that the inventory is a close representation of the actual emissions). When moving to smaller geographical areas the performance degrades for all three methods, with better performances of the Beirle and Fioletov methods, which account for transport effects. The estimated and inventory emissions show a reduction in the fitted slopes of the scatter plots, which can be explained further by the bar plot Figure 13. In this figure the emission distributions shown in Figure 11 are grouped based on local emission strength and compared to emissions reported for that location in the emission inventory. For all three methods the middle panel shows that lower emissions are overestimated, while the higher emissions are underestimated.

One of the explanations for the observed differences is the geographic misattribution of emissions, but part of the differences can furthermore be explained by other uncertainty terms. Next to uncertainties in the emission inventory itself (even though strong point sources are usually accurately represented, this does not always hold true for diffuse sources) differences

between the inventory and the emission estimates can come from inaccuracies in the used emission estimation method and data.

Firstly, there is the TROPOMI-NO₂ product. As stated earlier in this report the current TROPOMI-NO₂ product overestimates concentrations in background/low emission regions (+a few %) while having a negative bias in source regions (-35%, up to -50% in extreme cases). This is mostly due to inaccuracies in the air mass factor (AMF) which comes from uncertainties in the underlying modelled concentration fields and missing variations in the stratospheric NO₂ concentrations. A possible mitigation strategy would be using an overpass dependent bias correction which should resolve the variations in the AMF due to stratospheric Ozone, which spatially can vary significantly at a domain level. Local variations due to errors in the AMF cannot be corrected for without the use of a CTM and can lead to under and overestimation of emissions in high source and background regions.

Secondly, while the assumption of a 4(±25%) hour lifetime seems to be correct for 2019 Germany as a whole, an underestimation of the chemical losses could lead to an overall overestimation of the emissions, and vice versa an overestimation of the lifetime can lead to an underestimation of the emissions.

Other possible causes for over or underestimation of the emissions are the diurnal and seasonal variations (expected to be several % for the seasonal variations). Currently a fixed parameter was determined for the whole German domain, but locally especially the diurnal correction factor can be lower for the more continuous emissions, for example in the case of powerplants, and thus in effect create a negative bias for emissions. The NO_x to NO₂ ratio can also have local variations, which affect the total emissions. Beirle et al. (2021) recently gave a modelled estimate of the ratio, which was very close to the factor 1.32(±20%) given in his original study, with values moving towards 1.0 for industrial areas just north of the equator while values tended towards higher ranges (1.6) for less industrialized and high-latitude regions. Finally we have the wind fields, for which we estimate an uncertainty of up to 2m/s in mountainous and hilly areas. The effect can move in both directions and translates into an uncertainty of around 30% for average conditions over Germany (based on the matched wind fields).

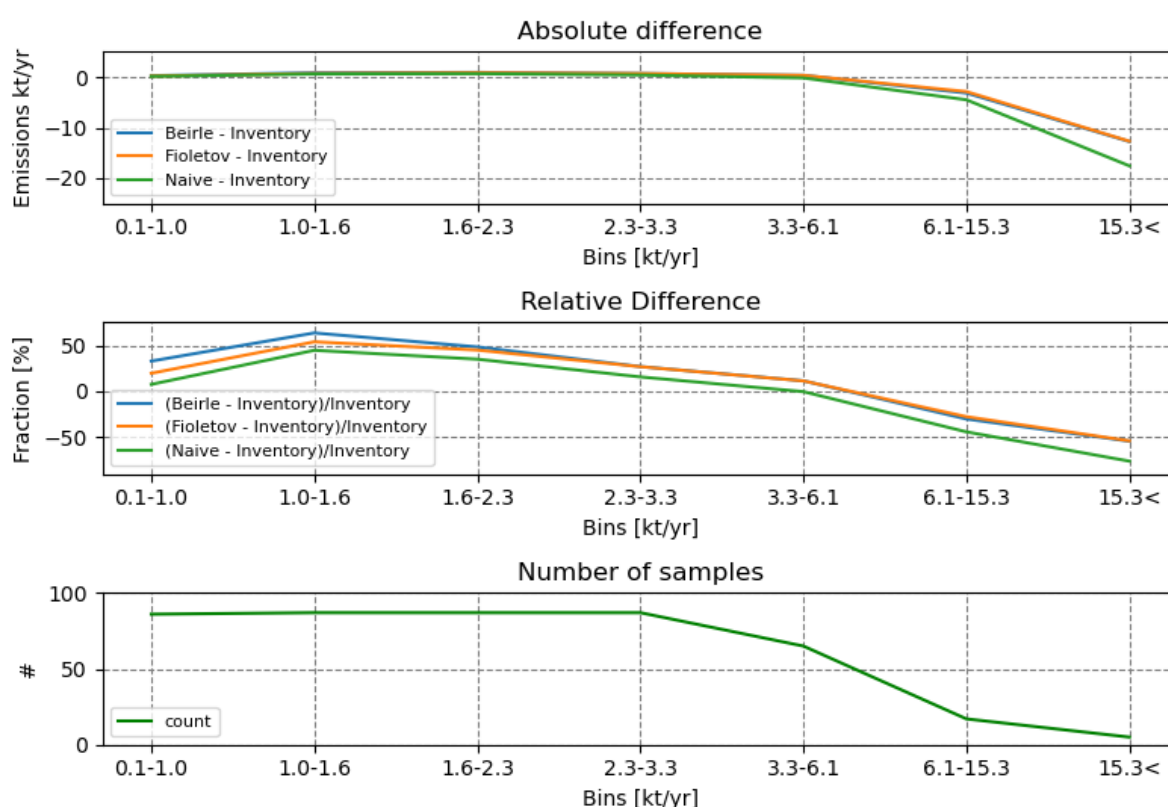
Taken together, these uncertainty terms translate into a Germany averaged uncertainty of around 51.6% for the Beirle approach, and 50.5% for the Gaussian plume method. These values should be seen as an upper limit, which would occur in the extremely unlikely case that the inaccuracy in NO_x:NO₂ ratio, lifetime, AMF and wind fields all nudge the estimate in the same direction for all locations in the domain of interest. In reality not all errors point in a similar direction, with the AMF/concentration term pointing in opposite directions for background and source regions.

Table 5: Statistics of the scatter plots in Figure 12 that quantify the performance of the various methods.

Admin code	Beirle slope intercept R*			Fioletov slope intercept R*			Naïve slope intercept R*		
Admin code 1 (Regions/states now including city-states)	1.03	7.12	0.96	1.00	7.62	0.95	0.88	7.47	0.93
Admin code 2 (governmental districts)	0.93	5.19	0.88	0.97	3.86	0.86	0.85	3.49	0.78
Admin code 3 (municipalities)	0.68	1.16	0.71	0.68	1.10	0.73	0.59	1.02	0.52

*Pearson correlation coefficient.

Figure 13: Line plots to compare the inventory with estimated emissions for the various methods applied at the ADM 3 level (admin code 3, i.e. district level).



Source: this study

3.5.2 Trends in German National Emissions based on OMI data

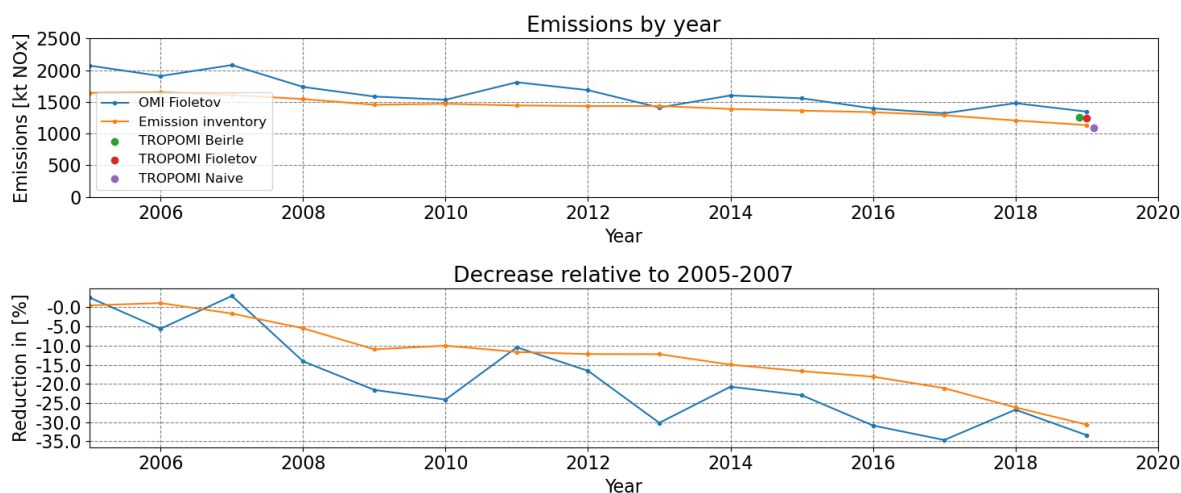
To assess how the German NO_x emissions have evolved between 2005 and 2019 OMI satellite data was downloaded and the Fioletov plume fitting routine was applied for each year separately. Since TROPOMI was launched on 13 October 2017 it can only be used to assess the

trend in recent years. OMI was launched on July 15, 2004 and hence allows exploration of longer time periods. The coarseness of OMI data ($13 \times 24 \text{ km}^2$) does not allow utilization of the divergence method (Beirle et al., 2019) with the default settings (0.027° spaced regular latitude-longitude grid which corresponds to 3 km in the latitudinal direction). To alter this resolution will lead to differentiation from the initial publication and would require an additional investigation of the validity of this method at a much coarser resolution.

The trend derived from OMI observations using the Fioletov method is presented in Figure 15 for the different reporting years. A general downward trend in NO_x emissions is found, which is in agreement with negative trends reported in emission inventories (Submission 2022). The derived emissions in 2017-2019 are on average about 25% lower than in 2005-2007. This observed reduction is in agreement with the reduction in the emissions as reported in 2021 (shown in Figure 15) and with the 23% reduction found between 2005-2007 and 2017-2019 period in the 2022 NFR reported totals based on fuel sold [Submission 2022]. When the emissions are split to individual NFR sectors, it can be seen that the downward trend in reported emissions is mainly realized through a reduction in traffic emissions (Figure 15).

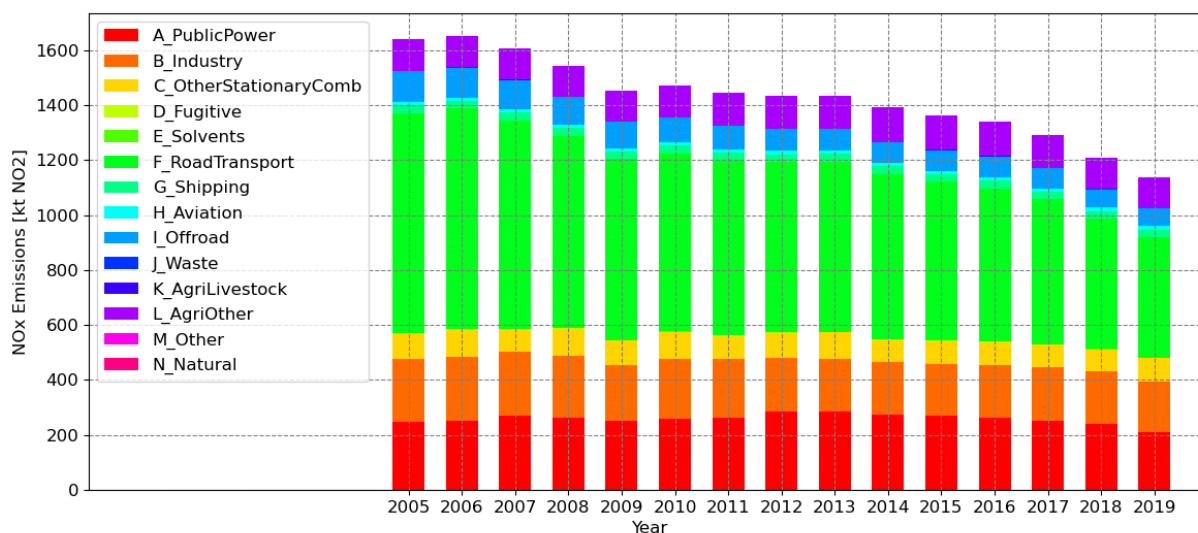
The yearly fluctuations seen in the derived emissions from OMI in Figure 15 can be a result of inaccuracies in the applied method that were discussed in the previous section, but can also reflect actual emission differences between years (even though these fluctuations are smaller as shown by the orange line in Figure 14). For example it might be that in cold winters power demand is higher which will result in higher emissions. An inaccuracy related to the method that is likewise weather dependent can be found in the lifetime. The same lifetime assumption was applied for all years, while meteorological conditions vary from one year to another. These conditions influence the chemical interaction in which NO_2 is lost. For example the amount of UV radiation influences the ozone concentration, and the temperature and humidity influence NO_x dry depositions. Both of which will affect the effective lifetime of NO_x . To investigate if the interannual fluctuations can be explained by any of these factors the impact of weather conditions of the individual years would have to be investigated in more detail. This could for example be done by simulating the NO_x concentrations fields for several years while keeping the emissions constant.

Figure 14: Trend line in national German NO_x emissions (in kt NO_x). The blue line in the top figure shows the emissions per year derived from OMI observations with the Gaussian plume fitting routine and the orange line shows the inventory. Colored dots show the TROPOMI-based estimates for 2019. The bottom graph shows the relative decrease with respect to the average annual emission estimate for the 2005-2007 period



Source: this study

Figure 15: Trend in reported German national NO_x emissions. Source: 2021 NFR submission. The contributions of the various sectors to the total emissions are distinguished. It is clear that the total reduction is mainly realized through a reduction in traffic emissions (F_RoadTransport).



Source: this study

3.5.3 Discussion on comparison of NFR national and satellite derived emission estimates

When comparing the results from the satellite observations to the inventory totals an important point to take into consideration is that the national inventory totals as reported in the NFR do not represent the actual total of all emissions within Germany. Furthermore, as explained in the previous paragraph the reported national total emissions in the inventories and the actual amount of pollutants in the atmosphere above a country are not directly comparable.

Due to the international reporting guidelines the emissions a number of sources are not included in the reported National total for compliance with the CLRTAP for Germany. These emissions are reported as so-called memo items in the NFR. The total NO_x emissions in 2019 of these sources are estimated at 207 Kton (2021 submission).

However not all these emissions will show up in the satellite observations. All satellite and inventory emissions reported in the previous sections only include those observed within the borders of Germany. This means that emissions at sea were not included in the emission totals. In this paragraph a further analysis (from the satellite perspective and the applied method) will be presented to elaborate on the issues which should be taken into account when comparing satellite based emission estimates with inventory totals. First the Memo items from the NFR will be discussed followed by additional overarching aspects in the comparison.

International aviation cruise (civil) (139.5 kt)³:

This category includes all emissions during the cruise phase of international flights. The emissions are calculated on the basis of fuel sold for international flights in the country. But these emission do only partly occur above the national territory as the emissions are calculated for the total distance of the international flights (by definition at a height above 3000 ft). This implies that a significant part of the emissions reported by Germany in this category occur over other countries, whereas emissions for this category in other countries may partially occur over Germany. Unlike the cruise phase, emissions from Landing and Take Off (LTO) are included in the inventory national totals and occur by definition below 3000 ft, and these are registered by the satellite observations.

The cruise emissions will typically occur between 31000 and 38000 ft which is reached at in proximately 10 minutes after Take Off and usually path through the troposphere to avoid turbulence in lower layers of the atmosphere (troposphere).

The satellite observed slant column total is split into a stratospheric and tropospheric part based on model simulations. At an altitude of 31000-38000 ft emissions typically take place in the lower stratosphere which is by principle not observed in the tropospheric column totals used in this study. Without direct insight into the emissions used in the model simulations, it is difficult to discuss the treatment of aviation emissions as the is not exactly known at what exact height they occur (somewhere between 3000ft, and the top of the troposphere (31000 ft). Furthermore emissions in the stratosphere will only be exchanged very slowly to lower altitudes. It is expected is that the overall effect of the lack of detection by the satellites of the aviation cruise emissions over Germany on the emission estimate is limited.

As a back of the envelope estimate let 's assume that a fraction of 10-20% of the estimated international cruise emissions flights take place over Germany, including long haul and short haul flights within Europe. Then assume that of those flights, at maximum 10% takes place

³ Between brackets: the German estimate as reported under Memo items in the NFR tables for 2019 in the 2021 submission.

within the troposphere, between 3000 and 31000ft, based on 10 minutes time between take off and cruising altitude, and a typical short flight within Europe of about 100 minutes, we end up with an emission fraction of 1-2% of the total emissions, which is about 1.5-3 kt NO_x. As these emissions occur at higher altitudes with stronger mixing, they are expected to be spread out over a larger domain. Compared to other emissions in the lower troposphere, which are more concentrated, the total effect of the aviation emissions on the tropospheric total columns can be expected to be very minor, especially when compared to other uncertainties in the retrieval as well as the inversion system used in this study and thus will not be a significant source of error.

Domestic aviation cruise (civil) (8.4 kton);

This category includes all emissions during the cruise phase of inland flights. The emissions are calculated on the basis of fuel sold and they will mostly occur above the national territory (by definition at a height above 3000 ft), although the flights will take the shortest route from one place to another which may also take it over other countries and/or water bodies when occurring near the German borders. Similarly as mentioned above, only a small fraction of the emissions will take place between the LTO emissions ceiling of 3000 ft and cruising altitude of 30.000 – 38000 ft which will have a minor to negligible effect on the tropospheric total columns and the derived emissions and thus will not be a significant source of error.

International maritime navigation (59.4 kt)

This category includes all emissions from fuels used by vessels (of all flags) engaged in international shipping. It includes emissions from journeys that depart in one country and arrive in a different country (e.g. departure in Germany and arrival in a foreign port). The emissions are calculated on the basis of fuel sold (bunkers) for international navigation in the country. These emissions only partly occur on the national territory as the reported emissions cover the whole international trip. Please note that the satellite derived emissions were clipped at the coast of Germany, so the off shore emissions of international shipping do not have to be included in the comparison. Some smearing of emissions can be expected near the borders where emissions are either misattributed to cells over the sea, or vice versa over land. Depending on the instruments footprint and sensitivity it has a limit for the maximum resolvability of the emissions. The TROPOMI instruments resolvability was estimated to be around 10-20km (personal communication; Chris McLinden, ECCC), with the variation related to the overall strength of the emissions. As the fraction of emissions mentioned here that take place near the German borders are quite low, the total smeared emissions can also be expected to be negligible compared to the other emissions within the domain and will not pose a significant source of error. As offshore emissions are not covered by the satellite view as used in this study, the emission from German fishing vessels and possibly other domestic shipping (which is returning in the same country as where it departed, and therefore included in the national total) should be taken out for a correct comparison between satellite and inventory. However, given the small emission from German fishery (0.38 kton NO_x) this is not a significant error in the comparison.

Multilateral operations (not estimated in Germany)

Emissions from fuels used for water-borne navigation and aviation in multilateral operations pursuant to the Charter of the United Nations. These include emissions from fuel delivered to the military in the country and delivered to the military of other countries. These emissions are expected to be minor and will not be a significant source of error.

Other not included in national total of the entire territory (not occurring in Germany)

Do not occur within the German memo emissions and will not be further discussed. Countries reporting emissions in this category however have to assess the relative contribution of these emissions to the total emissions and analyze if these emissions pose a possible error when comparing total inventory emissions with satellite estimates.

Volcanoes (not occurring in Germany)

There are no active volcanoes in Germany, and volcanoes do not emit significant amounts of NO₂ (Simpson et al., 1999).

But for other countries it is important to realize that these emissions should be included for a correct comparison of the inventory emissions with satellite observations. This is certainly the case for SO₂ emissions from volcanoes. Emissions from volcanoes have been estimated in the past using the Fioletov methodology (Fioletov et al., 2020) and results from these studies could be subtracted from the satellite based emission estimates to derive the anthropogenic emission totals. Besides satellite based estimates for volcanic emissions one could use inventories such as CAMS-GLOB-VOLC and NOVAC emissions (Galle et al., 2010; Arellano et al., 2021). A potential problem for the Divergence method, and up to a point for the Fioletov method, is that SO₂ plumes can travel over long distances, which is not modelled well in both methodologies. Long-distance plumes can in some cases cause attribution of emissions to regions where none take place. Furthermore, emissions from volcanoes can be sporadic, and short emission periods which in the inventories essentially get smoothed out over the whole year, while the actual emissions take place over a shorter period.

Forest fires (0.34 kt)

These emissions may vary from year to year and will be restricted to dry episodes during summer time. Therefore the effect of these emissions in the comparison of emission totals with satellite estimates should be judged on an annual basis. Forest fire emissions are not a dominant factor in Germany's emission total. In other countries might however have recurring forest fires and NO_x emissions from such fires can be noticeable. In the current methodology there is no filter implemented to remove periods with forest fires from the dataset, and thus fires will enhance the emissions found for the study region. Emissions of such fires can be accurately estimated, but these estimates are usually performed on a source to source basis (Adams et al., 2019; Griffin et al., 2019). On a yearly level emissions from fires are likely to cause enhanced emissions throughout the domain where the biomass burning plume overlaps the underlying cells. Especially outside the stronger source regions, this can cause a positive bias to the emissions. Without a more detailed study over a region with known fire emissions and long-distance NO_x plumes, it is not possible to give an estimate of the impact on the estimated yearly emissions. For Germany these emissions are expected to not be a significant source of error.

Other natural emissions: (Not occurring in Germany)

This category can be used to include the following categories of emissions (of which we only discuss those items relevant for the NO_x emissions, marked in italic):

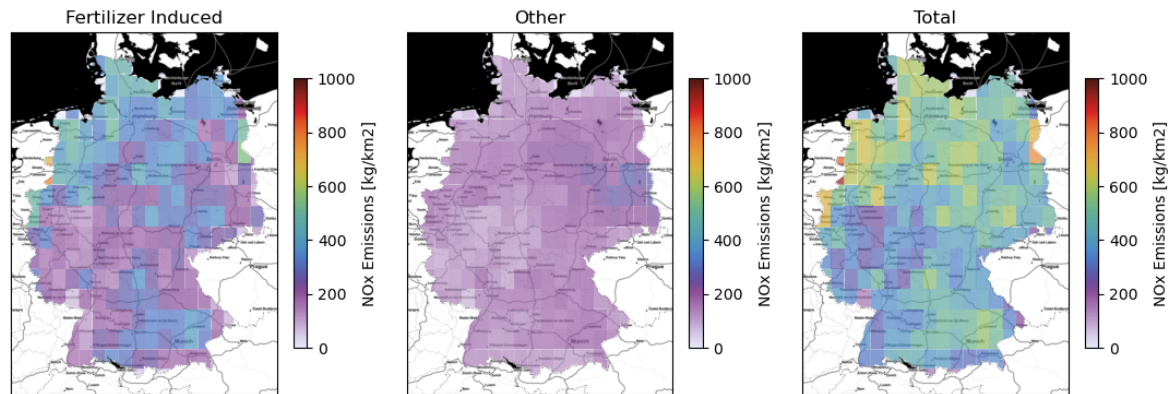
- *NO_x emissions from non-agricultural soils*
- *NO_x emissions from lightning.*
- NMVOC emissions from forests (for Germany these emissions can amount to approx. 5 % of the total manmade VOC emissions [EMEP Guidebook])
- NMVOC emissions from other types of vegetation
- CH₄ emissions from wetlands

- NH₃ emissions from wild animals, humans and pets
- GHG emissions from geological seepage
- GHG from Biomass stock changes
- GHG from Abandonment of Managed Lands
- CO₂ emissions from/or removal from soils
- Other Sources and Sinks: Other

NO_x emissions from non-agricultural soils

Due to widespread nitrogen pollution and deposition in Germany it is complicated to make an estimate of pure non-anthropogenic and non-agricultural soil emissions. There are several studies that looked at soil NO_x emissions for the European domain, mostly based on the Yienger and Levy method (1995), but fewer that focus on purely natural emissions. Simpson et al. (Simpson *et al.*, 1999) gave an estimate of 3-90 kt NO_x of forest emissions and 20 kt NO_x for grassland soils. This estimate was more recently updated by Simpson et al. (Simpson and Darras, 2021) and available as the CAMS-GLOB-SOIL inventory (REF), with a reported 2018 German emission total of about 160 kt NO_x. Within the inventory the emissions are split between fertilizer induced, biome, deposition related and pulsed emissions. There is always a danger of double counting such emissions but the fertilizer induced emissions of 100 kt match closely to those included within the 2019 GNFR data of about 110 kt. This leaves a remaining set of 60kt emissions, which is a combination of biome, deposition related and pulsed emissions. Figure 16 illustrates the spatial distribution of the fertilizer induced, *other* and total emissions. Note that the colormap range is a factor 10 smaller than those shown in Figure 11. The distribution of the *other* emissions are quite average throughout Germany, peaking somewhat towards the north eastern part of the country. When added to the inventory emissions (Figure 11) these emissions will raise the overall level of the emissions towards a slightly more purple tint, bringing the inventory set closer to the observed emissions. The inventory emission total mentioned in Table 4, 1119.1 will increase to 1179.5, which brings the total closer to the satellite estimated values. Note that Simpson et al. (2021) emissions stress that the derived soil emissions still have a large uncertainty range, mostly related to a lack of observations, missing data for some biomes, and the uncertainty of input parameters such as soil temperatures. Year to year variations can be expected to be large depending on variations in soil temperatures. The authors do not give an upper and lower range of the emissions.

Figure 16: Soil NO_x emissions split between fertilizer induced and other emissions as in the CAMS-GLOB-SOIL inventory (2018 emissions, 0.5°x0.5° resolution). Combined emissions (Total) are shown on the right). Note that the colormap upper range is 10x smaller than those used in Figure 11.



Source: this study

NO_x emissions from lightning

Globally the lightning NO constitutes about 3% of the total NO_x emission budget. Please note that according to the guidebook (EEA, 2019) only 20 % the lightning NO is formed in the lowest 1000 meter of the atmosphere and the remaining at higher altitude (all inter cloud lightning above 5 km height) (EEA, 2019). A back on the envelope estimate for the Lightning emissions can be made on the basis of the number of flashes per km² and the expected mol NO_x released per flash. A study by Anderson and Klugmann (Anderson and Klugmann, 2014) gives an average of about 2 flashes per km² throughout Germany, with fewer flashes in the central and northern parts. Assuming that on average the number of lightning flashes did not increase significantly in combination with a production of about 180 mol NO_x/flash (Bucsela et al., 2019) and German surface area of about 357.000 km², gives us a German Lightning NO_x emission total of about 5 kt NO_x per year. Similarly to the earlier points made for aviation emissions, this emission total is very minor and spread out over a large domain, and not expected to be a significant source of error when comparing satellite derived emission estimates with the emission inventory.

Other aspects to consider in the comparison of inventory totals and satellite estimates

Besides the above discussed memo items as reported in the NFR it should be noted that the emissions from road transport are required to be based on the fuels sold approach. This approach does not account for all the emissions which occur in Germany from vehicles which were fueled abroad and are driving in Germany (this might constitute an underestimation in the inventory). On the other hand the emissions from foreign vehicles (for instance from the Netherlands) which bought their fuel in Germany and were not driving in Germany are in this fuel sold approach allocated to Germany (this might constitute an overestimation of the German emissions). However it is not known how much emissions are associated with these cross border phenomena's for Germany. Data from The Netherlands show this might be a significant difference; the NO_x emission based on fuel used is approximately 5.5 % less than the emissions based on fuel sold as reported in the GNFR total. However as fuel prices in Belgium and Germany are cheaper than in The Netherlands, Dutch drivers fuel frequently in those countries thus the Dutch

case represents the higher end of the difference between fuel sold and fuel used approach, only surpassed by Luxemburg with one of the lowest fuel prices in Europe.

Another source of uncertainty are the emissions near the border regions. Emissions within 10-20km outside the border can be expected to be smeared out in the inversions. The stronger the source is the better resolvability. So for the larger sources 10 km can be assumed. Making a loop around the German borders there are a few areas of interest. Starting at the border of the Netherlands and moving clockwise on both sides of the border, there are several larger sources, such as the Weisweiler powerplant in Eschweiler, the Dolna Odra power station in Poland, and several powerplants near the border in the Czech Republic, but also several smaller and larger cities. By taking a polygon that is 10 km wider and narrower in shape than the existing German borders the smeared emissions near the borders can be approximated. Based on the CAMS-REG v5.1 inventory (emissions 2018, based on the in 2020 reported emissions) we find that around 120 kt of the German emissions take place within Germany and within 10 km of the borders, and around 75 kt just outside of Germany within 10 km of the border. Assuming that at most half of the full amount of these emissions smear out past the border, the smeared loss in emissions is about 22kt on the total emissions. This should be seen as an upper limit. Furthermore, of these emissions a large majority takes place in the western part of Germany, where the most common wind direction is wind coming from the west. In effect it can be expected that the smearing of those emissions will be reduced further.

To conclude only a few of the memo items can be expected to have a significant impact when comparing the inventory total with the satellite estimate. For Germany the largest contribution coming from the natural soil emissions which is estimated at about 60kt should be added to the NFR total reported for compliance. Of the non-memo items the smearing of emissions due to a lack of resolvability can be expected to have the largest effect with a value lying somewhere between the full 75kt just outside of the borders of Germany, and -120 kt within Germany. Assuming the most average “worst” case of the emissions not being resolvable and split to both sides of the border we find a total of 22 kt which should be added to the satellite observed value (or subtracted from the inventory).

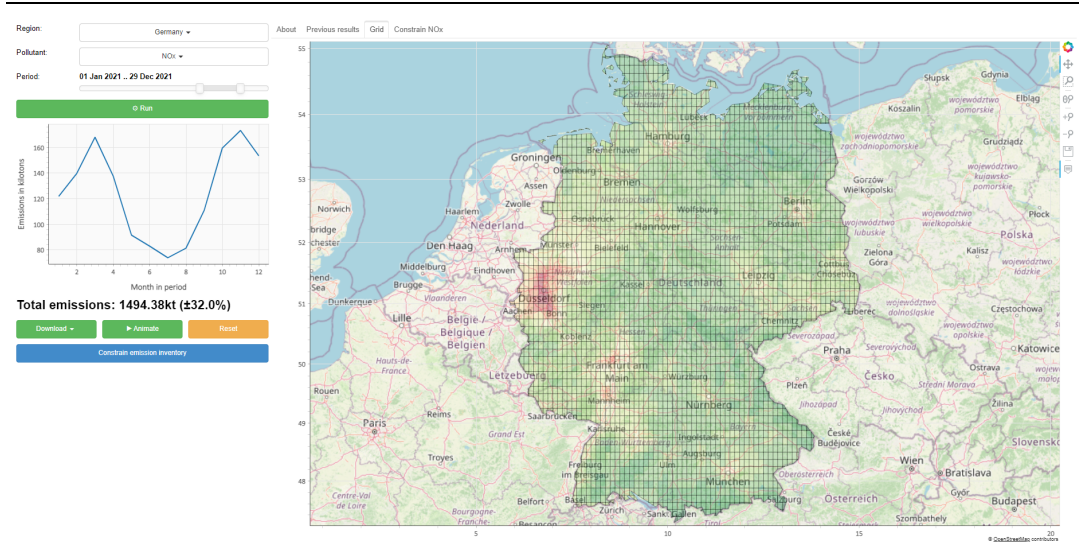
Quadratically adding these and the minor terms (those expected to be somewhat significant; lightning, soil, smearing) together we derive a total of 56 kt, bringing the inventory emission total up to a value of about 1175 kt NO_x. This final total is closer to the satellite based emissions derived with the Fioletov and Divergence method reported in Table 4.

3.6 Dissemination

The work described in this report was presented by Kevin Hausmann during the 2021 Joint EIONET (The European Environment Information and Observation Network) and TFEIP (Task Force on Emission Inventories and Projections) meeting in May 2021. The 2021 talk titled "The space emissions tool: constraining inventories using satellite data" can be found online (Hausman, 2021). In the presentation the general idea of the developed tool and a mock-up of the envisioned WebApp was presented. This meeting was attended by parties active in the field of the reporting of air pollutant emissions.

The WebApp, which is still under development, can already be accessed on <https://www.space-emissions.net/>. This page allows a user to select a region and period of interest and apply the methods described in this report to estimate NO_x emissions.

Figure 17: Screenshot of the WebApp Showing the NO_x emission estimate for Germany (in 2021) based on TROPOMI satellite data .



Source: this study

An update on the developments around the WebApp and satellite derived emissions was demonstrated at the 2022 Joint EIONET (The European Environment Information and Observation Network) and TFEIP (Task Force on Emission Inventories and Projections) meeting in May 2022. In the demonstration of the tool the reviewed methods were described in more detail and results from the two methods that are developed further are included.

To produce publicity for the presented work within the scientific community an article is under development for publication in a scientific journal. In this community the discussed methods are well established (Fioletov et al., 2013; McLinden et al., 2016; Beirle et al., 2019, 2021; Dammers et al., 2019) but access to their application is limited to a select group of scientists. The article will focus on the plume based fitting routine (Fioletov et al., 2017) to estimate national German emission for 2019-2021 at a high spatial resolution to see the effects of the COVID pandemic lockdown measures and relaxation thereof.

In both the presentations and publications attention will be drawn to the WebApp as well as the GitHub repository where the functionality described in this report and the underlying code will be freely available. Further developments towards other (short lived) species will be part of future endeavours. The open source nature of the work presented here hopefully sparks the interest and smoothens the development from other parties to bring satellite derived emission estimates further within the field of emission reporting and verification.

4 Conclusions and recommendations

4.1 Conclusions

The increasing capabilities of satellite products produce an ever growing potential to estimate NO_x emissions independently of CTMs, emission inventories or activity proxies, but through analysis of direct observations. It was shown that multiple physics informed methods, like for example a Gaussian plume-based fitting routine (Fioletov *et al.*, 2017), computation of the divergence of a pollutant flux field (Beirle *et al.*, 2019) or simply summing atmospheric concentration are able to estimate national total German NO_x emissions from TROPOMI satellite observations. For the year 2019 the methods produced an estimate of 1241.0 ($\pm 51.6\%$) kton, 1260.7 ($\pm 50.5\%$) kton and 1097.1 kton respectively, which are within 15% of NFR 2019 reported total emissions (1108.82 kton, reported in 2022). Likewise for the separate Bundesländer (with the exception of the city-states Berlin, Bremen, and Hamburg) emission totals are derivable from satellite observations and show strong correlations with emissions according to values found in the GNFR inventory data. Application of the method to the OMI observations revealed a $\pm 25\%$ decrease in total national German NO_x emissions for the 2017-2019 period compared to the 2005-2007 emissions which is in line with the decreasing trend in reported emissions.

Summarized, the uncertainty terms translated into a Germany total emission estimate uncertainty of 51.6 % for the Divergence approach, and 50.5% for the Gaussian plume method. These values should be seen as an upper limit, due to compensating errors. At a national level all three methods produce comparable results, showing that in Germany's case, the mass moving in and out of the country, to the sides of the domain, mostly cancel each other out. When moving towards Bundesländer and smaller administrative levels the performance degrades and differences between the methods become larger, with especially the Naïve method not being able to account for fluxes in and out of the regions. Towards the smallest administrative levels the Fioletov method shows promise to be more accurate than the Beirle method, although the Beirle method gives a better representation of the largest point sources. At such levels users are advised to fit the largest point sources with a Gaussian like approach as done by Beirle *et al.* (2019), before merging the emissions to the administrative boundaries. Furthermore, one should take into account the detection limit of TROPOMI for individual sources, which is at ~ 3.5 kt. An important issue when comparing emission estimates from satellite observations with the official inventory data is the fact that the inventories (by convention) do not include all emission sources which contribute to the observed concentrations. Adding estimates for natural emissions and emissions from the so called "memo" items from the IIR to the national total as reported in the IIR bring the inventory data and the satellite observation closer together.

4.2 Outlook

The tool has been developed with a focus on NO_x emission estimates from TROPOMI and OMI observations. Extensions to other pollutants should be straightforward under the reservation that the respective method is applicable to the selected pollutant. The methods developed here and available in the tool have been shown to work for at least carbon monoxide (CO), sulphur dioxide (SO₂) and ammonia (NH₃) (Beirle *et al.*, 2014; Dammers *et al.*, 2019; Lorente *et al.*, 2019; Fioletov *et al.*, 2017; 2020). Data products available from TROPOMI include CO and SO₂ so these pollutants seem like suitable candidates when an interest in their emissions exists although the TROPOMI and other satellite product quality varies a lot between the various products. Whereas most NO₂ observations can be used out of the box, the SO₂ product shows a lot more regional bias, and can only be used near emission sources or when using much stricter filter criteria

(Fioletov et al., 2020). In addition extensions to other satellites might allow the inclusion of more datasets and pollutants. Especially when extending the functionality to include NH_3 emission estimates the capability to download data from other satellites like IASI (A and B) and CrIS (SNPP and JPSS) needs to be developed.

In the future the geostationary Sentinel-4 satellite is planned to be launched and will provide hourly data on tropospheric constituents over Europe. This will allow the developed tool to explore additional functionality like the measurement of time profiles and might allow for emission estimates on a weekly or even daily basis. These capabilities are currently not fully developed within the tool but extensions in that direction are certainly possible.

Another interesting path to pursue further is the estimation of sector specific emissions. From high-resolution maps with emission estimates for e.g. Germany, busy roads and shipping routes are discernible. Obviously large point sources and cities can be detected with both the Beirle and Fioletov methods. These observations hint at the possibility to distinguish sectors within emission estimates directly. In an indirect way, time profiles can be used to differentiate between emissions from various sectors. This becomes especially interesting when hourly data is available which will be the case when Sentinel-4 is operational. For example road emissions will have two peaks reflecting morning and evening rush hours, while emissions from industries will have a more constant emission pattern. If time profiles per emissions source become derivable this provides another possibility to distinguish between sources. If these more high-resolution goals are attempted, more attention will need to be paid to variations of the lifetime, the $\text{NO}_x:\text{NO}_2$ ratios, and the local temporally varying bias, at higher spatial and temporal scales. Furthermore, developments in the direction of emission estimates of additional pollutants can help distinguish between sectors through the detection of co-emitted species for specific types of activity.

Next to the development of additional capabilities also the current capabilities can be further developed by for example incorporating more methods or additions to the current methods. If CTMs are considered, three additional methods (4dVar, EnKF and DECSO) for emission estimation are available that have already been discussed in detail in previous sections. But the CTM fields can also be used to better approximate the lifetimes and $\text{NO}_x:\text{NO}_2$ ratios. Continued use of purely satellite and meteorological data is also possible and an alternative method for daily emission estimates (Kuhlmann et al., 2019, 2020; Lorente et al., 2019) has recently been published. This method is very similar to the plume fitting routine incorporated in the developed tool but takes into account the evolution of the plume-based on a longer time period of meteorological data thereby accounting for bending of plumes due to changes in wind direction. Furthermore, the Fioletov method in its current state can be improved by applying a zoom like approach. First fitting emissions at a coarser resolution to account for regional fluxes, while step by step zooming to a smaller resolution with fewer sources and observations. Meanwhile the Beirle method can be extended with terms for deposition as well as a split in the chemical production and sink.

Within the developed functionality of the tool further standard improvements can also be made. An example is adding a location dependent lifetime (for example based on concentration of NO_2 , O_3 and OH), and the addition of local $\text{NO}_x:\text{NO}_2$ ratios and local corrections for diurnal and seasonal cycles) which all three would make sense from a physical perspective. Some of these improvements require simulated model fields, of which some are available (open-access) on the CAMS website (model fields). Other required variables such as temperature, UV radiation, precipitation and humidity, which would be used for adjusted lifetimes, are also available at the various ECMWF data storages. These quantities and/or estimates can be downloaded with the

ERA download tool and already make a relatively easy improvement to the lifetime estimates and thereby reduce the overall uncertainty of those terms.

A Appendices

A.1 Detailed description of satellite products - NO₂

In Table 6 and Table 7 an overview with a detailed description of the various available NO₂ satellite products (respectively L2 and L3) that were considered for this project is given.

Table 6: NO_x Level 2 products. Operational* means the product is still being provided, but a couple of days lag between the retrieval and the release of the processed data might be present.

Product name: OMI-Aura_L2-OMDOMINO Satellite: OMI Coverage period: 2018-01-01 – Operational* Provider: KNMI/TEMIS Data location: https://www.temis.nl/airpollution/no2col/no2regioomi_v2.php Description: Tropospheric NO ₂ columns are derived from satellite observations based on slant column NO ₂ retrievals with the DOAS (Differential Optical Absorption Spectroscopy) technique and a combined modelling/retrieval/assimilation approach. The Dutch OMI NO ₂ (DOMINO) retrieval algorithm version 2 (Boersma <i>et al.</i> , 2011) is used which has a new look-up table (LUT) for altitude-dependent AMFs based on more realistic atmospheric profile parameters, and include more surface albedo and surface pressure reference points than version 1.				
Product name: OMI-Aura_L2-QA4ECV_NO2_PSD_v1.1 Satellite: OMI Coverage period: 1995-01-01 – Operational* Provider: KNMI/TEMIS Data location: http://www.qa4ecv.eu/ecv/no2-pre Description: The QA4ECV NO ₂ Essential Climate Variable precursor product contains harmonized vertical NO ₂ columns for the period 1995-2017. The dataset contains three products: (1) the tropospheric vertical column density, (2) the stratospheric vertical column density, and (3) the total vertical column density. The NO ₂ ECV precursor data will provide geophysical information for each and every ground pixel observed by GOME, SCIAMACHY, OMI, and GOME-2(A), without the additional binning, averaging or gridding typically applied for Level 3 data. In addition to vertical NO ₂ columns, the product contains intermediate results, such as the result for the spectral fit, fitting diagnostics, the averaging kernel, cloud information, and algorithm and product error estimates.				
Product name: OMI/Aura Nitrogen Dioxide (NO ₂) Total and Tropospheric Column 1-orbit L2 Swath 13x24 km V003 (OMNO2) Satellite: OMI Coverage period: 2004-10-01 – Operational* Provider: NASA Data location: https://disc.gsfc.nasa.gov/datasets/OMNO2_003/summary				

Description: The Version 4.0 updates include: (1) use of a new daily and OMI field of view specific geometry dependent surface Lambertian Equivalent Reflectivity (GLER) product in both NO₂ and cloud retrievals; (2) use of improved cloud parameters (effective cloud fraction and cloud optical centroid pressure) from a new cloud algorithm (OMCDO2N) that are retrieved consistently with NO₂ using a new algorithm for O₂-O₂ slant column data and the GLER product for terrain reflectivity; (3) use of a more accurate terrain pressure calculated using OMI ground pixel-averaged terrain height and monthly mean GMI terrain pressure; and (4) improved treatment over snow/ice surfaces by using the concept of scene LER and scene pressure. The OMNO2 product contains slant column NO₂ (total amount along the average optical path from the sun into the atmosphere, and then toward the satellite), the total NO₂ vertical column density (VCD), the stratospheric and tropospheric VCDs, air mass factors (AMFs), scattering weights for calculation of AMFs, and other ancillary data. Other OMNO2-associated NO₂ products include the Level-2 gridded column product, OMNO2G, and the Level-3 gridded column product, OMNO2d.

Product name: TM5-MP-DOMINO version 1.2.x & 1.3.x, OFFLINE (2018-):

Satellite: TROPOMI

Coverage period: 2018-01-01 – Operational*

Provider: KNMI/TEMIS

Data location: https://www.temis.nl/airpollution/no2col/no2regio_tropomi.php

Description: Tropospheric NO₂ columns are derived from TROPOMI observations based on slant column NO₂ retrievals with the DOAS technique and a combined modelling/retrieval/assimilation approach is used. The TM5-MP (Tracer Model v5 Massively Parallelized) model is used for assimilation.

Product name: Sentinel-5P TROPOMI Tropospheric NO₂ 1-Orbit L2 5.5km x 3.5km V1 (S5P_L2_NO2___HiR)

Satellite: TROPOMI

Coverage period: 2019-08-06 – Operational*

Provider: NASA

Data location: <https://catalog.data.gov/dataset/Sentinel-5p-tropomi-tropospheric-no2-1-orbit-l2-5-5km-x-3-5km-v1-s5p-l2-no2-hir-at-ges-dis>

Description: Starting from August 6th in 2019, Sentinel-5P TROPOMI along-track high spatial resolution (~5.5km at nadir) has been implemented. For data before August 6th of 2019, please check S5P_L2_NO2___ data collection. The TROPOMI retrieval of total and tropospheric NO₂, is based on the DOMINO approach, a DOAS retrieval, a pre-calculated air-mass factor (AMF) look-up table, and a data assimilation/chemistry transport model for the separation of the stratospheric and tropospheric contributions to the NO₂ column. It also include many retrieval developments of the European Quality Assurance for Essential Climate Variables (QA4ECV) project.

Product name: SVELD_S5P_NO2TROPO_P1D

Satellite: TROPOMI

Coverage period: 2019-07-30 – Operational*

Provider: DLR

Data location:

<https://download.geoservice.dlr.de/SVELD/files/>

Description: This collection contains tropospheric NO₂ columns for Germany and surrounding areas derived from Sentinel-5P/TROPOMI Level-1B data. The Sentinel-5P tropospheric NO₂ data is generated by DLR and provided in the framework of the mFUND-Project "S-VELD". The tropospheric NO₂ data are vertical column densities with the unit "μmol/m²". Sentinel-5P observes Germany once per day at ~12:00 UTC. These daily observations are gridded onto a regular UTM grid. The day and measurement time are included in the netCDF data file. Only tropospheric NO₂ data for cloud-free Sentinel-5P measurements are provided (cloud fraction < ~0.2). Sentinel-5P cloud fraction data is included in this collection as well.

Table 7: Level 3 products:

Product name: S5P_L3_NO2_TM

Satellite: TROPOMI

Coverage period: 2019-07-30 – Operational*

Provider: VITO

Data location: <https://viewer.terrascope.be>

Description: L3 product regridded from the Sentinel-5P level 2 (L2) data products as provided by ESA from the Sentinel Hub.

Product name: OMI/Aura NO₂ Cloud-Screened Total and Tropospheric Column L3 Global Gridded 0.25 degree x 0.25 degree V3 (OMNO2d)

Satellite: OMI

Coverage period: 2004-10-01 – Operational*

Provider: NASA

Data location: https://disc.gsfc.nasa.gov/datasets/OMNO2d_003/summary

Description: This is Level-3 daily global gridded (0.25x0.25 degree) Nitrogen Dioxide Product (OMNO2d). OMNO2d data product is a Level-3 Gridded Product where pixel level data of good quality are binned and "averaged" into 0.25x0.25 degree global grids. This product contains Total column NO₂ and Total Tropospheric Column NO₂, for all atmospheric conditions, and for sky conditions where cloud fraction is less than 30 percent.

Product name: Sentinel-5P NRTI NO2: Near Real-Time Nitrogen Dioxide & Sentinel-5P OFFL NO2: Offline Nitrogen Dioxide

Satellite: TROPOMI

Coverage period: 2018-07-10 – Operational*

Provider: European Union/ESA/Copernicus

Data location: https://developers.google.com/earth-engine/datasets/catalog/COPERNICUS_S5P_NRTI_L3_NO2 & https://developers.google.com/earth-engine/datasets/catalog/COPERNICUS_S5P_OFFL_L3_NO2

Description: The NO2 S5P datasets, has two versions: Near Real-Time (NRTI) and Offline (OFFL). The NRTI assets cover a smaller area than the OFFL assets, but appear more quickly after acquisition. The OFFL assets contain data from a single orbit (which, due to half the earth being dark, contains data only for a single hemisphere). Because of noise on the data, negative vertical column values are often observed in particular over clean regions or for low SO₂ emissions. It is recommended not to filter these values except for outliers, i.e. for vertical columns lower than -0.001 mol/m².

The original Sentinel 5P Level 2 (L2) data is binned by time, not by latitude/longitude. To make it possible to ingest the data into Earth Engine, each Sentinel 5P L2 product is converted to L3, keeping a single grid per orbit (that is, no aggregation across products is performed).

The conversion to L3 is done by the harp convert tool using the bin_spatial operation. The source data is filtered to remove pixels with QA values less than: 75% for the tropospheric_NO2_column_number_density band of NO₂.

Product name: SVELD_S5P_NO2TROPO_P1D

Satellite: TROPOMI

Coverage period: 2019-07-30 – Operational*

Provider: DLR

Data location:

<https://download.geoservice.dlr.de/SVELD/files/>

Description: This collection contains tropospheric NO₂ columns for Germany and surrounding areas derived from Sentinel-5P/TROPOMI Level-1B data. The Sentinel-5P tropospheric NO₂ data is generated by DLR and provided in the framework of the mFUND-Project "S-VELD". The tropospheric NO₂ data are vertical column densities with the unit "μmol/m²". Sentinel-5P observes Germany once per day at ~12:00 UTC. These daily observations are gridded onto a regular grid. The day and measurement time are included in the netCDF data file. Only tropospheric NO₂ data for cloud-free Sentinel-5P measurements are provided (cloud fraction < ~0.2). Sentinel-5P cloud fraction data is included in this collection as well.

A.2 Detailed description of satellite products - NH₃

In Table 8 an overview with a detailed description of the various available NH₃ satellite products that were considered for this project (L2 and L3) is given.

Table 8: Summary of the openly available ammonia satellite products (L2/L3), with a summary of the period of observations, provider, summary of quality, and download location. Operational* means the product is still being provided, but a couple of days lag between the retrieval and the release of the processed data might occur.

<p>Product name: CrIS-FPR v1.5 Satellite: CrIS Coverage period: 2012-05– Operational* Provider: ECCC Data location: https://hpfx.collab.science.gc.ca/~mas001/satellite_ext/cris/snpp/nh3/v1_5/, account available on request (mark.shephard@canada.ca) Description: The CrIS-NH₃ (v1.5) product provides NH₃ total columns and vertical profiles. Both a complete and lite version of the product are available, with fewer number of variables included in the lite version. The current version does not include a cloud filter, but in theory this should be included intrinsically as there are no retrievals performed for regions with no ammonia signature. The lack of retrievals for locations with no ammonia(non-detects) in effect can produce a high bias within the product. The next version (v1.6) is planned for mid-end of 2021 and will include a cloud filter-based on VIIRS observations. It will also include all observations for which no retrieval was performed, with a possibility to use a best estimate for such low values. Typically a quality filter value of 5 is used to only use the best quality data which filters observations with low information content (DOF<0.1) as well as removing outliers in both retrieval terms (CHISQ>5) and concentrations (>200ppb).</p>
<p>Product name: IASI-ANNI-v3 Satellite: IASI Coverage period: A: 2007-10– Operational*; B: 2013- Operational*; C: 2020- Operational* Provider: ULB & L'ATMOS/IPSL Data location: https://iasi.aeris-data.fr/nh3/; L3 data: https://iasi.aeris-data.fr/catalog/ Description: The IASI-ANNI-v3 product is the latest iteration of the IASI-NH₃ product. It is produced using the Artificial Neural Network for IASI (ANNI) retrieval framework. The satellite product includes a cloud filter which enables filtering for cloudy scenes. The most recent products do not include the pixel shape nor does the product produce an averaging kernel which makes accounting for vertical sensitivity and spatial representativity more complicated.</p>

5 Bibliography

- van der A, R.J. *et al.* (2020) 'Connecting the dots: NO_x emissions along a West Siberian natural gas pipeline', *npj Climate and Atmospheric Science*, 3(1), pp. 1–7. doi:10.1038/s41612-020-0119-z.
- Adams, C. *et al.* (2019) 'Satellite-derived emissions of carbon monoxide, ammonia, and nitrogen dioxide from the 2016 Horse River wildfire in the Fort McMurray area', *Atmospheric Chemistry and Physics*, 19(4), pp. 2577–2599. doi:10.5194/acp-19-2577-2019.
- Anderson, G. and Klugmann, D. (2014) 'A European lightning density analysis using 5 years of ATDnet data', *Natural Hazards and Earth System Sciences*, 14(4), pp. 815–829. doi:10.5194/nhess-14-815-2014.
- Arellano, A.F. and Hess, P.G. (2006) 'Sensitivity of top-down estimates of CO sources to GCTM transport', *Geophysical Research Letters*, 33(21), pp. 1–5. doi:10.1029/2006GL027371.
- Arellano, S. *et al.* (2021) 'Synoptic analysis of a decade of daily measurements of SO₂ emission in the troposphere from volcanoes of the global ground-based Network for Observation of Volcanic and Atmospheric Change', *Earth System Science Data*, 13(3), pp. 1167–1188. doi:10.5194/essd-13-1167-2021.
- Babenhauserheide, A. *et al.* (2015) 'Comparing the CarbonTracker and M5-4DVar data assimilation systems for CO₂ surface flux inversions', *Atmospheric Chemistry and Physics*, 15(17), pp. 9747–9763. doi:10.5194/acp-15-9747-2015.
- Barbu, A.L. *et al.* (2009) 'A multi-component data assimilation experiment directed to sulphur dioxide and sulphate over Europe', *Atmospheric Environment*, 43(9), pp. 1622–1631. doi:10.1016/j.atmosenv.2008.12.005.
- Bauwens, M. *et al.* (2020) 'Impact of Coronavirus Outbreak on NO₂ Pollution Assessed Using TROPOMI and OMI Observations', *Geophysical Research Letters*, 47(11), pp. 1–9. doi:10.1029/2020GL087978.
- Beer, R. *et al.* (2008) 'First satellite observations of lower tropospheric ammonia and methanol', *Geophysical Research Letters*, 35(9), pp. 1–5. doi:10.1029/2008GL033642.
- Beirle, S. *et al.* (2003) 'Weekly cycle of NO₂ by GOME measurements: A signature of anthropogenic sources', *Atmospheric Chemistry and Physics*, 3(6), pp. 2225–2232. doi:10.5194/acp-3-2225-2003.
- Beirle, S. *et al.* (2011) 'Megacity emissions and lifetimes of nitrogen oxides probed from space', *Science*, 333(6050), pp. 1737–1739. doi:10.1126/science.1207824.
- Beirle, S. *et al.* (2014) 'Estimating the volcanic emission rate and atmospheric lifetime of SO₂ from space: A case study for Kilauea volcano, Hawai'i', *Atmospheric Chemistry and Physics*, 14(16), pp. 8309–8322. doi:10.5194/acp-14-8309-2014.
- Beirle, S. *et al.* (2019) 'Pinpointing nitrogen oxide emissions from space', *Science Advances*, 5(11), pp. 1–7. doi:10.1126/sciadv.aax9800.
- Beirle, S. *et al.* (2021) 'Catalog of NO_x emissions from point sources as derived from the divergence of the NO₂ flux for TROPOMI', *Earth System Science Data*, 13(6), pp. 2995–3012. doi:10.5194/essd-13-2995-2021.
- Bergamaschi, P. *et al.* (2000) 'Inverse modeling of the global CO cycle', *Journal of Geophysical Research*, 105, pp. 1909–1927.
- Bergamaschi, P. *et al.* (2010) 'Inverse modeling of European CH₄ emissions 2001–2006', *Journal of Geophysical Research*, 115(D22), p. D22309. doi:10.1029/2010JD014180.
- Bergamaschi, P., Alexe, M. and Segers, A. (2014) *Upgraded CH₄ flux inversion system*.
- Biswal, A. *et al.* (2020) 'COVID-19 lockdown and its impact on tropospheric NO₂ concentrations over India using satellite-based data', *Heliyon*, 6(9), p. e04764. doi:10.1016/j.heliyon.2020.e04764.

- Boersma, K.F. *et al.* (2011) 'An improved tropospheric NO₂ column retrieval algorithm for the Ozone Monitoring Instrument', *Atmospheric Measurement Techniques*, 4(9), pp. 1905–1928. doi:10.5194/amt-4-1905-2011.
- Bucsela, E.J. *et al.* (2019) 'Midlatitude Lightning NO_x Production Efficiency Inferred From OMI and WWLLN Data', *Journal of Geophysical Research: Atmospheres*, 124(23), pp. 13475–13497. doi:10.1029/2019JD030561.
- Cao, H. *et al.* (2020) 'Inverse modeling of NH₃ sources using CrIS remote sensing measurements', *Environmental Research Letters*, 15(10). doi:10.1088/1748-9326/abb5cc.
- Castellanos, P. and Boersma, K.F. (2012) 'Reductions in nitrogen oxides over Europe driven by environmental policy and economic recession', *Scientific Reports*, 2(2), pp. 1–7. doi:10.1038/srep00265.
- Chen, Y. *et al.* (2020) 'High-resolution Hybrid Inversion of IASI Ammonia Columns to Constrain U.S. Ammonia Emissions Using the CMAQ Adjoint Model', *Atmospheric Chemistry and Physics*, (June), pp. 1–25. doi:10.5194/acp-2020-523.
- Clarisse, L. *et al.* (2009) 'Global ammonia distribution derived from infrared satellite observations', *Nature Geoscience*, 2(7), pp. 479–483. doi:10.1038/ngeo551.
- Clarisse, L. *et al.* (2010) 'Global to local observations of atmospheric ammonia with IASI Global to local observations of atmospheric ammonia with IASI', (January).
- Clarisse, L. *et al.* (2019) 'Tracking down global NH₃ point sources with wind-adjusted superresolution', *Atmospheric Measurement Techniques*, 12(10), pp. 5457–5473. doi:10.5194/amt-12-5457-2019.
- Coheur, P.-F. *et al.* (2009) 'IASI measurements of reactive trace species in biomass burning plumes', *Atmospheric Chemistry and Physics*, 9(15), pp. 5655–5667. doi:10.5194/acp-9-5655-2009.
- Cooper, M. *et al.* (2017) 'Comparing mass balance and adjoint methods for inverse modeling of nitrogen dioxide columns for global nitrogen oxide emissions', *Journal of Geophysical Research*, 122(8), pp. 4718–4734. doi:10.1002/2016JD025985.
- Curier, R.L. *et al.* (2011) 'Synergistic use of Iotos-euros model and OMI NO₂ tropospheric column to evaluate the nox emission trends over Europe', *34th International Symposium on Remote Sensing of Environment - The GEOSS Era: Towards Operational Environmental Monitoring*, (2), pp. 2–5.
- Curier, R.L. *et al.* (2012) 'Improving ozone forecasts over Europe by synergistic use of the LOTOS-EUROS chemical transport model and in-situ measurements', *Atmospheric Environment*, 60, pp. 217–226. doi:10.1016/j.atmosenv.2012.06.017.
- Curier, R.L. *et al.* (2014) 'Synergistic use of OMI NO₂ tropospheric columns and LOTOS-EUROS to evaluate the NO_x emission trends across Europe', *Remote Sensing of Environment*, 149(2), pp. 58–69. doi:10.1016/j.rse.2014.03.032.
- van Damme, M., Wichink Kruit, R.J., *et al.* (2014) 'Evaluating 4 years of atmospheric ammonia (NH₃) over Europe using IASI satellite observations and LOTOS-EUROS model results', *Journal of Geophysical Research: Atmospheres*, 119(15), pp. 9549–9566. doi:10.1002/2014JD021911.
- van Damme, M., Clarisse, L., *et al.* (2014) 'Global distributions, time series and error characterization of atmospheric ammonia (NH₃) from IASI satellite observations', *Atmospheric Chemistry and Physics*, 14(6), pp. 2905–2922. doi:10.5194/acp-14-2905-2014.
- van Damme, M. *et al.* (2015) 'Worldwide spatiotemporal atmospheric ammonia (NH₃) columns variability revealed by satellite', *Geophysical Research Letters*, 42(20), pp. 8660–8668. doi:10.1002/2015GL065496.
- Van Damme, M. *et al.* (2015) 'Towards validation of ammonia (NH₃) measurements from the IASI satellite', *Atmospheric Measurement Techniques*, 8(3), pp. 1575–1591. doi:10.5194/amt-8-1575-2015.

- Van Damme, M. *et al.* (2018) 'Industrial and agricultural ammonia point sources exposed', *Nature*, 564(7734), pp. 99–103. doi:10.1038/s41586-018-0747-1.
- Van Damme, M. *et al.* (2020) 'Global, regional and national trends of atmospheric ammonia derived from a decadal (2008–2018) satellite record', *Environ. Res. Lett.*, p. ERL-110252.R1.
- Dammers, E. *et al.* (2015) 'Retrieval of ammonia from ground-based FTIR solar spectra', *Atmospheric Chemistry and Physics*, 15(22), pp. 12789–12803. doi:10.5194/acp-15-12789-2015.
- Dammers, E. *et al.* (2016) 'An evaluation of IASI-NH₃ with ground-based Fourier transform infrared spectroscopy measurements', *Atmospheric Chemistry and Physics*, 16(16), pp. 10351–10368. doi:10.5194/acp-16-10351-2016.
- Dammers, E. *et al.* (2017) 'Validation of the CrIS fast physical NH₃ retrieval with ground-based FTIR', *Atmospheric Measurement Techniques*, 10(7), pp. 2645–2667. doi:10.5194/amt-10-2645-2017.
- Dammers, E. *et al.* (2019) 'NH₃ emissions from large point sources derived from CrIS and IASI satellite observations', *Atmospheric Chemistry and Physics*, 19(19), pp. 12261–12293. doi:10.5194/acp-19-12261-2019.
- Ding, J. *et al.* (2018) 'Maritime NO_x Emissions Over Chinese Seas Derived From Satellite Observations', *Geophysical Research Letters*, 45(4), pp. 2031–2037. doi:10.1002/2017GL076788.
- Ding, J. *et al.* (2020) 'NO_x Emissions Reduction and Rebound in China Due to the COVID-19 Crisis', *Geophysical Research Letters*, 47(19), pp. 1–9. doi:10.1029/2020GL089912.
- van Donkelaar, A. *et al.* (2010) 'Global estimates of ambient fine particulate matter concentrations from satellite-based aerosol optical depth: Development and application', *Environmental Health Perspectives*, 118(6), pp. 847–855. doi:10.1289/ehp.0901623.
- Duncan, B.N. *et al.* (2013) 'The observed response of Ozone Monitoring Instrument (OMI) NO₂ columns to NO_x emission controls on power plants in the United States: 2005–2011', *Atmospheric Environment*, 81(2), pp. 102–111. doi:10.1016/j.atmosenv.2013.08.068.
- EEA (2019) 'EMEP/EEA air pollutant emission inventory guidebook 2019: Technical guidance to prepare national emission inventories', *EEA Technical report* [Preprint], (12/2019). Available at: <https://www.eea.europa.eu/publications/emep-eea-guidebook-2019>.
- Elissavet Koukouli, M. *et al.* (2018) 'Updated SO₂ emission estimates over China using OMI/Aura observations', *Atmospheric Measurement Techniques*, 11(3), pp. 1817–1832. doi:10.5194/amt-11-1817-2018.
- Erisman, J.W. *et al.* (1988) 'Vertical distribution of gases and aerosols: The behaviour of ammonia and related components in the lower atmosphere', *Atmospheric Environment* (1967), 22(6), pp. 1153–1160. doi:10.1016/0004-6981(88)90345-9.
- Eskes, H. *et al.* (2013) *Data Assimilation and Air Quality Forecasting*, *NATO Science for Peace and Security Series C: Environmental Security*. doi:10.1007/978-94-007-5577-2_32.
- Evangeliou, N. *et al.* (2020) '10–Year Satellite–Constrained Fluxes of Ammonia Improve Performance of Chemistry Transport Models', *Atmospheric Chemistry and Physics Discussions*, (November), pp. 1–41. doi:10.5194/acp-2020-1008.
- Fioletov, V. *et al.* (2017) 'Multi-source SO₂ emission retrievals and consistency of satellite and surface measurements with reported emissions', *Atmospheric Chemistry and Physics*, 17(20), pp. 12597–12616. doi:10.5194/acp-17-12597-2017.
- Fioletov, V. *et al.* (2019) 'Multi-Satellite Air Quality Sulfur Dioxide (SO₂) Database Long-Term L4 Global V1', *Goddard Earth Science Data and Information Services Center (GES DISC)* [Preprint]. doi:10.5067/MEASURES/SO2/DATA403.

- Fioletov, V. *et al.* (2020) 'Anthropogenic and volcanic point source SO₂ emissions derived from TROPOMI onboard Sentinel 5 Precursor: first results', *Atmospheric Chemistry and Physics Discussions*, (2018), pp. 1–30. doi:10.5194/acp-2019-1095.
- Fioletov, V.E. *et al.* (2011) 'Estimation of SO₂ emissions using OMI retrievals', *Geophysical Research Letters*, 38(21), pp. 1–5. doi:10.1029/2011GL049402.
- Fioletov, V.E. *et al.* (2013) 'Application of OMI, SCIAMACHY, and GOME-2 satellite SO₂ retrievals for detection of large emission sources', *Journal of Geophysical Research Atmospheres*, 118(19), pp. 11399–11418. doi:10.1002/jgrd.50826.
- de Foy, B. *et al.* (2014) 'Model evaluation of methods for estimating surface emissions and chemical lifetimes from satellite data', *Atmospheric Environment*, 98, pp. 66–77. doi:10.1016/j.atmosenv.2014.08.051.
- Fu, G. *et al.* (2017) 'Data assimilation for volcanic ash plumes using a satellite observational operator: A case study on the 2010 Eyjafjallajökull volcanic eruption', *Atmospheric Chemistry and Physics*, 17(2), pp. 1187–1205. doi:10.5194/acp-17-1187-2017.
- Galle, B. *et al.* (2010) 'Network for Observation of Volcanic and Atmospheric Change (NOVAC) - A global network for volcanic gas monitoring: Network layout and instrument description', *Journal of Geophysical Research Atmospheres*, 115(D5), pp. 1–19. doi:10.1029/2009JD011823.
- Goldberg, D.L. *et al.* (2019) 'Enhanced Capabilities of TROPOMI NO₂: Estimating NO_x from North American Cities and Power Plants', *Environmental Science and Technology*, 53(21), pp. 12594–12601. doi:10.1021/acs.est.9b04488.
- van der Graaf, S. *et al.* (2021) 'Data assimilation of CrIS-NH₃ satellite observations for improving spatiotemporal NH₃ distributions in LOTOS-EUROS.', *in prep* [Preprint].
- Griffin, D. *et al.* (2019) 'High-Resolution Mapping of Nitrogen Dioxide With TROPOMI: First Results and Validation Over the Canadian Oil Sands', *Geophysical Research Letters*, 46(2), pp. 1049–1060. doi:10.1029/2018GL081095.
- Gui, K. *et al.* (2019) 'Satellite-derived PM_{2.5} concentration trends over Eastern China from 1998 to 2016: Relationships to emissions and meteorological parameters', *Environmental Pollution*, 247, pp. 1125–1133. doi:10.1016/j.envpol.2019.01.056.
- Guo, X. *et al.* (no date) 'Validation of IASI satellite ammonia observations at the pixel scale using in-situ vertical profiles', *Journal of Geophysical Research: Atmospheres*, n/a(n/a), p. e2020JD033475. doi:https://doi.org/10.1029/2020JD033475.
- Hausman, K. (2021) 'On-line presentation: "The space emissions tool: constraining inventories using satellite data"', in *The 2021 Joint EIONET and TFEIP meeting*. Available at: https://www.tfeip-secretariat.org/_files/ugd/e5a9c7_b78137e60df04fdca7f639b7eb6a1bce.pdf.
- Heald, C.L. *et al.* (2012) 'Atmospheric ammonia and particulate inorganic nitrogen over the United States', *Atmospheric Chemistry and Physics*, 12(21), pp. 10295–10312. doi:10.5194/acp-12-10295-2012.
- Hilboll, A., Richter, A. and Burrows, J.P. (2013) 'Long-term changes of tropospheric NO₂ over megacities derived from multiple satellite instruments', *Atmospheric Chemistry and Physics*, 13(8), pp. 4145–4169. doi:10.5194/acp-13-4145-2013.
- Houweling, S. *et al.* (2017) 'Global inverse modeling of CH₄ sources and sinks: An overview of methods', *Atmospheric Chemistry and Physics*, 17(1), pp. 235–256. doi:10.5194/acp-17-235-2017.
- Janjić, T. *et al.* (2018) 'On the representation error in data assimilation', *Quarterly Journal of the Royal Meteorological Society*, 144(713), pp. 1257–1278. doi:10.1002/qj.3130.

- Jiang, Z. *et al.* (2017) 'A 15-year record of CO emissions constrained by MOPITT CO observations', *Atmospheric Chemistry and Physics*, 17(7), pp. 4565–4583. doi:10.5194/acp-17-4565-2017.
- Konovalov, I.B. *et al.* (2010) 'Multi-annual changes of NO_x emissions in megacity regions: Nonlinear trend analysis of satellite measurement based estimates', *Atmospheric Chemistry and Physics*, 10(17), pp. 8481–8498. doi:10.5194/acp-10-8481-2010.
- Kranenburg, R. *et al.* (2013) 'Source apportionment using LOTOS-EUROS: module description and evaluation', *Geoscientific Model Development*, 6(3), pp. 721–733. doi:10.5194/gmd-6-721-2013.
- Krol, M. *et al.* (2005) 'The two-way nested global chemistry-transport zoom model TM5: algorithm and applications', *Atmospheric Chemistry and Physics*, 5, pp. 417–432.
- Kuhlmann, G. *et al.* (2019) 'Detectability of CO₂ emission plumes of cities and power plants with the Copernicus Anthropogenic CO₂ Monitoring (CO₂M) mission', *Atmospheric Measurement Techniques*, 12(12), pp. 6695–6719. doi:10.5194/amt-12-6695-2019.
- Kuhlmann, G. *et al.* (2020) 'Quantifying CO₂ emissions of a city with the Copernicus Anthropogenic CO₂ Monitoring satellite mission', *Atmospheric Measurement Techniques Discussions*, 1, pp. 1–33. doi:10.5194/amt-2020-162.
- Kuhlmann, G. *et al.* (2021) 'Quantifying CO₂ Emissions of Power Plants With CO₂ and NO₂ Imaging Satellites', *Frontiers in Remote Sensing*, 2(2), pp. 1–18. doi:10.3389/frsen.2021.689838.
- Lamsal, L.N. *et al.* (2011) 'Application of satellite observations for timely updates to global anthropogenic NO_x emission inventories', *Geophysical Research Letters*, 38(5), pp. 1–5. doi:10.1029/2010GL046476.
- Lamsal, L.N. *et al.* (2015) 'U.S. NO₂ trends (2005–2013): EPA Air Quality System (AQS) data versus improved observations from the Ozone Monitoring Instrument (OMI)', *Atmospheric Environment*, 110(April), pp. 130–143. doi:10.1016/j.atmosenv.2015.03.055.
- Liu, X. *et al.* (2017) 'Assimilation of satellite NO₂ observations at high spatial resolution using OSSEs', *Atmospheric Chemistry and Physics*, 17(11), pp. 7067–7081. doi:10.5194/acp-17-7067-2017.
- Lonsdale, C.R. *et al.* (2017) 'Modeling the diurnal variability of agricultural ammonia in Bakersfield, California, during the CalNex campaign', *Atmospheric Chemistry and Physics*, 17(4), pp. 2721–2739. doi:10.5194/acp-17-2721-2017.
- Lorenc, A.C. and Payne, T. (2007) '4D-Var and the butterfly effect: Statistical four-dimensional data assimilation for a wide range of scales', *QUARTERLY JOURNAL OF THE ROYAL METEOROLOGICAL SOCIETY*, 133, pp. 607–614. doi:DOI: 10.1002/qj.36.
- Lorente, A. *et al.* (2019) 'Quantification of nitrogen oxides emissions from build-up of pollution over Paris with TROPOMI', *Scientific Reports*, 9(1), pp. 1–10. doi:10.1038/s41598-019-56428-5.
- Lu, S. *et al.* (2016) 'Estimation of volcanic ash emissions through assimilating satellite data and ground-based observations', *Journal of Geophysical Research*, 121(18), pp. 10,971–10,994. doi:10.1002/2016JD025131.
- Lu, Z. *et al.* (2015) 'Emissions of nitrogen oxides from US urban areas: Estimation from Ozone Monitoring Instrument retrievals for 2005–2014', *Atmospheric Chemistry and Physics*, 15(18), pp. 10367–10383. doi:10.5194/acp-15-10367-2015.
- McLinden, C.A. *et al.* (2016) 'Space-based detection of missing sulfur dioxide sources of global air pollution', *Nature Geoscience*, 9(7), pp. 496–500. doi:10.1038/ngeo2724.
- Mijling, B. and Van Der A, R.J. (2012) 'Using daily satellite observations to estimate emissions of short-lived air pollutants on a mesoscopic scale', *Journal of Geophysical Research Atmospheres*, 117(17), pp. 1–20. doi:10.1029/2012JD017817.

- Miyazaki, K. *et al.* (2016) 'Decadal changes in global surface NO_x emissions from multi-constituent satellite data assimilation', *Atmospheric Chemistry and Physics Discussions*, (2), pp. 1–48. doi:10.5194/acp-2016-529.
- Miyazaki, K. *et al.* (2017) 'Decadal changes in global surface NO_x emissions from multi-constituent satellite data assimilation', *Atmospheric Chemistry and Physics*, 17(2), pp. 807–837. doi:10.5194/acp-17-807-2017.
- Miyazaki, K., Eskes, H.J. and Sudo, K. (2012) 'Global NO_x emission estimates derived from an assimilation of OMI tropospheric NO₂ columns', *Atmospheric Chemistry and Physics*, 12(5), pp. 2263–2288. doi:10.5194/acp-12-2263-2012.
- Nowak, J.B. *et al.* (2012) 'Ammonia sources in the California South Coast Air Basin and their impact on ammonium nitrate formation', *Geophysical Research Letters*, 39(7).
- Pang, J. *et al.* (2018) 'Assimilating AOD retrievals from GOCI and VIIRS to forecast surface PM_{2.5} episodes over Eastern China', *Atmospheric Environment*, 179(October 2017), pp. 288–304. doi:10.1016/j.atmosenv.2018.02.011.
- Paraschiv, S. and Paraschiv, L.S. (2019) 'Analysis of traffic and industrial source contributions to ambient air pollution with nitrogen dioxide in two urban areas in Romania', *Energy Procedia*, 157(2018), pp. 1553–1560. doi:10.1016/j.egypro.2018.11.321.
- Qu, Z., Henze, D.K., Theys, N., *et al.* (2019) 'Hybrid Mass Balance/4D-Var Joint Inversion of NO_x and SO₂ Emissions in East Asia', *Journal of Geophysical Research: Atmospheres*, 124(14), pp. 8203–8224. doi:10.1029/2018JD030240.
- Qu, Z., Henze, D.K., Li, C., *et al.* (2019) 'SO₂ Emission Estimates Using OMI SO₂ Retrievals for 2005–2017', *Journal of Geophysical Research: Atmospheres*, 124(14), pp. 8336–8359. doi:10.1029/2019JD030243.
- Randall V.Martin (2008) 'Satellite remote sensing of surface air quality', *Atmospheric Environment*, 42(34), pp. 7823–7843. doi:10.1016/j.atmosenv.2008.07.018.
- Russell, A.R., Valin, L.C. and Cohen, R.C. (2012) 'Trends in OMI NO₂ observations over the United States: Effects of emission control technology and the economic recession', *Atmospheric Chemistry and Physics*, 12(24), pp. 12197–12209. doi:10.5194/acp-12-12197-2012.
- De Ruyter De Wildt, M., Eskes, H. and Boersma, K.F. (2012) 'The global economic cycle and satellite-derived NO₂ trends over shipping lanes', *Geophysical Research Letters*, 39(1), pp. 2–7. doi:10.1029/2011GL049541.
- Schaap, M. *et al.* (2013) 'Assessing the sensitivity of the OMI-NO₂ product to emission changes across europe', *Remote Sensing*, 5(9), pp. 4187–4208. doi:10.3390/rs5094187.
- Schiferl, L.D. *et al.* (2016) 'Interannual variability of ammonia concentrations over the United States: Sources and implications', *Atmospheric Chemistry and Physics*, 16(18), pp. 12305–12328. doi:10.5194/acp-16-12305-2016.
- Schneider, P., Lahoz, W.A. and Van Der A, R. (2015) 'Recent satellite-based trends of tropospheric nitrogen dioxide over large urban agglomerations worldwide', *Atmospheric Chemistry and Physics*, 15(3), pp. 1205–1220. doi:10.5194/acp-15-1205-2015.
- Schwartz, C.S. *et al.* (2012) 'Simultaneous three-dimensional variational assimilation of surface fine particulate matter and MODIS aerosol optical depth', *Journal of Geophysical Research Atmospheres*, 117(13), pp. 1–22. doi:10.1029/2011JD017383.
- Segers, A.J. *et al.* (2010) 'Study on the value of the MSG/SEVIRI derived AOD operational air quality forecast', *TNO report*, [Preprint], (TNO-034-UT-2010-00085).
- Seinfeld, J.H. (1989) 'Urban Air Pollution: State of the Science', *Science*, 243(4892), pp. 745 LP – 752. doi:10.1126/science.243.4892.745.

- Shephard, M.W. *et al.* (2011) 'TES ammonia retrieval strategy and global observations of the spatial and seasonal variability of ammonia', *Atmospheric Chemistry and Physics*, 11(20), pp. 10743–10763. doi:10.5194/acp-11-10743-2011.
- Shephard, M.W. *et al.* (2015) 'Tropospheric Emission Spectrometer (TES) satellite validations of ammonia, methanol, formic acid, and carbon monoxide over the Canadian oil sands, Atmos', *Meas. Tech. Discuss*, 8, pp. 9503–9563.
- Shephard, M.W. *et al.* (2020) 'Ammonia measurements from space with the Cross-track Infrared Sounder: Characteristics and applications', *Atmospheric Chemistry and Physics*, 20(4), pp. 2277–2302. doi:10.5194/acp-20-2277-2020.
- Shephard, M.W. and Cady-Pereira, K.E. (2015) 'Cross-track Infrared Sounder (CrIS) satellite observations of tropospheric ammonia', *Atmospheric Measurement Techniques*, 8(3), pp. 1323–1336. doi:10.5194/amt-8-1323-2015.
- Simpson, D. *et al.* (1999) 'Inventorying emissions from nature in Europe derived here amount of biogenic NO_x emissions cover a wide range , Gg NO_x (as N) yr - •. In terms of relative contribution to total European emissions for', 104(98), pp. 8113–8152.
- Simpson, D. and Darras, S. (2021) 'Global soil NO emissions for Atmospheric Chemical Transport Modelling: CAMS-GLOB-SOIL v2.2', *Earth System Science Data Discussions*, 2021, pp. 1–35. doi:10.5194/essd-2021-221.
- Someya, Y. *et al.* (2020) 'Atmospheric ammonia retrieval from the TANSO-FTS/GOSAT thermal infrared sounder', *Atmospheric Measurement Techniques*, 13(1), pp. 309–321. doi:10.5194/amt-13-309-2020.
- Stavrakou, T. *et al.* (2008) 'Assessing the distribution and growth rates of NO_x emission sources by inverting a 10-year record of NO₂ satellite columns', *Geophysical Research Letters*, 35(10), pp. 1–5. doi:10.1029/2008GL033521.
- Streets, D.G. *et al.* (2013) 'Emissions estimation from satellite retrievals: A review of current capability', *Atmospheric Environment*, 77, pp. 1011–1042. doi:10.1016/j.atmosenv.2013.05.051.
- Sun, K. *et al.* (2017) 'Validation of TES ammonia observations at the single pixel scale in the San Joaquin Valley during DISCOVER-AQ', *Journal of Geophysical Research : Atmospheres*, pp. 1–12. doi:10.1002/2014JD022846.Received.
- Tack, F. *et al.* (2021) 'Assessment of the TROPOMI tropospheric NO₂ product based on airborne APEX observations', *Atmospheric Measurement Techniques*, 14(1), pp. 615–646. doi:10.5194/amt-14-615-2021.
- Tevlin, A.G. *et al.* (2017) 'Tall Tower Vertical Profiles and Diurnal Trends of Ammonia in the Colorado Front Range', *Journal of Geophysical Research: Atmospheres*, 122(22), pp. 12,468–12,487. doi:10.1002/2017JD026534.
- Timmermans, R. *et al.* (2019) 'Impact of synthetic space-borne NO₂ observations from the Sentinel-4 and Sentinel-5P missions on tropospheric NO₂ analyses', *Atmospheric Chemistry and Physics*, 19(19), pp. 12811–12833. doi:10.5194/acp-19-12811-2019.
- Timmermans, R.M.A. *et al.* (2009) 'The Added Value of a Proposed Satellite Imager for Ground Level Particulate Matter Analyses and Forecasts', *IEEE Journal of Selected Topics in Applied Earth Observations and Remote Sensing*, 2(4), pp. 271–283. doi:10.1109/JSTARS.2009.2034613.
- Tong, D.Q. *et al.* (2015) 'Long-term NO_x trends over large cities in the United States during the great recession: Comparison of satellite retrievals, ground observations, and emission inventories', *Atmospheric Environment*, 107(2), pp. 70–84. doi:10.1016/j.atmosenv.2015.01.035.

- Verhoelst, T. *et al.* (2021) 'Ground-based validation of the Copernicus Sentinel-5P TROPOMI NO₂ measurements with the NDACC ZSL-DOAS, MAX-DOAS and Pandonia global networks', *Atmospheric Measurement Techniques*, 14(1), pp. 481–510. doi:10.5194/amt-14-481-2021.
- Vinken, G.C.M., Boersma, K.F., Van Donkelaar, A., *et al.* (2014) 'Constraints on ship NO_x emissions in Europe using GEOS-Chem and OMI satellite NO₂ observations', *Atmospheric Chemistry and Physics*, 14(3), pp. 1353–1369. doi:10.5194/acp-14-1353-2014.
- Vinken, G.C.M., Boersma, K.F., Maasakkers, J.D., *et al.* (2014) 'Worldwide biogenic soil NO_x emissions inferred from OMI NO₂ observations', *Atmospheric Chemistry and Physics*, 14(18), pp. 10363–10381. doi:10.5194/acp-14-10363-2014.
- Vira, J. and Sofiev, M. (2012) 'On variational data assimilation for estimating the model initial conditions and emission fluxes for short-term forecasting of SO_x concentrations', *Atmospheric Environment*, 46, pp. 318–328. doi:10.1016/j.atmosenv.2011.09.066.
- Wang, C. *et al.* (2020) 'Comparison and validation of TROPOMI and OMI NO₂ observations over China', *Atmosphere*, 11(6). doi:10.3390/atmos11060636.
- Wang, Y. and Wang, J. (2020) 'Tropospheric SO₂ and NO₂ in 2012–2018: Contrasting views of two sensors (OMI and OMPS) from space', *Atmospheric Environment*, 223(July 2019), p. 117214. doi:10.1016/j.atmosenv.2019.117214.
- Warner, J.X. *et al.* (2016) 'The global tropospheric ammonia distribution as seen in the 13-year AIRS measurement record', *Atmospheric Chemistry and Physics*, 16(8), pp. 5467–5479. doi:10.5194/acp-16-5467-2016.
- Warner, J.X. *et al.* (2017) 'Increased atmospheric ammonia over the world's major agricultural areas detected from space', *Geophysical Research Letters*, 44(6), pp. 2875–2884. doi:10.1002/2016GL072305.
- Whitburn, S. *et al.* (2015) 'Ammonia emissions in tropical biomass burning regions: Comparison between satellite-derived emissions and bottom-up fire inventories', *Atmospheric Environment*, 121, pp. 42–54. doi:10.1016/j.atmosenv.2015.03.015.
- Zhang, L. *et al.* (2008) 'An adjoint sensitivity analysis and 4D-Var data assimilation study of Texas air quality', *Atmospheric Environment*, 42(23), pp. 5787–5804. doi:10.1016/j.atmosenv.2008.03.048.
- Zhang, L. *et al.* (2016) *Sources and Processes Affecting Fine Particulate Matter Pollution over North China: An Adjoint Analysis of the Beijing APEC Period*, *Environmental Science and Technology*. doi:10.1021/acs.est.6b03010.
- Zhang, Z. *et al.* (2018) 'Enhanced response of global wetland methane emissions to the 2015-2016 El Niño-Southern Oscillation event', *Environmental Research Letters*, 13(7). doi:10.1088/1748-9326/aac939.
- Zheng, T., French, N. and Baxter, M. (2016) 'Development of the WRF-CO₂ 4DVar assimilation system', *Geoscientific Model Development Discussions*, pp. 1–37. doi:10.5194/gmd-2016-289.
- Zhou, Y. *et al.* (2012) 'Changes in OMI tropospheric NO₂ columns over Europe from 2004 to 2009 and the influence of meteorological variability', *Atmospheric Environment*, 46(2), pp. 482–495. doi:10.1016/j.atmosenv.2011.09.024.
- Zhu, L. *et al.* (2013) 'Constraining U.S. ammonia emissions using TES remote sensing observations and the GEOS-Chem adjoint model', *Journal of Geophysical Research: Atmospheres*, 118(8), pp. 3355–3368. doi:10.1002/jgrd.50166.
- Zondlo, M. *et al.* (2016) 'Ammonia emissions, transport, and deposition downwind of agricultural areas at local to regional scales', in *EGU General Assembly Conference Abstracts*, p. 16552.